

# Performance and Analysis of Solitons in Optical Domain

*Thesis submitted in partial fulfillment of the requirement for the award of the degree of*

**MASTER OF ENGINEERING**

*In*

**ELECTRONICS & COMMUNICATION ENGINEERING**

*Submitted by*

**Jaspreet Singh**

**Roll no. 800961008**

*Under the Guidance of*

**Dr. Sanjay Sharma**

**Associate Professor**



**Electronics and Communication Engineering Department**

**Thapar University, Patiala-147004 (PUNJAB)**

**July 2011**

## CERTIFICATE

---

I hereby declare that the work which is being presented in the thesis entitled "Solitons, Interactions and Soliton Systems" in partial fulfillment of the requirement for the award of degree of Master in Engineering at Electronics and Communication department of Thapar University, Patiala is an authentic record of my own work carried out under the supervision of Dr. Sanjay Sharma, Associate Professor, ECED.

The matter presented in this thesis has not been submitted in any other University/Institute for the award of my degree.

Date:

*Jaspreet Singh*  
Jaspreet Singh 08/8/2011  
Roll No. 800961008

It is certified that the above statement made by the student is correct to the best of my knowledge and belief.

*Sanjay Sharma* 10/8/2011  
Dr. Sanjay Sharma  
Associate Professor  
ECED, Thapar University

Counter signed by:

*A.K. Chatterjee* 17/8/11  
Dr. A.K. Chatterjee  
Professor & Head  
ECED, Thapar University  
Patiala-147004

*S.K. Mohapatra*  
Dr. S.K. Mohapatra  
Dean of Academic Affairs  
Thapar University  
Patiala-147004

## ACKNOWLEDGEMENT

---

No volume of words is enough to express my gratitude towards my guide, **Dr. Sanjay Sharma**, Associate Professor, Electronics and Communication Engineering Department, Thapar University, who has been very concerned and has aided for all the material essential for the preparation of this thesis report. He has helped me to explore this vast topic in an organized manner and provided me with all the ideas on how to work towards a research-oriented venture.

I am also thankful to **Dr. A. K. Chatterjee**, Head of Department, ECED and **Dr. Alpana Aggarwal**, P.G. Coordinator, for the motivation and inspiration that triggered me for the thesis work.

I would also like to thank the staff members and my colleagues who were always there in the need of the hour and provided with all the help and facilities, which I required, for the completion of my thesis.

Most importantly, I would like to thank my parents and the Almighty for showing me the right direction out of the blue, to help me stay calm in the oddest of the times and keep moving even at times when there was no hope.

*Jaspreet Singh*

Jaspreet Singh 08/8/2011

Roll No. – 800961008

## ABSTRACT

---

From the stripes of a zebra, to the spirals of cream in a hot cup of coffee, we are surrounded by patterns in the natural world. But why are there patterns? Why drives their formation? In this thesis we study some of the diverse ways patterns can arise due to the interactions between solitary waves in nonlinear systems, sometimes starting from nothing more than random noise.

What follows is a set of three studies:

In the first study, we study about solitons as what soliton is? From where it is generated, soliton types and optical solitons.

In the second study, we study about spatial solitons, soliton properties such as diffraction and Kerr effect.

In the third study, we study as what will happen when number of soliton pulses having same phases interact with each other as the interaction enhances the refractive index at the point where they meet or not. This enhancement depends on the intensities of the participating pulses individually. This character can be exploited very nicely in long distance remote switching through optical fiber. The change of refractive index in optical fiber media by interaction between two or among more numbers of soliton pulses can lead leakage of light from the fiber at the interaction point.

Many other similar incidences can be organized by this interaction and these can be directly utilized in long distance switching. Optical logic operation can be conducted from a long distance if the interaction can be organized properly. We can see also from the above discussion that the change of refractive index will not depend at all of the frequencies of the carrier waves of the interacting soliton pulses.

In the final study, we study about soliton systems & find out the results of various soliton systems with the help of Optisystem simulation software.

# TABLE OF CONTENTS

<b>CERTIFICATE</b>	<b>i</b>
<b>ACKNOWLEDGEMENT</b>	<b>ii</b>
<b>ABSTRACT</b>	<b>iii</b>
<b>TABLE OF CONTENTS</b>	<b>iv</b>
<b>LIST OF FIGURES</b>	<b>vi</b>
<b>LIST OF ABBREVIATIONS</b>	<b>xii</b>
<b>CHAPTER 1: INTRODUCTION</b>	<b>1</b>
1.1 Solitons	1
1.2 Brief History of Solitons	3
1.3 Optical Solitons	8
1.3.1 Optical Temporal Solitons	8
1.3.2 Optical Spatial Solitons	11
1.4 Incoherent Solitons	14
1.5 Modulation Instability Problem Statement	17
<b>CHAPTER 2: SPATIAL SOLITONS AND DIFFRACTION</b>	<b>19</b>
2.1 1-D Spatial Solitons	19
2.2 Kerr Effect in Spatial Solitons	23
2.3 Soliton Diffraction	25
2.3.1 Sampling	26
2.3.2 Sampling in Linear Propagation Simulations	26
2.3.3 Sampling in Nonlinear Diffraction Simulation	27
2.4 Spatial Solitons	28
<b>CHAPTER 3: SOLITONS AND THEIR INTERACTIONS</b>	<b>34</b>
3.1 Soliton Interactions	35
3.2 Phase Sensitive Interactions	37
3.3 Soliton Collision	40

3.4 Soliton Attraction	42
3.5 Soliton Repulsion	43
3.6 Interaction of Soliton Pulses in Long Distance Switching	45
3.6.1 Effect of interaction between two soliton pulses with different frequencies but in same phase.	47
3.6.2 Effect of interaction among three soliton pulses with different frequencies but in same phase.	50
<b>CHAPTER 4: OPTISYSTEM SIMULATION RESULTS</b>	<b>54</b>
4.1 Fundamental and Higher Order Solitons	56
4.2 Interaction of Optical Solitons	61
4.2.1 Interaction between Identical, In-Phase Solitons	62
4.2.2 Interaction between Identical, $\pi$ -out of Phase Solitons within one Collision length	67
4.3 Decay of Higher order Solitons in the Presence of Third-Order Dispersion(TOD)	70
4.4 Stability of Solitons in Birefringent Optical Fibers	78
4.5 Soliton Amplifier as In-Line Amplifier in Soliton Communication Systems	85
4.6 Decay of Higher order Solitons in the presence of Intrapulse Raman(IR) Scattering	92
4.7 Decay of Higher order Solitons in the presence of Self-Steepening	100
<b>CHAPTER 5: CONCLUDING REMARKS AND FUTURE SCOPE</b>	<b>107</b>
<b>REFERENCE</b>	<b>109</b>

## LIST OF ABBREVIATIONS

KDV	Korteweg,de Vries
NSE	Nonlinear Schroedinger Equation
LED	Light Emitting Diodes
FFT	Fast Fourier Transform
GVD	Group Velocity Dispersion
SPM	Self Phase Modulation
TOD	Third Order Dispersion
LMS	Least mean square
LS	Least square
MSE	Mean square
MMSE	Minimum mean square error
LAN	Local Area Network

# CHAPTER 1

## INTRODUCTION

---

### 1.1 SOLITONS

A soliton is a special form of light pulses that can be transmitted over fiber optic channel. Potentially, a soliton retains its shape or wavelength over a longer distance than ordinary light pulses, permitting a higher rate of information bits to be transmitted or in other words a soliton is a self-reinforcing solitary wave that maintains its shape while it travels at constant speed.

In mathematics, solitons arise as the solutions of a widespread class of weakly nonlinear dispersive partial differential equations. Solitons are caused by a cancellation of nonlinear & dispersive effects in the medium. John Scott Russell produced the phenomenon in a wave tank and named it as “Wave of Translation”. After performing a Galilean and variety of scaling transformations, the Korteweg, de Vries (KdV) equation can be written in simplified form

$$u_t + 6uu_x + u_{xxx} = 0 \quad (1.1)$$

One soliton solution of this nonlinear PDE:

$$u(x, t) = \frac{1}{2} c \operatorname{sech}^2 \frac{1}{2} \sqrt{c} (x - ct + \delta) \quad (1.2)$$

Where  $c$  is the speed of the soliton and  $\delta$  is the phase. This equation shows that peak amplitude is exactly half the speed. Thus larger solitary waves have greater speed.

The KdV equation can admit also a multi-soliton solutions.

Following are the properties associated to solitons:

1. They are of permanent form;
2. They are localized within a region;
3. They can interact with other solitons, and emerge from the collision unchanged, except for a phase shift.

Dispersion and non-linearity can interact to produce permanent and localized wave forms. Consider a pulse of light traveling in glass. This pulse can be thought of as consisting of light of several different frequencies. Since glass shows dispersion, these different frequencies will travel at different speeds and the shape of the pulse will therefore change over time. However, there is also the non-linear Kerr effect: the refractive index of a material at a given frequency depends on the light's amplitude or strength. If the pulse has just the right shape, the Kerr effect will exactly cancel the dispersion effect, and the pulse's shape won't change over time.

Many exactly solvable models have soliton solutions, including the Korteweg–de Vries equation, the nonlinear Schrödinger equation, the coupled nonlinear Schrödinger equation, and the sine-Gordon equation. The soliton solutions are typically obtained by means of the inverse scattering transform and owe their stability to the integrability of the field equations. The mathematical theory of these equations is a broad and very active field of mathematical research.

Some types of tidal bore, a wave phenomenon of a few rivers including the River Severn, are 'undular': a wavefront followed by a train of solitons. Other solitons occur as the undersea internal waves, initiated by seabed topography, that propagate on the oceanic pycnocline. Atmospheric solitons also exist, such as the Morning Glory Cloud of the Gulf of Carpentaria, where pressure solitons travelling in a temperature inversion layer produce vast linear roll clouds. The recent and not widely accepted soliton model in neuroscience proposes to explain the signal conduction within neurons as pressure solitons.

A topological soliton, also called a topological defect, is any solution of a set of partial differential equations that is stable against decay to the "trivial solution." Soliton stability is due to topological constraints, rather than integrability of the field equations. The constraints arise almost always because the differential equations must obey a set of boundary conditions, and the boundary has a non-trivial homotopy group, preserved by the differential equations. Thus, the

differential equation solutions can be classified into homotopy classes. There is no continuous transformation that will map a solution in one homotopy class to another. The solutions are truly distinct, and maintain their integrity, even in the face of extremely powerful forces. Examples of topological solitons include the screw dislocation in a crystalline lattice, the Dirac string and the magnetic monopole in electromagnetism, the Skyrmion and the Wess–Zumino–Witten model in quantum field theory, and cosmic strings and domain walls in cosmology.

On a fundamental level, the origin of nonlinear response is related to an harmonic motion of bound electrons under the influence of an applied field. As a result, the total polarization  $\mathbf{P}$  induced by electric dipoles is not linear in the electric field  $\mathbf{E}$ ,

$$\mathbf{P} = \epsilon_0 (\chi^{(1)} \cdot \mathbf{E} + \chi^{(2)} : \mathbf{E}\mathbf{E} + \chi^{(3)} : \mathbf{E}\mathbf{E}\mathbf{E} + \dots) \quad (1.3)$$

where  $\epsilon_0$  is the vacuum permittivity and  $\chi^{(j)}$  ( $j = 1; 2; \dots$ ) is  $j$ th order susceptibility preserved by the differential equations. Thus, the differential equation solutions can be classified into homotopy classes. There is no continuous transformation that will map a solution in one homotopy class to another. The solutions are truly distinct, and maintain their integrity.

## 1.2 A Brief History of Solitons

It was in 1834 that the first officially documented observation of a soliton occurred. John S. Russell, a Scottish scientist, was riding his horse along a shallow canal, when he noticed in it a “well defined heap of water” elevated above the smooth water around it travelling “without change of form or diminution of speed” [1]. He was able to follow it on horseback for some distance until it finally disappeared. Today, science recognizes what Russell saw as a soliton, a phenomena related to tsunamis and tidal waves. Solitons are by no means restricted to water waves; the mechanism is universal, appearing in numerous nonlinear systems capable of supporting waves. Loosely speaking, a soliton may refer to any solitary, localized wave packet that remains unchanged as it propagates.

Soliton formation results from the interplay between the linear and non-linear responses of the propagation medium. In linear systems, dispersion or diffraction generally will cause wave-packets to spread as they propagate. Any wave-packet can be decomposed into a linear superposition of plane-waves of different frequencies using Fourier methods; broadening of a pulse will occur if these plane-waves of different frequencies travel at different velocities (chromatic dispersion) or at different angles (diffraction). Although the spectral contents of the pulse will remain unchanged, the dispersion (or diffraction) will introduce a frequency dependent phase-shift to each of the plane wave components, causing the overall intensity profile that is their superposition to grow wider. In non-linear materials, these broadening tendencies can be countered by focusing of the wave-packet caused by intensity dependent properties of the propagation medium.



Figure 1.1: Modern day re-creation of the soliton observed by Russell in 1834. [Union Canal near Edinburgh, Scotland, July 1995, at a conference on nonlinear waves at Heriot-Watt University]

(Figure Source: Non linear fibre optics by G.P Aggarwal)

In optics, for example, the refractive index of the material may be affected by the presence of light; in self-focusing materials the refractive index will increase with the intensity of the beam. This can in turn lead to the effective creation of an induced “lens” which “focuses” the beam. To think about this in another way, both the linear and nonlinear responses introduce phase differences among different plane wave components of the beam. These changes can offset one another, and the nonlinear effect may cause a beam widened by dispersion (diffraction) to narrow again. If the characteristics of the wave-packet and the properties of the material are such that the linear spreading and non-linear self-focusing effects exactly counter one another, a soliton will be created.

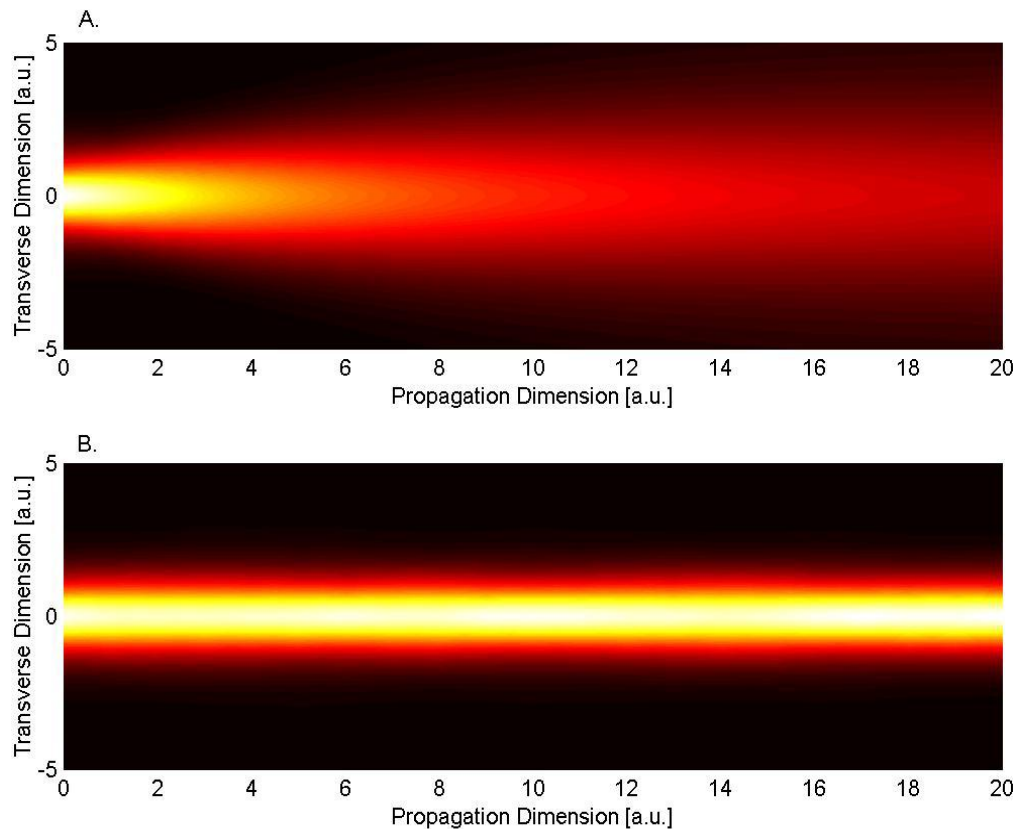


Figure 1.2. A. Diffraction (or dispersion) of a one-transverse dimensional beam propagating in linear media. B. Propagation of a similar beam in non-linear media: the properties of the material and beam are such that the linearity and nonlinearity exactly balance, resulting in a soliton.

(Figure Source: Non linear fibre optics by G.P Aggarwal)

While soliton formation is in itself a very interesting phenomena, interactions between solitons are one of their most fascinating aspects. Intriguing parallels can be drawn between soliton interaction “forces” and those of particles. In some respects, solitons behave like “quasi-particles”. A single soliton travels as a unique, well formed, unchanging entity. These defining properties are indifferent to close-range interactions (or even collisions) with other solitons. For the class of integrable systems, soliton collisions have been proven to be fully elastic [9,11]; not only is the number of solitons conserved, but also each soliton retains its respective power and velocity. Furthermore, soliton collisions are not just the result of two solitons blindly crossing paths; rather effective “forces” exist between solitons and the particle-like wave-packets may either attract or repel one another, depending on their phase properties. Unique and quite varied dynamics, such as spiraling, fusion, and fission may be observed [10].

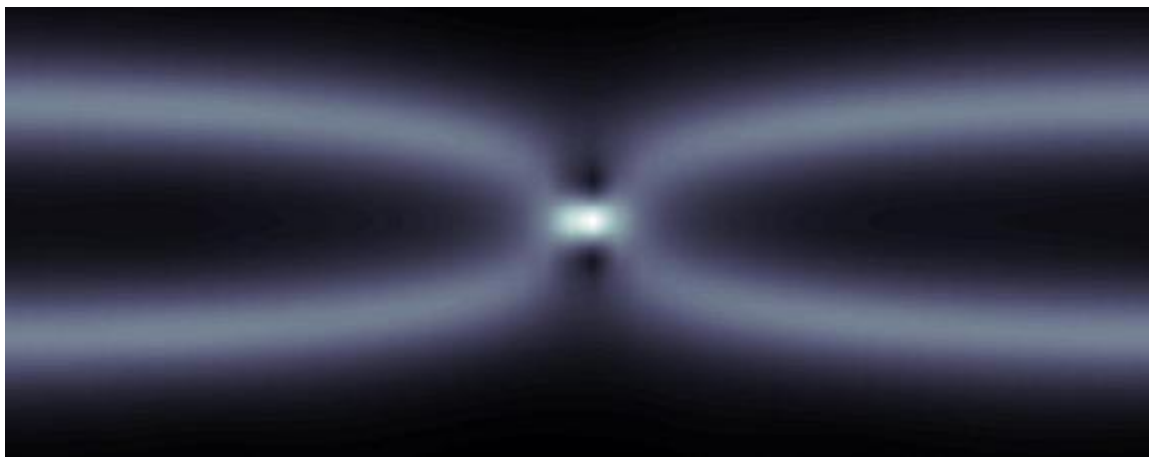


Figure 1.3. Two one dimensional solitons collide and recover.

(Figure Source:Non linear fibre optics by G.P Aggarwal)

While Russell observed solitons in nature as far back as 1834, it was not until 1964, after the invention of the laser, that self-focusing behavior was reported in the laboratory [12]. Narrow wave-packets could propagate undistorted for seemingly indeterminate distances. Many fundamental results in soliton science followed within a few years. In 1965, Kruskal showed mathematically that, like particles, the beams could intersect with one another and continue to

propagate undisturbed. This behavior was likened to “collisions” and the new “particles” were christened “solitons” [11]. After more pioneering work such as the superposition of soliton solutions and Lax-pairs, inverse-scattering methods were used in 1972 to find exact solutions to the (1+1)D Nonlinear Schroedinger Equation (NLS) with Kerr non-linearity [9]. (The Kerr-type non-linearity  $\Delta n_{NL} = n_2 I$  is a real quantity, linear in the local intensity  $I$ . To first order, the non-linearity in almost any system can be modeled this way, provided the frequency is far from any resonances so that the anharmonicity is relatively weak. Typical values of  $\Delta n$  giving rise to optical spatial solitons are on the order  $10^{-4}$ ).

In the years since then, solitons have been found in many other systems, illustrating their universality. The solitons first discovered in 1964 were optical spatial solitons. That is, these solitons were optical and had constant spatial profiles. In 1973, another sort of optical soliton, the optical temporal soliton, was theoretically shown to be possible by Hasegawa and Tappert [14]. These are one dimensional solitons consisting of a beam of light trapped in its transverse spatial dimensions by a waveguide, while pulsed in the direction of propagation; it is this temporal profile which is solitonic and remains unchanged during propagation over huge distances. The first temporal solitons were observed experimentally in optical fibers by Mollenauer, Stolen, and Gordon in 1980 [13] and have since then been much studied for potential use in long-haul communication systems [14-16]. Although optical solitons are probably the easiest to study nowadays, and the most commonly researched, solitons are universal and have been discovered in many non-linear media allowing the propagation of waves. Plasma waves [2], sound waves in  $^3\text{He}$  [3], and waves in  $\text{CS}_2$  [5], glass [6], semiconductor [7], and polymer waveguides [8] have all been shown to support solitons. An incredible variety of solitons have been classified since the early days, exhibiting a remarkable range of forms: photorefractive solitons [39,40], quadratic solitons [41,42], multicomponent vector solitons [43], incoherent solitons [44-46], discrete solitons [47,48], optical “bullets” [49], and cavity solitons [50,51] are just a few examples.

## 1.3 Optical Solitons

### 1.3.1 Optical Temporal Solitons

In optics, we speak of two generic kinds of solitons: temporal and spatial. Temporal solitons can be seen in optical fibers, where the propagation of light is governed by the Non-Linear Schrödinger equation (NLS),

$$\frac{\partial A}{\partial z} = \frac{i}{2} \beta \frac{\partial^2 A}{\partial \tau^2} + i\gamma |A|^2 A, \quad (1.4)$$

where  $A$  refers to the slowly varying electric field envelope of a short pulse of light with carrier frequency  $\omega_0$ ;  $\beta$  and  $\gamma$  are real constants reflecting, respectively, the strength of the linear and non-linear responses. The coordinate,  $z$ , corresponds to the distance the light pulse has propagated along the fiber, and  $\tau$  is the time coordinate in the reference frame of the pulse (the time variable has been shifted linearly as a function of  $z$  so that the coordinate frame moves at the group velocity of the pulse). Although, of course, there are three spatial dimensions, only one appears in the equation; this is because the light is assumed to be an unchanging mode of the optical fiber waveguide in the transverse  $x$  and  $y$  directions, which cancels out of the equations. Such a system is referred to as (1 + 1) D, meaning 1 transverse (or trapping) dimension and 1 propagation dimension.

Examining Eq (1.4), we can see both dispersion and non-linear focusing, or self-phase modulation, at work. The first term on the right hand side represents linear chromatic dispersion, and the second, the nonlinear response of the medium resulting from the dipole movements of the electrons in the material in response to the electric field waves passing through it. Eq. (1.4) is known as the Non-Linear Schrödinger equation (NLS) due to its resemblance to the Schrödinger equation in quantum mechanics. Along these lines, we can intuitively think of the non-linear term as creating a “potential well”. In this case, a soliton can be thought of as being a “bound state” of the potential which it itself induces (the so-called “self-consistency principle”) [20]. To better understand this important equation, it is instructive to consider its origin [17]. As stated above,  $A(\tau, z)$  represents the slowly varying envelope of the electric field at a carrier frequency  $\omega_0$ :

$$\bar{E}(t, z) = A(t, z)e^{i(k_0 z - \omega_0 t)} \hat{x} \quad (1.5)$$

where we are back in the true coordinate frame,  $(t,z)$ , and linear polarization in the  $\hat{x}$ -direction is assumed; the wavevector of the carrier in vacuum is  $k_0 = \frac{2\pi}{\lambda_{VAC}}$ , where  $\lambda_{VAC}$  is the wavelength. The response of the medium to the light, (both the dispersion and the non-linearity), are embodied in the form of its index of refraction:

$$n^2(\omega, |\vec{E}|^2) = n_0^2(\omega) + n_2 |\vec{E}|^2 \quad (1.6)$$

where  $n_0(\omega)$  represents chromatic dispersion, and (far from the resonances of the material) may be well approximated by the Sellmeier equation  $n_0^2(\omega) = 1 + \sum_{j=1}^M \frac{\alpha_j \omega_j^2}{\omega_j^2 - \omega^2}$ , where the sum,  $j$ , is over each of the  $M$  resonances of the material [18]. The non-linear response of the medium is assumed to be linear in the intensity, proportional to the constant,  $n_2$ . This results by assuming that the electric field is sufficiently weak enough for the response to be approximated as a Taylor's series with only the lowest non-zero term retained; for centro-symmetric materials this must be proportional to  $\vec{E} \cdot \vec{E}^*$ , and not  $\vec{E}$ , since an  $E_r$  term would indicate a directional preference in the material. The wave-vector,  $k$ , is related to the index of refraction (keeping first order terms only):

$$\frac{ck}{\omega} = n_0(\omega) + \frac{n_2}{2n_0} |\vec{E}|^2 \quad (1.7)$$

Thus  $k = k(\omega, |\vec{E}|^2)$ , and for frequencies near to the carrier frequency,  $\omega_0$ , we may approximate

$$k - k_0 = \frac{\partial k}{\partial \omega} (\omega - \omega_0) + \frac{1}{2} \frac{\partial^2 k}{\partial \omega^2} (\omega - \omega_0)^2 + \frac{\partial k}{\partial |\vec{E}|^2} (|\vec{E}|^2 - |\vec{E}_0|^2) \quad (1.8)$$

where all of the derivatives are constants evaluated at  $k_0, \omega_0$ , and  $|\vec{E}_0|^2$  (the average amplitude). Knowing that the electric field may be represented in the Fourier domain as well as in time and space, and that, at infinity,  $E \rightarrow 0$ , we can use integration by parts to replace  $k - k_0$  with the spatial

operator  $-i \frac{\partial}{\partial z}$  and  $\omega - \omega_0$  with the temporal operator  $i = \frac{\partial}{\partial t}$ . Making these replacements in the equation above, and operating on the field envelope,  $A(t,z)$ , we get:

$$i \left( \frac{\partial A}{\partial z} + \frac{\partial k}{\partial \omega} \frac{\partial A}{\partial t} \right) - \frac{1}{2} \frac{\partial^2 k}{\partial \omega^2} \frac{\partial^2 A}{\partial t^2} + \frac{\partial k}{\partial |A|^2} (|A|^2 - |A_0|^2) A = 0, (1.9)$$

where we have used the fact  $|\vec{E}|^2 = |A|^2$ . Remembering that the derivatives with respect to  $k$  are constants, and moving to a frame of reference,  $\tau = t - \frac{z}{v_g}$ ,  $z$  that moves with the group velocity of the pulse ( $v_g = \partial \omega / \partial k$ ), we have

$$\frac{\partial A}{\partial z} = \frac{i}{2} \beta \frac{\partial^2 A}{\partial \tau^2} + i\gamma (|A|^2 - |A_0|^2) A \quad (1.10)$$

where we have introduced the notation  $\beta$  and  $\gamma$  for the constants in Eq. (1.9). Note that  $|A_0|^2$  is a constant and thus this term will simply introduce a phase  $e^{i\gamma|A_0|^2 z}$  that is constant across the profile of the pulse, introduces no new physics, and may be renormalized out, reducing Eq. (1.10) to the NLS as desired. If the dispersion constant,  $\beta > 0$ , then the material is said to have anomalous dispersion, and the equation can be solved exactly using the inverse-scattering method developed by Zakharov and Shabat [9] for bright solitons of the form

$$A(\tau, z) = \sqrt{P_0} \operatorname{sech}(\tau/\tau_0) \exp\left(\frac{i}{2} z |\beta| / \tau_0^2\right) \quad (1.11)$$

where  $P_0$  is the peak power of the pulse and  $\tau_0$  is the temporal width of the pulse. The intensity profile of the pulse,  $|A(\tau, z)|^2 = f(\tau)$ , has no  $z$  dependence and thus the pulse is truly stationary and a **soliton**.

Since the 1980s, most of the research on temporal solitons has focused on applications to long-distance fiber optic communications [14-16]. However, temporal solitons are also intrinsically interesting from a scientific point of view and much about the general behavior of self-trapped waves in non-linear systems can be learned by examining their behavior. As discussed in the

introduction, two solitons in close proximity to one another will interact. If two solitons of the form of Eq. (1.11) are near to one another with no relative phase difference between them, then the two pulses will attract one another, and eventually pass right through one another, “colliding”. The solitons have momentum and will continue to separate after the collision, but the attraction will act as a restoring force, eventually drawing the two back together. The pair of solitons will continue to pass through one another, again and again, with perfect periodicity. On the other hand, if the solitons are initially  $\pi$  out of phase with respect to one another, then they will repel.

A phenomenon related to solitons is that of “higher-order” solitons. If  $N$  solitons, all in phase, are initially exactly overlapping in both time and space, then the initial pulse profile will look like

$$A_N(\tau, z = 0) = N\sqrt{P_0} \operatorname{sech}(\tau/\tau_0) \quad (1.12)$$

As the solitons propagate, the interactive forces between the solitons will cause them to oscillate, and various patterns will form as the pulse eventually breaks into peaks. The behavior is periodic, and the pulse shape will continually return to the same profile as in Eq. (1.12).

### 1.3.2 Optical Spatial Solitons

The temporal solitons in Section 1.3.1 are able to exist because temporal changes in the intensity of the pulse create a temporal gradient in the index of refraction of the material, causing it to act as a time-dependent waveguide for the pulse. Since the electric field in Eq. (1.5) is essentially uniform in space (the fluctuations in space and time due to the envelope’s carrier wave are very rapid and average out) only the derivative of the slowly varying electric field envelope with respect to time matters. However, time is a coordinate like any other, and in fact, variations in the intensity of a beam in space can also give rise to an altered index of refraction and an optically-induced waveguide. If the characteristics of the incident beam coincide with those of a mode of the waveguide which it induces, then the light will propagate, (“self-trapped” by its own waveguide), as a soliton.

Spatial soliton can occur in dielectric planar waveguides, or by using beams which are very broad and uniform in one transverse dimension, and narrow in the other.

Immediately, an important difference between spatial and temporal solitons becomes apparent: (as far as we know) only one time dimension exists, therefore temporal solitons are inherently limited to be one-dimensional! Work over recent years has shown a rich variety of possibilities for spatial solitons, and solitons trapped in two transverse spatial dimensions ((2+1)D) have been shown to exist as well as solitons trapped in both transverse spatial dimensions and the time dimension ((2+1+1)D solitons, or “light bullets”).

In addition to providing an extra dimension for solitons to propagate in, moving to the spatial domain also allows an extra dimension for solitons to interact in, and for the definition of inherently high-dimensional quantities such as angular momentum. Now, intriguing behaviors such as soliton spiralling and vortex solitons are possible. Overall, the spatial domain provides a very rich environment for studying the fundamental properties of solitons.

One simple way to understand the existence of spatial solitons is to view them as a balance between spreading due to linear diffraction, and focusing caused by a non-linearly induced “lens”. An alternative, and very illustrative, picture of spatial soliton phenomena was presented by Askar’yan in 1962 and expanded upon by Snyder et al in 1991 [20]. Consider a material of the self-focusing type - for bright beams, the refractive index will be highest at the center of the beam where the intensity of the beam is greatest. The structure is identical to a graded-index waveguide: a higher index core is surrounded by material with a lower index of refraction, causing waves to reflect internally. Such waveguides may have guided modes for which these reflections interfere constructively, allowing these modes to propagate in the waveguide with their intensity profiles unchanged. Our spatial soliton example is no different: the higher index of refraction in the center sets up a waveguide which may allow the propagation of certain modes. If the profile of the incident beam is the same as one of the modes of the waveguide, then the incident beam can propagate unchanged. In such a case, the incident beam induces a waveguide in the material, and then proceeds to propagate in it as a guided mode! The soliton is said to be “self-trapped”.

## Spatial Solitons

In order to understand how a spatial soliton can exist, we have to make some considerations about a simple convex lens. As shown in the picture on the right, an optical field approaches the lens and then it is focused. The effect of the lens is to introduce a non-uniform phase change that causes focusing. This phase change is a function of the space and can be represented with  $\varphi(x)$ , whose shape is approximately represented in the picture.

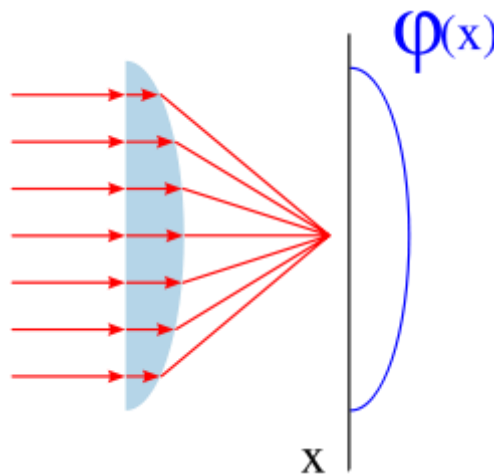


Figure 1.4: Convex lens showing spatial solitons

(Figure Source: Wikipedia(Internet))

The phase change can be expressed as the product of the phase constant and the width of the path the field has covered. We can write it as:

$$\varphi(x) = k_0 n L(x) \quad (1.13)$$

where  $L(x)$  is the width of the lens, changing in each point with a shape that is the same of  $\varphi(x)$  because  $k_0$  and  $n$  are constants. In other words, in order to get a focusing effect we just have to introduce a phase change of such a shape, but we are not obliged to change the width. If we leave

the width  $L$  fixed in each point, but we change the value of the refractive index  $n(x)$  we will get exactly the same effect, but with a completely different approach.

That's the way graded-index fibers work: the change in the refractive index introduces a focusing effect that can balance the natural diffraction of the field. If the two effects balance each other perfectly, then we have a confined field propagating within the fiber.

Spatial solitons are based on the same principle: the Kerr effect introduces a Self-phase modulation that changes the refractive index according to the intensity:

$$\varphi(x) = k_0 n(x) L = k_0 L [n + n_2 I(x)] \quad (1.14)$$

if  $I(x)$  has a shape similar to the one shown in the figure, then we have created the phase behavior we wanted and the field will show a self-focusing effect. In other words, the field creates a fiber-like guiding structure while propagating. If the field creates a fiber and it is the mode of such a fiber at the same time, it means that the focusing nonlinear and diffractive linear effects are perfectly balanced and the field will propagate forever without changing its shape (as long as the medium does not change and if we can neglect losses, obviously). In order to have a self-focusing effect, we must have a positive  $n_2$ , otherwise we will get the opposite effect and we will not notice any nonlinear behavior.

The optical waveguide the soliton creates while propagating is not only a mathematical model, but it actually exists and can be used to guide other waves at different frequencies. This way it is possible to let light interact with light at different frequencies (this is impossible in linear media).

## 1.4 Incoherent Solitons

All of the solitons discussed in Sec. 1.3 above are coherent solitons; that is to say, if the phase of the electric field is known at one particular time (place) then the phase of the electric field at any other time (place) can also be predicted. For example, consider the temporal soliton solution of Eq. (1.4) given in Eq. (1.11); at the input, we know the amplitude and phase of the electric field at every point and time:

$$\vec{E}(\tau, z = 0) = \sqrt{P_0} \operatorname{sech}(\tau/\tau_0) \hat{x} \quad (1.15)$$

(The phase is simply uniform everywhere). The solution, Eq. (1.11), also dictates the amplitude and phase of the electric field at every point in time and space. Furthermore, for any input electric field amplitude whatsoever, Eqs. (1.4) and (1.14) can be used to calculate the phase at any later point, provided the phase of the initial condition is specified. This is what is meant by **coherent**.

While coherence is certainly not a property of light in general, it is a reasonably good characterization of the light produced by the lasers used in many experiments. Since lasers produce light by stimulated emission, their beams are indeed highly coherent. On the other hand, light from Light Emitting Diodes (LEDs) and from natural sources, such as the sun or light bulbs, is incoherent, and the phase varies randomly with time and space across the beam. Some light is partially incoherent, and for distances smaller than the coherence length,  $l_c$ , (or times shorter than the coherence time), the phase is correlated (for coherent light  $l_c \rightarrow \infty$ ).

For many years, only coherent optical solitons were known to exist, and it was assumed that this property was a necessity. It was thought that the instantaneous speckles inherent in incoherent beams would each be individually self-focused by the non-linearity, resulting in filamentation and the breakup of the wavefront. This all changed, when in 1995, Mitchell, Chen, Shih, and Segev from Princeton University experimentally demonstrated self-trapping of incoherent light, (with randomly varying phase both in time and in space), using an SBN photorefractive crystal with a slow non-linearity [26]. Key to the success of the experiment was the use of a medium with a response time long compared to the characteristic phase fluctuation time across the beam. In this way, the non-linearity could respond only to the smooth and steady time-averaged intensity profile, and was not affected by the momentary speckles. Since then, much research has been done both experimentally and theoretically in nonlinear media in general, greatly increasing understanding of this new type of soliton and propagation of incoherent optical beams.

Perhaps the simplest way to explain incoherent solitons is the multi-modal theory. Whether the wave is incoherent or not, in a self-focusing medium, the refractive index will be highest where

the intensity of the incident beam is highest. In crystals with a slow non-linearity, the refractive index of the material will increase where the time-averaged intensity of the beam increases and, for example, for a Gaussian beam with highest intensity in the center, this will lead to the creation of an induced wave-guide.

In this way, the time-averaged intensity of the soliton can be decomposed into a sum of the modes of the induced waveguide. Of course, the time-averaged population of each of the modes will remain stationary as it propagates in the waveguide, so the sum of their time-averaged populations must also remain stationary. Since the waveguide was induced by the intensity profile in the first place, what we have is a genuine soliton. This explanation implies three requirements for the existence of incoherent solitons: (1) the response time of the non-linearity must be slower than the characteristic time of phase fluctuations, (2) the incoherent beam must be able to induce a multi-mode waveguide, and (3) the slowly varying envelope of the partially incoherent beam must be an appropriate superposition

of these is the Fourier transform of the correlation function. Although the modal perspective of incoherent soliton formation is informative and useful for finding stationary soliton solutions, it offers no insight into the dynamic properties of incoherent solitons and cannot say anything at all about incoherent non-solitonic beams. A quite different approach, the coherent-density method[27], is excellently suited to studying these problems. In this model, infinitely many “coherent components” propagate at all possible angles (i.e. values of the wave-vector  $(k_x, k_y)$ ) and interact with one another only through the non-linearity, which is a function of the time-averaged total intensity. The shapes of the initial intensity profile for each of these coherent components are the same, but the relative weights are given by the angular power spectrum of the source beam, which much use to thoroughly detail it now. First, consider an incoherent field of uniform time-averaged intensity, representing only the statistical fluctuations of 0.

The coherent-density approach can easily be adapted for computer; all that is required is to supply the initial conditions and to approximate the infinite number of coherent components by a discrete, finite number (replacing integrals by summations). In practice, a large number of components are required to simulate beams with even a small partial incoherence; in two spatial dimensions, the number can exceed  $100 \times 100$ . For problems with a fair amount of spatial variation, each of the  $100 \times 100$  components may require on the order of  $2048 \times 2048$  spatial grid

points as well. Thus, a modest problem might require 41,943,040,000 points just for the grid, and due to the sensitive nature of non-linear dynamics, these usually are required to be 32-bit double precision (that's more than 156 Giga-Bytes just to store the incoherent wave profile!). The amount of computational power required for the problem quickly escalates! In fact, without access to a supercomputer, most problems can not reasonably be attempted. Fortunately, the nature of the problem is highly parallel and naturally suited to massively parallel machines. In Chapters 2 and 3, research was made possible thanks to the use of the Pittsburg Supercomputing facility; computations were performed using parallel programming techniques on up to as many as 512 processors.

## 1.5 Modulation Instability

Closely related to the formation of solitons is the process of modulation instability (MI). In the regime of soliton formation, a very broad, flat beam (a beam much wider than the corresponding soliton of equivalent peak intensity) propagating under the influences of linear and non-linear influences will be unstable, since the linear diffraction effect is quite small compared to the non-linear effects. Interestingly, due to random background noise, the wavefront may have small amplitude perturbations of width similar to little "quasi-solitons" and each may individually start to "self-focus". These initially infinitesimal fluctuations may grow in amplitude, causing the beam to fragment and breakup into narrow *filaments* [28-31] that often are almost ideal solitons [32,33]. In the context of certain pursuits, the behavior is undesirable; it is well known in fiber optic communications that signals containing long, broad pulses may disintegrate into random trains of short pulses. This mechanism is known as modulation instability (MI) and is observed with both temporal and spatial optical wavefronts, in both one and two dimensions<sup>2</sup>. MI is not exclusive to optics, but is a universal phenomena, occurring in many non-linear environments including waves in fluids [36], plasmas [37], and dielectr han they are being washed-out by linear diffusion. Above this point, MI will occur. Such a "threshold" is unique to incoherent MI and has no counterpart in coherent systems. ic materials [38].

While the existence of MI in coherent non-linear systems has been well known for many years, MI in incoherent systems remained largely unexplored for a long time. Approaching the topic

naively, it might at first appear that incoherence would eliminate modulation instability. The less coherent a wavepacket is, the more rapidly it will diffuse, and so any growth of “filaments” due to MI tends to be “washed-out” by this linear diffusion. However, recent theoretical and experimental work has established the presence of MI in partially-coherent systems [34,35]. As the strength of the non-linear response of the material is increased, the strength of the MI mechanism also “increases”: filaments will form more and more quickly. It has been shown that by continuing to increase the non-linearity, eventually the filaments will form faster than 2 (1+1)D solitons formed by propagating an two-transverse-dimensional optical beam which is broad in one transverse dimension and narrow and solitonic in the other are subject to breakup in the broad dimension due to the related “transverse instability”.

Not only is the onset of MI different in incoherent and coherent systems, but interesting differences in the dynamics of the resulting filaments can be seen between the two systems as well. In coherent systems, solitonic filaments of random phases are created and forces between any pair of solitons can be either attractive or repulsive depending upon the phase difference between the solitons. In incoherent system, as I show in this thesis, on scales greater than the correlation length only attractive forces will be of significance since incoherent solitons can never be out of phase with one another and the effect of increased intensity nearby always deepens the effective potential well. As a result, the solitons group together and soliton “clusters” are created. We show this behavior experimentally and theoretically, using numerical simulations, in Chapter 4. We believe this phenomena important not only in that it offers an opportunity to observe rich non-linear dynamics, but also in that clustering behavior is common to many non-linear systems. Natural systems are often impossible to control or explore in different parameter regimes or initial conditions and optical spatial solitons provide a well-controlled and very flexible environment to study clustering.

## CHAPTER 2

### SPATIAL SOLITONS AND DIFFRACTION

---

1-D soliton solutions are known to be stable. In other words, the perfect balance between the linear (diffraction) and nonlinear (self focusing) effects prevents small field fluctuations from destroying the soliton. Specifically, if the fluctuation results in a bit of soliton widening, the self-focusing effect gets into the situation to squish the soliton back to its original spatial width. Alternatively, if the fluctuation causes the soliton to get compressed in space, diffraction takes over and makes sure that the soliton is back in its proper form. However, 2-D soliton solutions could potentially become unstable when the diffraction does not balance self focusing, leading to a mathematical singularity. As noted before, the optical consequence of this singularity is (typically) crystal damage.

#### **2.11-D spatial solitons**

The following figure illustrates the idea behind spatial solitons. The expanding wavefront due to diffraction is exactly compensated by the converging wavefront due to self focusing to produce a soliton with a plane wavefront.

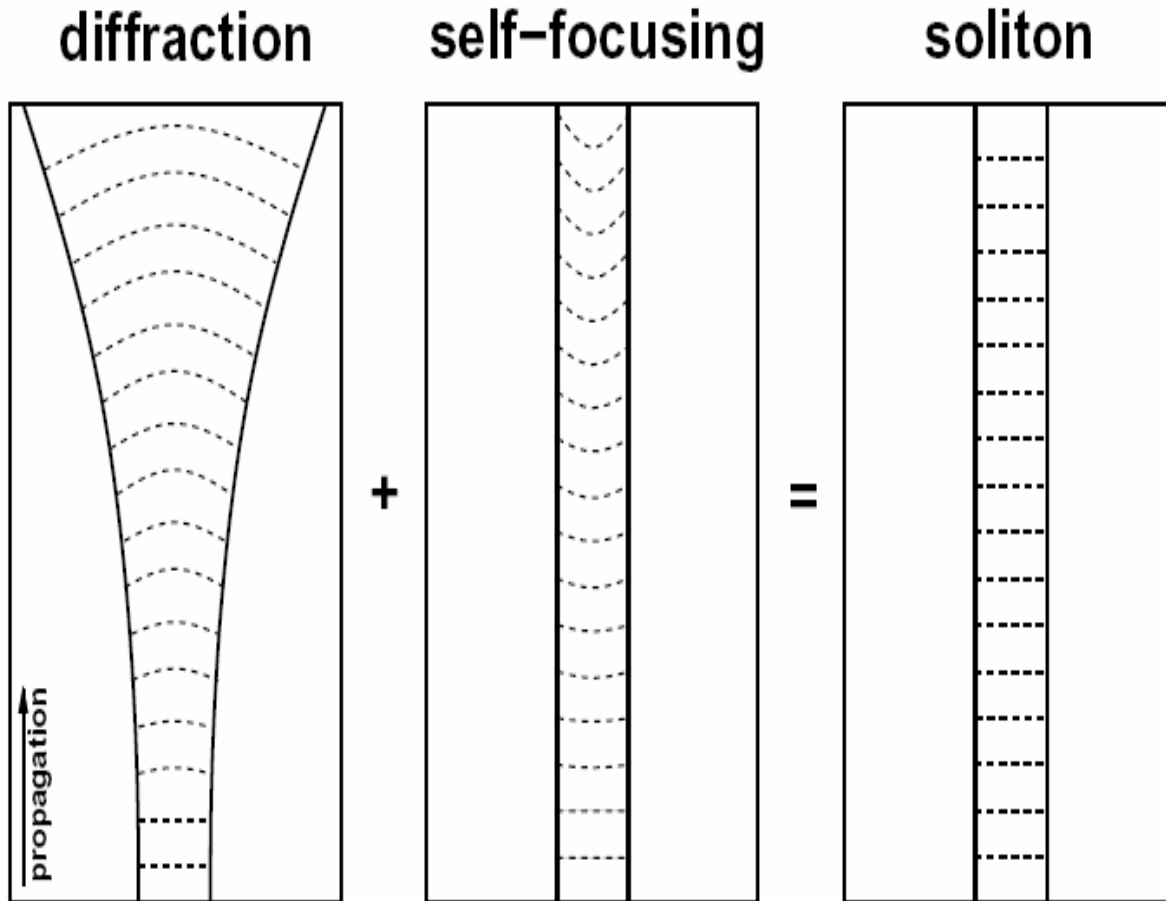


Figure 2.1:1 D spatial solitons

(Figure Source: Non linear fibre optics by G.P Aggarwal)

As with all other propagation wave solutions, soliton solutions have to satisfy the wave equation. But, now we should consider the nonlinear wave equation. Since we are in the 1D world, we assume that the beam is confined in y axis (physically, consider a slab waveguide). Further, if we assume that the linearly guided and nonlinear soliton envelopes are separable, the general Helmholtz equation reduces to

$$\frac{\partial^2 \bar{A}}{\partial z^2} + \frac{\partial^2 \bar{A}}{\partial x^2} + k_0^2 \bar{A} + 2k_0^2 \frac{n_2}{n_0} |A|^2 \bar{A} = 0 \quad (2.1)$$

Where  $A$  is the soliton amplitude,  $k_0$  is the wave number, and  $n_2$  is the nonlinear coefficient. Since a soliton is a stationary solution by definition, we have

$$\bar{A}(x, z) = A(x)e^{i\beta z} \quad (2.2)$$

Which when substituted into the nonlinear 1D separable wave function, becomes

$$\frac{d^2 A(x)}{dx^2} + \left[ k_0^2 - \beta^2 + 2k_0^2 \frac{n_2}{n_0} |A(x)|^2 \right] A(x) = 0 \quad (2.3)$$

where  $\beta$  represents the total wave number. The transverse envelope is assumed to be of the form

$$A(x) = A_0 \operatorname{sech} \left( \frac{x}{w_0} \right) \quad (2.4)$$

where

$$A_0 = \frac{1}{\kappa_0 w_0} \sqrt{\frac{n_0}{n_2}}$$

$$\beta^2 = k_0^2, \quad \frac{1}{w_0^2} = k_0^2 \left[ 1, \frac{n_2 A_0^2}{n_0} \right] \quad (2.5)$$

Since the wave equation is invariant under unitary transformation, a more general stationary soliton solution can be written as

$$A(x', z') = A_0 \operatorname{sech} \left[ \frac{\cos \theta x' - \sin \theta z'}{w_0} \right] e^{i\beta[\cos \theta z' + \sin \theta x']} \quad (2.6)$$

This is the complete non-paraxial 1D solution. Since it is mathematically [1] and numerically difficult to analyze the non-paraxial solution, we make a parabolic approximation that leads to a simple paraxial 1D solution. Assume (for simplicity)

$$\bar{A}(x, z) = A(x, z)e^{ik_0z}. \quad (2.7)$$

Assume SVEA and make the following approximation

$$\left| \partial^2 A / \partial z^2 \right| = \frac{1}{2k_0} \left| \frac{\partial^3 A}{\partial z^3} + \frac{\partial^3 A}{\partial z \partial x^2} + 2k_0^2 \frac{n_2}{n_0} \frac{\partial |A|^2 A}{\partial z} \right| \ll |2k_0 \partial A / \partial z| \quad (2.8)$$

to end up in the following nonlinear Schrödinger equation

$$2ik_0 \frac{\partial A}{\partial z} + \frac{\partial^2 A}{\partial x^2} + 2k_0^2 \frac{n_2}{n_0} |A|^2 A = 0. \quad (2.9)$$

Note that this expression is valid only for propagation along directions very close to z axis. The first two terms of the above expression just represents linear diffraction, while the third term is due to the Kerr nonlinearity.

## 2.2 Kerr Effect in Spatial Soliton

The following k-space diagram illustrates the paraxial approximation. Diffraction in 1+1D is represented by slicing the (2+1)D k-surface (sphere) with a plane passing through the origin. As can be seen, the paraxial approximation approximates the k-circle as a parabola, and so, it's accurate only within a small range of angles close to the optical axis. Mathematically,

$k_z = \sqrt{k_0^2 - k_x^2}$  is approximated as  $k_z \approx k_0 - k_x^2 / 2k_0$  (retain only the first two terms of binomial expansion).

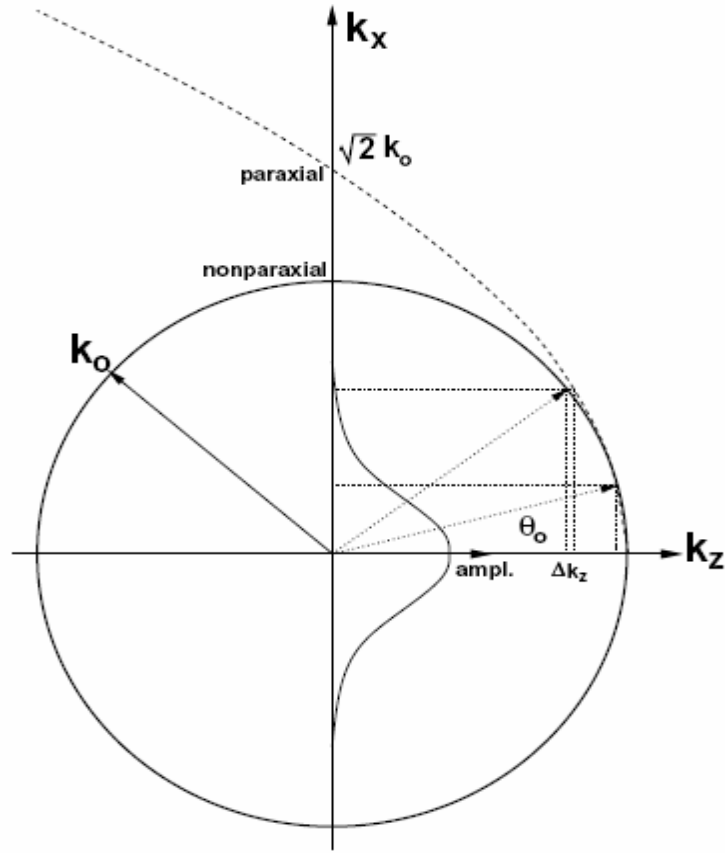


Figure 2.2: Showing kerr effects in spatial solitons

(Figure Source: Yu. N. Karamzin and A. P. Sukhorukov, Sov. Phys. JETP **42**, 842 (1976))

In the paraxial regime, the general soliton propagation solution can be written as

$$A(x, z) = e^{i\phi^{NL}(x,z)} A(x, 0) \quad (2.10)$$

Where  $A(x,0)$  is the initial field amplitude and  $A(x,z)$  is the field amplitude after propagation through a distance  $z$ . The nonlinear phase is the scaled integral of the intensity from 0 to  $z$ .

$$\phi^{NL}(x, z) = k_f n_2 \int_0^z |A(x, z')|^2 dz'. \quad (2.11)$$

When  $z$  is small, the above equation can be approximated to

$$\phi^{NL}(x, \Delta z) \approx k_f n_2 |A(x, \Delta z/2)|^2 \Delta z \quad (2.12)$$

The accuracy of numerical beam propagation simulations in linear media does not depend on the  $z$  sampling rate. In other words, in linear regime, successively propagating a field through a distance of  $10z_0$  ( $z_0 = \text{confocal distance}$ ) in steps of  $z_0$ , will produce the same result as propagating the field directly through  $10z_0$ . However, in a nonlinear regime, if the above approximation ( $z$  is small) is made,  $z$  sampling indeed determines the accuracy of propagation. The above paraxial version of the 1D soliton solution forms the basis of the second section of this project.

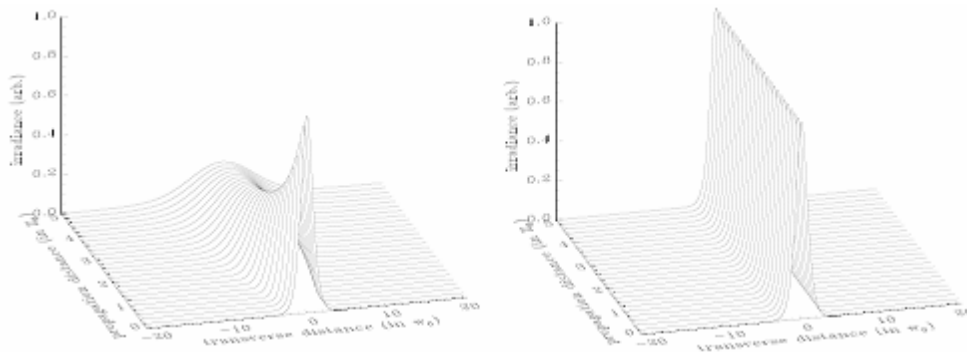


Figure 2.3: Paraxial version of 1D solitons

(Figure Source: Yu. N. Karamzin and A. P. Sukhorukov, Sov. Phys. JETP **42**, 842 (1976))

The above simulation compares the propagation of a beam (diffracting) in a linear media with a spatial soliton. Note that the initial beam profile was same (hyperbolic secant) in both cases. Clearly, the spatial profile of the soliton remains the same as the initial profile even after propagation through  $5z_0$ !

Such nonlinear simulations involve operations both in space and spectral domains. Propagation is typically done in the Fourier domain while the nonlinear effect is added after transforming the field back to the space domain.

By using the stationary ansatz specified before,

$$\frac{d^2 A(x)}{dx^2} + 2k_0 \left[ -\beta + k_f n_2 |A(x)|^2 \right] A(x) = 0. \quad (2.13)$$

Assuming the soliton to be of the form of a hyperbolic secant (defined earlier), the amplitude and phase become

$$\begin{aligned} A_0 &= \frac{1}{k_0 w_0} \sqrt{\frac{n_0}{n_2}} \\ \beta &= 1/2 \kappa_0 w_0^2 = \kappa_f n_2 A_0^2 / 2 \end{aligned} \quad (2.14)$$

The amplitude remains the same as before while the phase has clearly been changed by the paraxial approximation. Now that we know the amplitude and phase, the full paraxial solution can be expressed as

$$\bar{A}(x, y, z) = \frac{1}{k_0 w_0} \sqrt{\frac{n_0}{n_2}} \Phi(y) \operatorname{sech} \left( \frac{x}{w_0} \right) e^{i[k_0 + 1/2 \kappa_0 w_0^2]z} \quad (2.15)$$

Let's analyze the above solution. At  $z = 0$ , we have a real hyperbolic secant. As the soliton propagates ( $z > 0$ ), the amplitude remains the same (amplitude has no  $z$  dependence), while there's a linear phase accumulation. As the intensity of the beam is given as square of the absolute value of amplitude, we see that the intensity has no  $z$  dependence too! Hence, as advertised, the spatial profile of the soliton is unaffected by propagation.

### 2.3 Soliton Diffraction

Soliton propagation involves simultaneous action of linear diffraction and nonlinear self focusing. Linear diffraction can be thought of as a filtering problem. In other words, the diffracted field is calculated (well, defined) as the convolution of the input field and the impulse response of free space. Since the FFT era, Fourier domain processing has become so

fast( $N\log(N)$ ) that almost all digital filtering operations are performed in the spectral domain, where spatial convolution transforms to spectral multiplication. Hence, the diffraction is implemented in the Fourier domain by just multiplying the Fourier transform of the input field with the free space transfer function. Self-focusing is a nonlinear effect, and so, is generally implemented in the spatial domain.

The following simulations come under the category of (1+1)D beam propagation, where we consider only one transverse dimension (y or x), and the propagation dimension (z). Consider the input field to be  $A(x, z = 0)$ . The transverse plane at every  $z > 0$  represents the propagated field at that particular z.

### **2.3.1 Sampling**

Digital simulations operate on discrete spatial coordinates, where a continuous function (in x) is represented as a series of quantized samples. In order to avoid aliasing, Nyquist must be obeyed in the transverse dimension. However, this is not necessarily true in the propagation (z) dimension.

### **2.3.2 Sampling in linear propagation simulations**

Since diffraction can be modeled as a linear system, repeated ('n' times) filtering of a signal with a filter H is entirely equivalent to applying *one* new filter T to the signal, where the new filter T is just the product of all the repeated filters H in Fourier domain. In other words,  $T = H.H.H....H = H^n$ . Hence, in a linear propagation problem low z sampling will not result in a numerical error. Nevertheless, linear beam propagation simulations used for display generally obey Nyquist (they don't have to). If Nyquist is violated in z, while looking at the entire simulation, there would be very prominent blocking artifacts, which essentially are manifestations of a higher spatial frequencies being misrepresented as lower spatial frequencies.

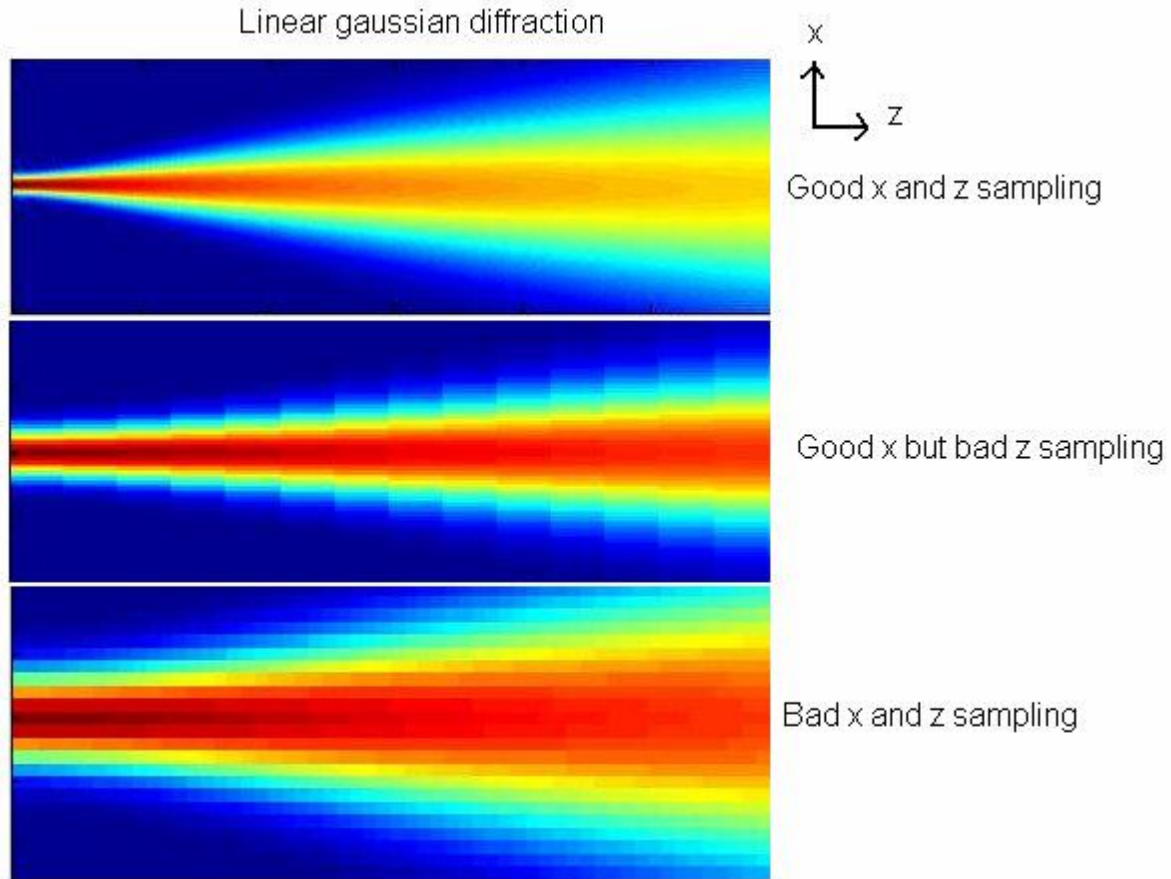


Figure 2.4: linear gaussian diffraction in spatial solitons

(Figure Source: Yu. N. Karamzin and A. P. Sukhorukov, Sov. Phys. JETP **42**, 842 (1976))

To summarize, in linear propagation, Nyquist is necessary in the transverse dimension but not in the propagation dimension ( $z$ ), although obeying Nyquist in  $z$  would result in visually appealing simulations.

### 2.3.3 Sampling in nonlinear diffraction simulations

In nonlinear propagation simulations involving nonlinear operations in the real space, a very high sampling rate (at least Nyquist) must be maintained in both transverse and the propagation dimensions. High sampling rate in transverse dimension, as before, is to avoid aliasing, while high sampling in the propagation dimension is necessary to ensure the accuracy of the

simulation. A low  $z$ -sampling rate will almost certainly result in steep numerical errors. This is because of the following reason:

$$\phi^{NL}(x, z) = k_f n_2 \int_0^z |A(x, z')|^2 dz'. \quad (2.16)$$

The above function represents the phase to be multiplied in real space in each propagating step. When  $z$  is small, this can be approximated to

$$\phi^{NL}(x, \Delta z) \approx k_f n_2 |A(x, \Delta z/2)|^2 \Delta z \quad (2.17)$$

The above phase is relatively much simpler to numerically implement than the earlier expression. But, it's an approximation, and just like any other approximation, it breaks down if it's used in unwarranted regimes. In this case, the valid regime is "small  $z$ ", which corresponds to high sampling rate.

## 2.4 Spatial Solitons

We now simulate the various properties of solitons that we described in section 1. While so, we'll also compare soliton propagation with linear diffraction, assuming identical initial fields  $A(x, z = 0)$ . Hyperbolic secant soliton solutions will be used in all of the following simulations.

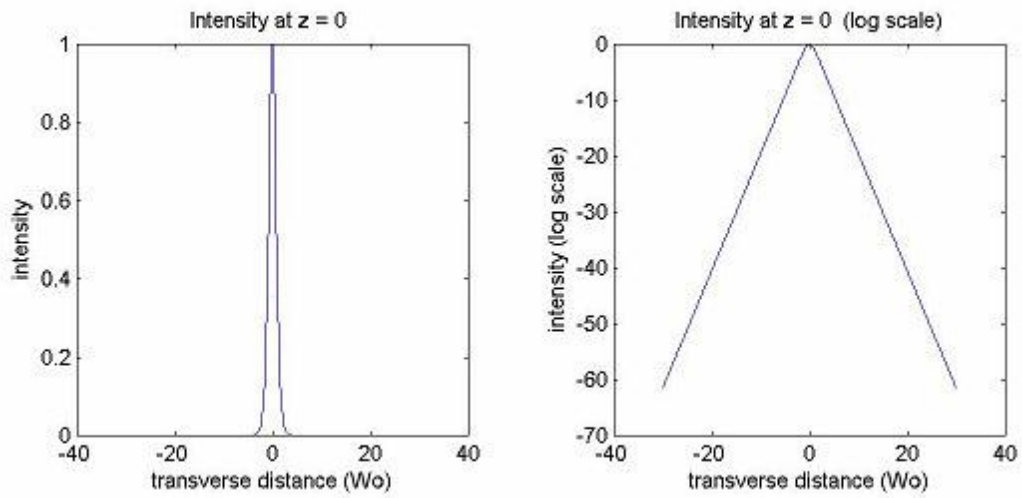


Figure 2.5: Hyperbolic secant soliton

(Figure Source: Non linear fibre optics by G.P Aggarwal)

When these sech fields propagate in a linear medium, they diffract.

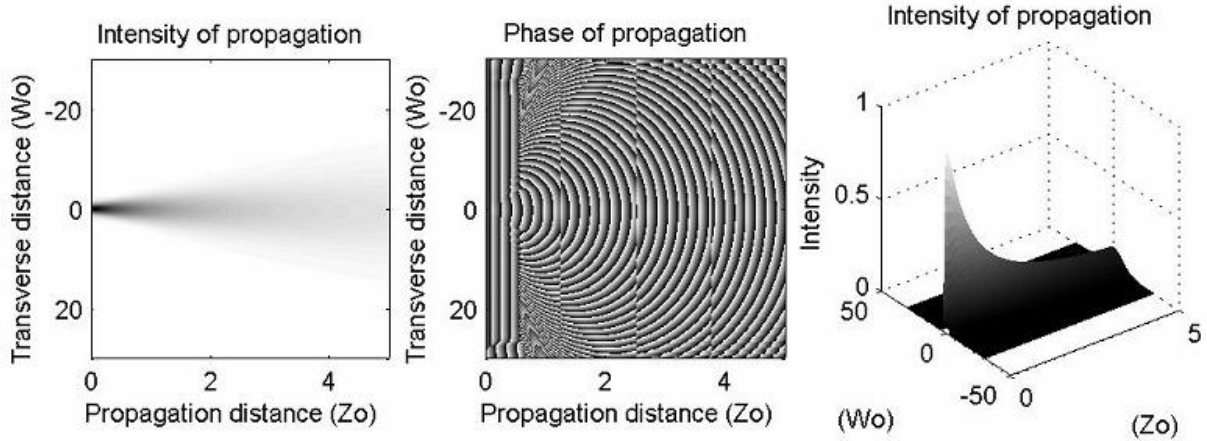


Figure 2.6: Intensity and phase propagation in spatial solitons

(Figure Source: Non linear fibre optics by G.P Aggarwal)

The intensity image clearly shows the energy spreading out as the sech propagates in  $z$ . The phase shows expanding spherical wavefronts. The three apparent vertical discontinuities in the phase plot are not real.

The 3D intensity plot shows the intensity draining out as it propagates.

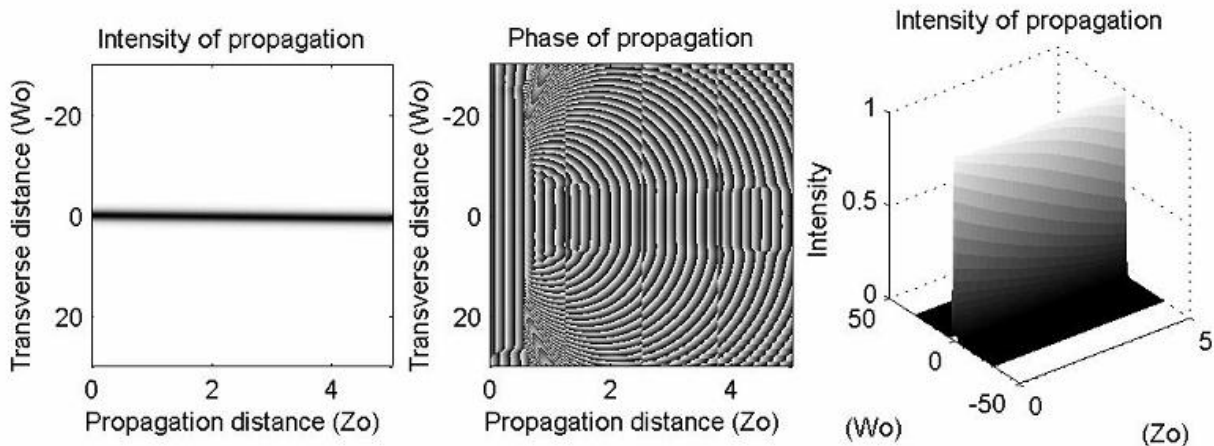


Figure 2.7: Intensity draining in spatial solitons

(Figure Source: Non linear fibre optics by G.P Aggarwal)

We now consider the paraxial soliton propagation with exactly the same specifications (sampling rate, distances, etc) as before. This was implemented by adding an additional “focusing” step in real space. Specifically, after every diffraction step in fourier space, we come back to the real space and multiply the field with the nonlinear phase defined earlier.

The intensity image shows that there’s no spreading out of energy as the sech propagates until  $5Z_0$ . The number  $5Z_0$  was chosen from [1]. The phase image has interesting facts to observe. Any unchanging wave (Ex: Collimated beam) should have a plane wave front, and so should a soliton. It can be clearly seen from the phase image that the central region (where the soliton propagates) has plane wavefronts throughout  $5Z_0$ . The 3D plot also indicates that the beam loses no energy as it propagates.

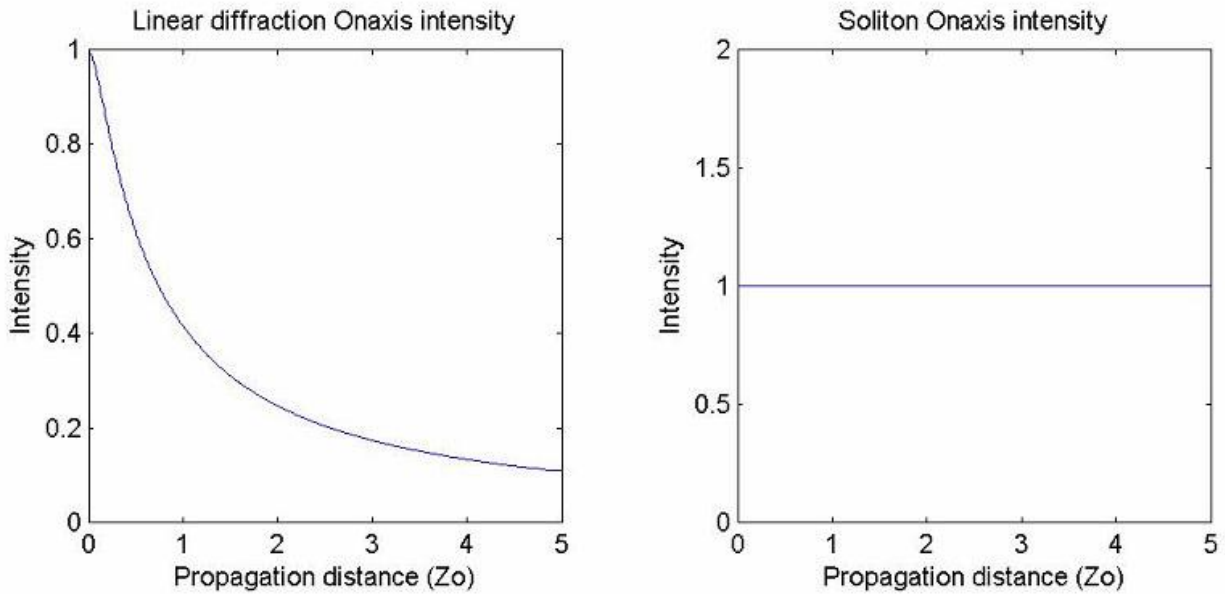


Figure 2.8: Onaxis intensity in spatial solitons

(Figure Source: Non linear fibre optics by G.P Aggarwal)

Welcome to the world of solitons! Since we now have a fully working soliton numerical algorithm, soliton interactions can be implemented with ease. Before jumping into soliton interactions, it might be worth while to analyze the importance of nonlinear phase that exactly compensates diffraction.

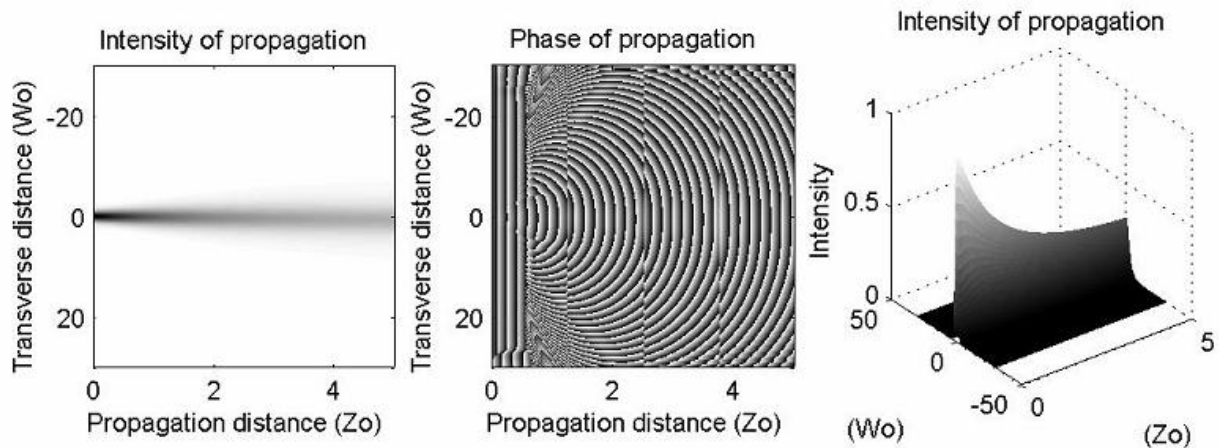


Figure 2.9: Intensity and phase propagation in spatial solitons

(Figure Source: Non linear fibre optics by G.P Aggarwal)

If the magnitude of the self focusing effect is lesser than that of diffraction, then the beam will start diffracting as it propagates (although, the diffraction will be at a much smaller rate than what would have been without self focusing). In the above simulation, the self focusing does not exactly compensate diffraction. Compare this with the first simulation, where we did not have self focusing at all. It can be immediately seen that with self focusing, the beam diffracts at a slower rate.

Now, let us consider the other case, where the magnitude of self focusing is larger than that of diffraction. Theoretically, we'd expect the beam to focus down as it propagates. In order to implement this, we slightly increase the magnitude of the nonlinear phase. The results match with theoretical predictions quite amazingly.

Consider the intensity image below. A careful look would reveal that as the beam propagates, the intensity increases and decreases as a continuous function due to "overfocusing".

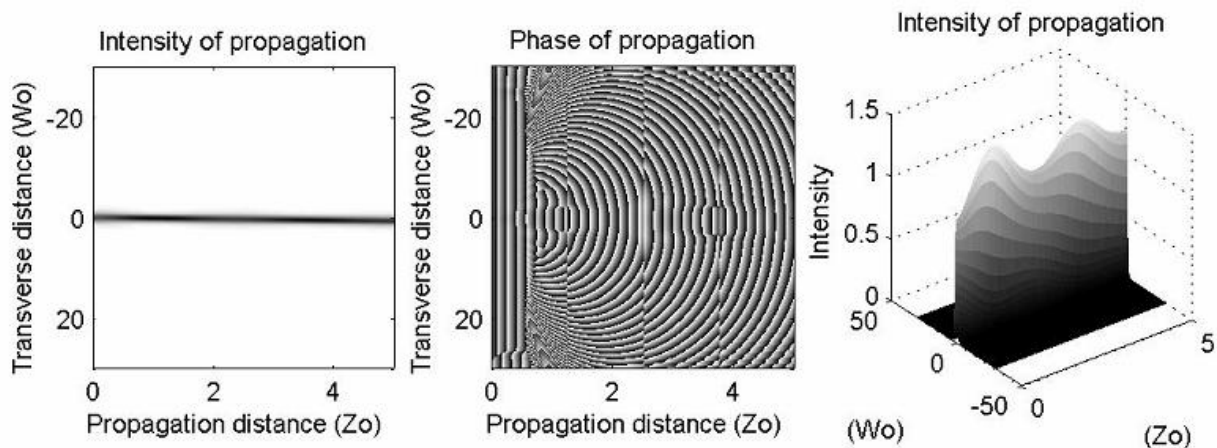


Figure 2.10: Effect of focusing on spatial solitons

(Figure Source: Non linear fibre optics by G.P Aggarwal)

The phase image is more intuitive. It clearly indicates two “focal points” within the propagation regime. The “focal points” can be identified by the transformation of a converging spherical wavefront into a plane wavefront and then to a diverging spherical wavefront. The 3D intensity image also gives this intuition. In each of the two “focal points”, the intensity is clearly higher.

It’s interesting to analyze how diffraction and self focusing try to dominate each other in this simulation. To start with, as self focusing magnitude is higher, the beam starts converging towards a focal point. Beyond the focal point, the beam diverges. Diffraction seems to facilitate this divergence until self focusing starts dominating again.

Therefore, for the creation of a soliton, self focusing should exactly (magic?) compensate diffraction.

## CHAPTER 3

### SOLITONS AND THEIR INTERACTIONS

---

This lesson demonstrates the particle-like nature of the solitons through some basic features of their interactions. The fundamental optical soliton propagates (see "Self-phase modulation and group velocity dispersion" from the Tutorials) undistorted due to the exact balance between the nonlinear (SPM) and dispersive (GVD) effects. Thus the soliton propagates as a "particle" (i.e. maintains its shape) rather than as a linear wave packet.

The particle-like nature of solitons manifests itself clearly through the interactions between neighboring solitons. Soliton pulses remain unaffected after interacting with each other. Besides, soliton interaction is phase-sensitive. In-phase solitons "attract"  $\pi$  - but out-of-phase ones repel each other. The intermediate cases (phase difference between zero and  $\pi$ ) pertain to an initial attraction followed by repulsion.

When two identical, in-phase solitons, separated in time by  $T$ , interact with each other, the time separation between them evolves periodically and the period (the collision length) given by the inverse scattering theory [55] is:

$$L_{coll} = L_D \frac{\pi \sinh \frac{T}{T_0} \cosh \frac{T}{2T_0}}{\frac{T}{T_0} + \sinh \frac{T}{T_0}}$$

In above equation,  $L_D$  is the dispersion length, and  $T_0$  is the pulse width. At 40 Gb/s, and 0.5 bit pulse width for sech pulses,  $T_0 = 7.0902 ps$ .

The dispersion length is then:

$$L_D = \frac{T_0^2}{|\beta_2|} = \frac{(7.0902)^2}{20} = 2.513 \text{ km}$$

Soliton phenomena exist on two conditions. First, there must exist stable solitary waves that travel with constant configurations (shape, speed, etc.) as long as they do not meet any external obstacles. Second, if a solitary wave meets another of its kind, they interact, but without destroying each other's identities (elastic interaction). Such solitary waves are called solitons.

The soliton phenomenon is essentially a nonlinear phenomenon. First, solitons can exist due to a delicate equilibrium between (linear) scattering (the dispersion phenomenon) and (nonlinear) convective (the shock wave phenomenon) actions. And second, the world path (the trajectory in space-time space) of a soliton suffers phase shifts caused by interactions with other solitons. The values of the phase shifts depend on the amplitudes of interaction solitons.

Soliton phenomena can certainly be observed in Nature. In order to take advantage of the existence of solitons for practical applications, it is important to learn more about the interaction process between solitons. The question "What actually happens during the interaction process of solitons?" is fundamental also from a theoretical point of view. For example, one of the most robust tests for a mathematical model to be (non-)integrable, is to study interactions of its solitary waves. If the interaction is inelastic, then the model is unlikely to be integrable.

### 3.1 Soliton Interactions

The time interval  $T_B$  between two neighboring bits or pulses determines the bit rate of a communication system as  $B = 1/T_B$ . It is thus important to determine how close two solitons can come without affecting each other. Interaction between two solitons has been studied both analytically and numerically. This section discusses the origin of mutual interaction and its affect on individual solitons.

It is clear on physical grounds that two solitons would begin to affect each other only when they are close enough that their tails overlap. Mathematically, the total field  $u = u_1 + u_2$ , where

$$u_j(\xi, \tau) = \eta_j \operatorname{sech}[\eta_j(\tau - q_j)] \exp(i\phi_j - i\delta_j\tau) \quad (3.1)$$

With  $j=1,2$ . It is  $u$  that satisfies the NLS equation, rather than  $u_1 + u_2$  individually. The first detailed study on interaction forces in solitons was done by J.P. Gordon in 1983[2]. Some notable soliton interactions are collision, attraction, repulsion, trapping, and dragging.

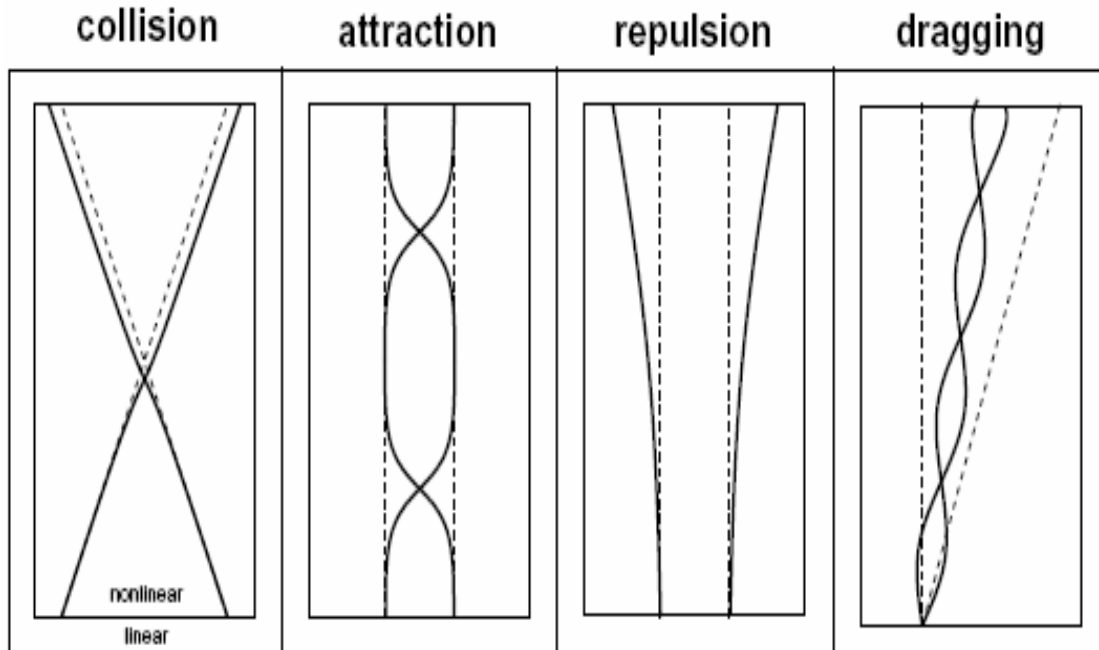


Figure 3.1: Soliton interaction pattern

(Figure Source: Non linear fibre optics by G.P Aggarwal)

Collision interaction between two similarly polarized solitons almost does nothing to the solitons, but for a very small spatial shift, as shown above. As the attractive forces between solitons are balanced both before and after the point of collision, the interaction is symmetric. However, collision interaction between two orthogonally polarized solitons can result in a permanent angle change.

When two similarly polarized solitons with same phase propagate close to each other, they attract. The attraction is periodic in the sense that the two interacting solitons swap spatial positions repeatedly at the same rate as they propagate. Other than this periodic spatial movement, the solitons remain intact. On similar lines, when two similarly polarized solitons with phase difference of  $\pi/2$  propagate close to each other, they repel.

In contrast to attraction, there is no spatial periodicity in repulsion – The two interacting solitons keep moving away from each other. Attraction and repulsion occur in orthogonally polarized solitons too.

Spatial trapping and dragging are asymmetric interactions, where two solitons overlap in the beginning of the nonlinear medium. Since there is no interaction force before overlap, and since the force after overlap is unbalanced, the interacting solitons incur a permanent angle change.

Threshold contrast is a metric to evaluate the potential for a soliton interaction to be useful in applications like logic gates. It is defined as the ratio of the power of the input fundamental signal to the power of the deviated pump that exits the aperture. Pump power, signal power, gate length, aperture size, and interaction length are few parameters that determine threshold contrast. As hinted earlier, an interaction with high threshold contrast is suitable for logic gates.

Soliton interactions can be classified as phase sensitive (same polarization) and phase insensitive interactions (orthogonal polarization).

### **3.2 Phase Sensitive Interactions**

The amount of spectral overlap between two solitons determines the phase sensitivity of an interaction. A very small spectral overlap will almost result in a phase insensitive interaction as the solitons will pass through each other with relatively large velocity. This would result in a weak interaction. On the other hand, if the spectral overlap is significant, the phase sensitive interaction is strong (useful for high contrast logic gates).

Since the interaction heavily depends on the relative phase of the two solitons, it might be experimentally difficult to control the interaction, and so, these phase sensitive interactions are

not widely used for robust logic gates [55] In a collision interaction, the spatial shift decreases with increasing angle of collision. (This is sometimes a problem, because long interaction lengths are required to achieve high contrast by using small collision).

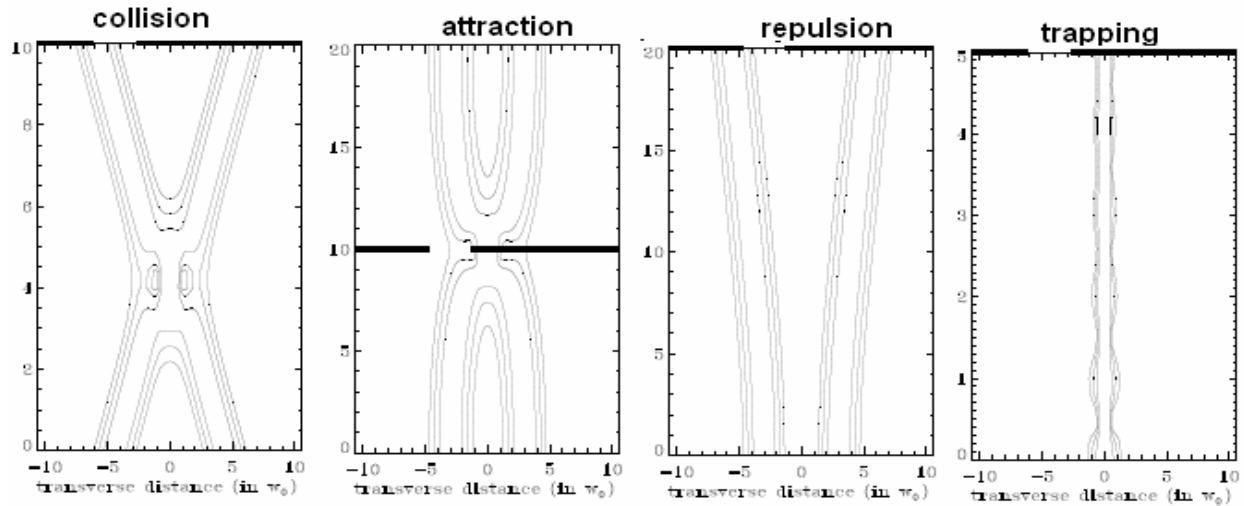


Figure 3.2: Phase sensitive interactions in solitons

(Figure Source: Non linear fibre optics by G.P Aggarwal)

Consider the phase sensitive interactions shown above. The collision interaction ( $10Z_0$ ) gives a threshold contrast of 1.5. While the attraction interaction ( $20Z_0$ ) has a threshold contrast of 4.8, the repulsion interaction ( $20Z_0$ ) gives a contrast of 5.5. Finally, the trapping interaction ( $5Z_0$ ) achieves a contrast of 11. In the collision, repulsion, and trapping interactions, the angular shift due to the interaction can be clearly seen. Note that in each of the above scenarios; had it not been for the interaction, the soliton propagating from right to left would have impinged on the region shown with a small discontinuity.

In large scale computing systems, phase dependence of an interaction might be annoying. Phase independent interactions can be achieved using orthogonally polarized solitons. For example, in a nonlinear Kerr material, phase-insensitive nonlinear cross-focusing can be used to achieve soliton interactions. In a pseudo-1D soliton interactions, the phase dependence can be completely eliminated. The phase dependence can be reduced in the case of orthogonal linear polarizations

by using waveguide birefringence to mismatch the phase dependent terms in the induced nonlinear material polarizations.

Consider the first phase insensitive collision interaction illustrated below. Here the twosolitons have equal amplitudes. The top interaction (5Zo) has a threshold contrast of 1.1while the bottom interaction (15Zo) has a threshold contrast of 23. In the second phase insensitive collision interaction, the amplitudes of the two solitons are unequal. The topinteraction (5Zo) has a threshold contrast of 9.6 and the bottom interaction has athreshold contrast greater than 1000! The attraction interaction (20Zo) between two equal amplitude solitons achieves a contrast of 9.8, while the repulsion interaction (20Zo) between unequal amplitude (3:1) solitons achieves a contrast of 69! The dragging interaction (contrast > 1000) clearly shows an angle shift due to mutual trapping.

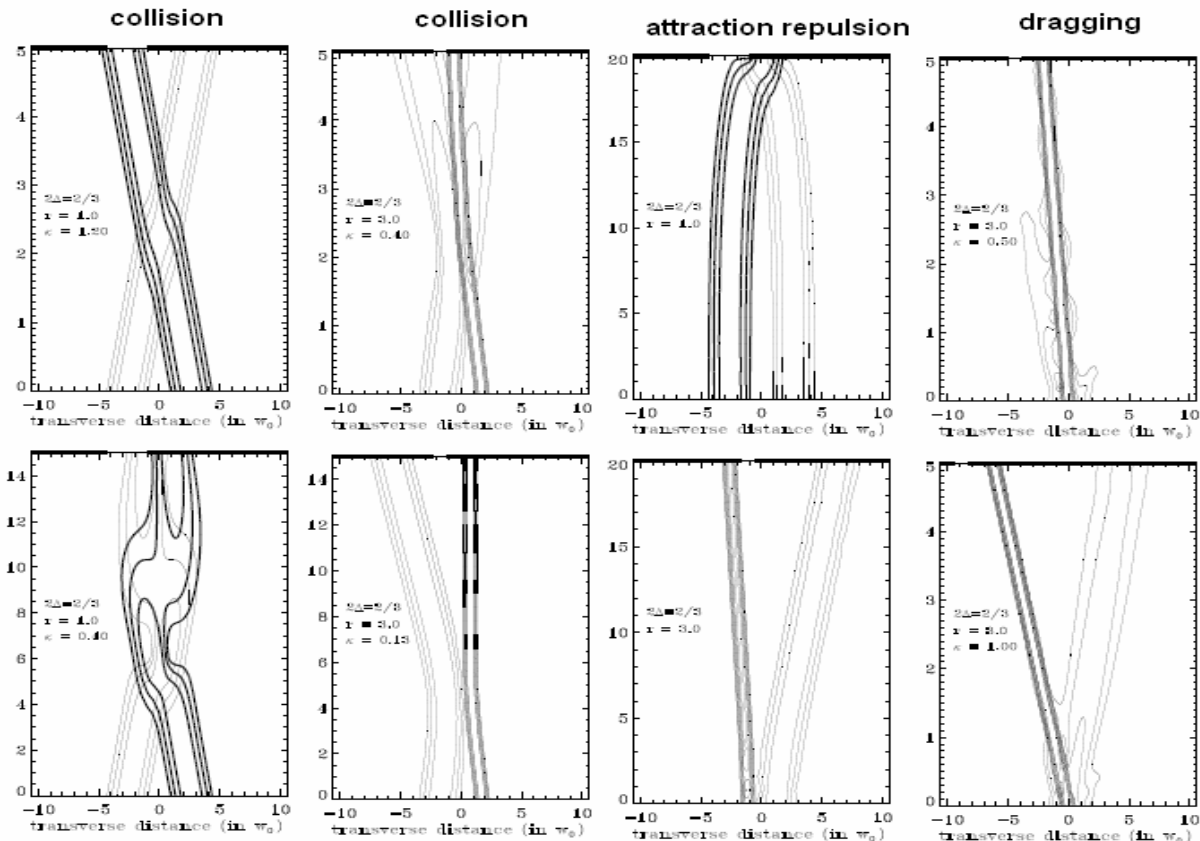


Figure 3.3: Dragging interactions in solitons

(Figure Source: Non linear fibre optics by G.P Aggarwal)

### 3.3 Soliton Collision

In this section, we will work with multiple sech fields to analyze soliton interactions. First, we'll let two sech fields to collide both in a linear medium and in the more interesting nonlinear medium (soliton collision).

We implement collision by adding equal but opposite linear phases to two such fields located close to each other.

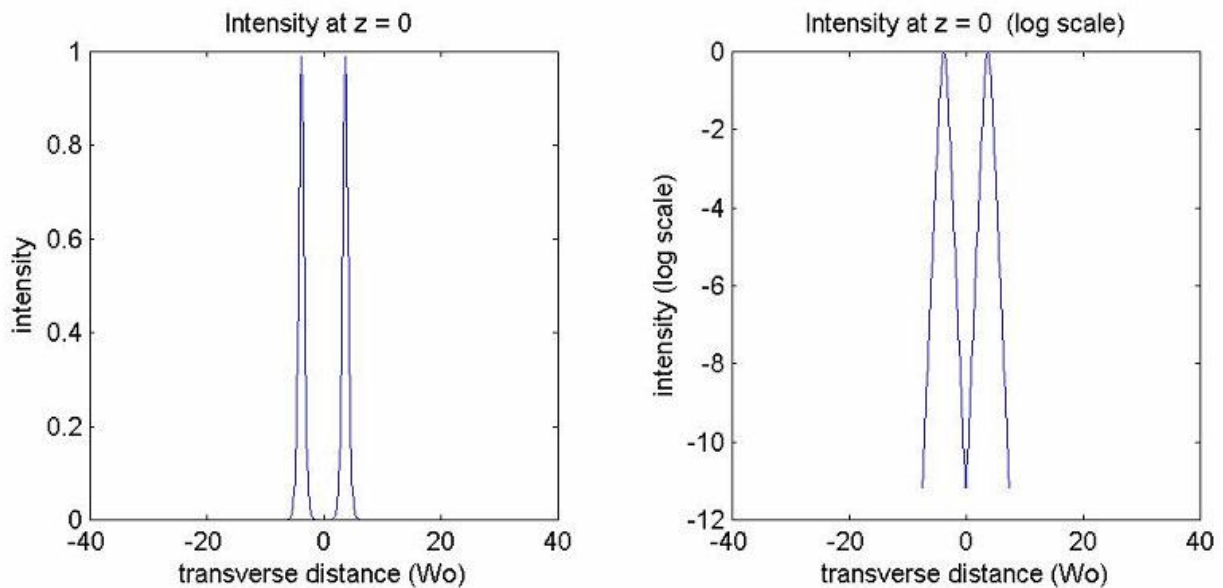


Figure 3.4: Intensity variations in solitons

(Figure Source: Non linear fibre optics by G.P Aggarwal)

Optically, it's akin to passing two sech fields through two prisms with equal but opposite slopes. An axicon with its center matched to the center of the two sech fields could be one possible lab setup.

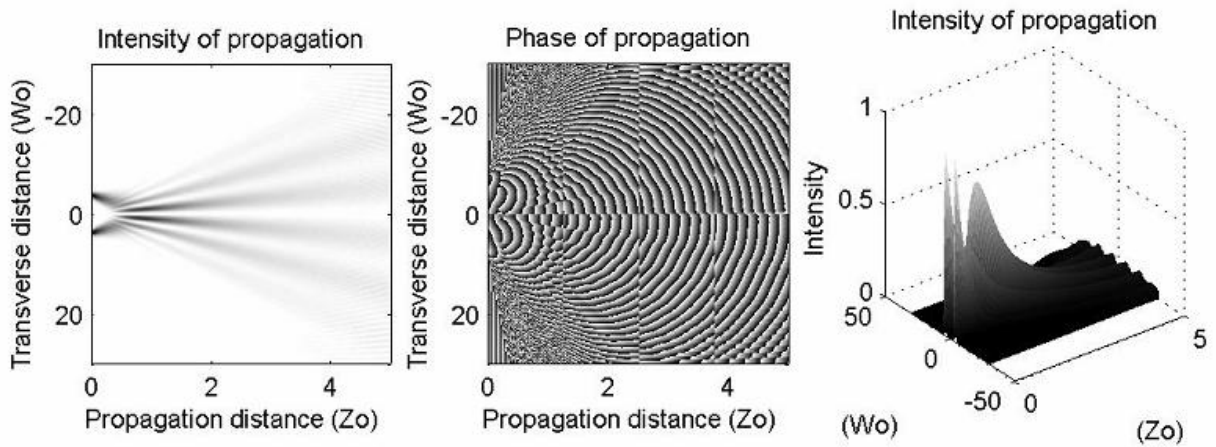


Figure 3.5: Intensity and phase propagation for soliton collision

(Figure Source: Non linear fibre optics by G.P Aggarwal)

The above simulation illustrates the “collision” of two sech beams in a linear medium. Interference fringes can be seen in the far field.

We now implement a two soliton collision. The intensity image clearly shows that the solitons remain unchanged after collision.

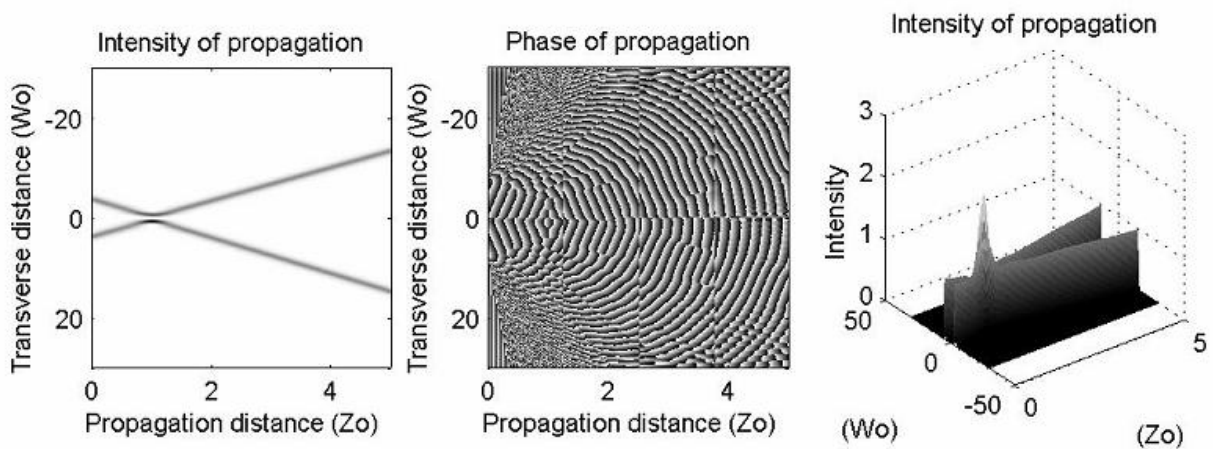


Figure 3.6: Intensity and phase propagation for soliton collision

(Figure Source: Non linear fibre optics by G.P Aggarwal)

It is interesting to see an (on axis) amplitude null exactly when the two solitons collide. The solitons seem to exactly destructively interfere in that region. Due to the on-axis null, there's an on-axis phase discontinuity in the phase plot. A careful observation of the phase plot would reveal plane wavefronts in regions of the phase image where the two solitons propagate. There's a symmetric (transverse) increase in intensity near the overlap region, which can be clearly seen in the 3D intensity plot.

### 3.4 Soliton Attraction

To implement soliton repulsion, we come in which two sech fields as before, but with nonlinear phase. In other words, the sech beams are propagating parallel to each other. The tails of the two sech beams overlap a “bit” in linear scale and a “bit more” in log scale.

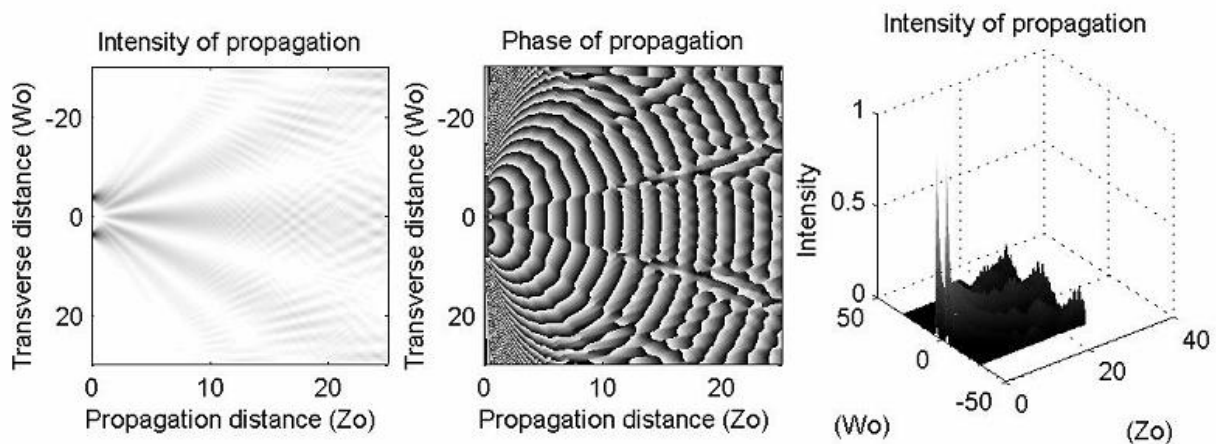


Figure 3.7: Intensity and phase propagation for soliton attraction

(Figure Source: Non linear fibre optics by G.P Aggarwal)

In the linear simulation, note that on-axis far field is bright. (constructive interference).

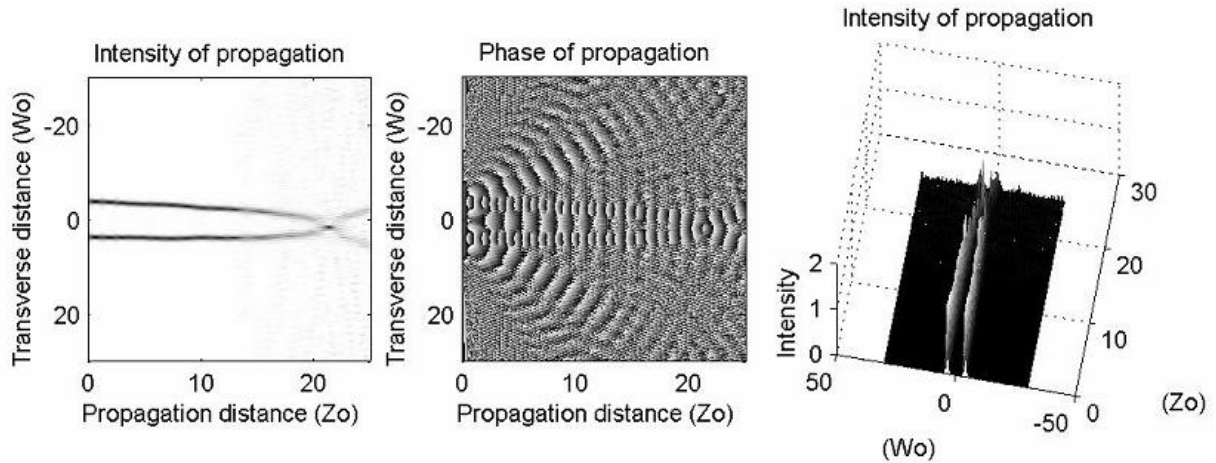


Figure 3.8: Intensity and phase propagation in solitons

(Figure Source: Non linear fibre optics by G.P Aggarwal)

The linear and nonlinear results are shown above. For observing attraction, the author had to propagate the beam through at least  $25Z_0$ . This probably could be done better if the two sech fields were located even closer. The problem with going through  $25Z_0$  is that the  $z$  samples become enormous, and in order to make the algorithm execute in a reasonable amount of time, the  $z$  sampling frequency was reduced (bad). Since nonlinear propagation numerical errors increase drastically at low sampling frequencies, the above simulation isn't all that accurate.

Specifically, the energy of the soliton seems to be decreasing as it propagates (although the locality of the field is conserved). Nevertheless, the point here is to prove that solitons do attract, and the attraction can be clearly seen at about  $20Z_0$  in all three images shown above.

### 3.5 Soliton Repulsion

Soliton repulsion is implemented by making one of the two sech fields  $\pi/2$  out of phase with respect to the other. The results are shown below.

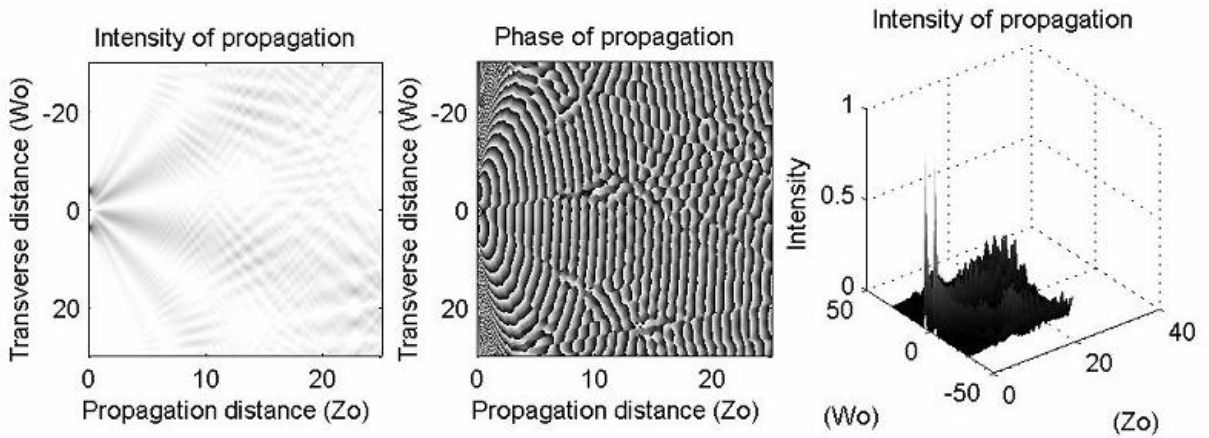


Figure 3.9: Intensity and phase propagation for soliton repulsion

(Figure Source: Non linear fibre optics by G.P Aggarwal)

In the linear simulation, note that because of the  $\pi/2$  out of phase, on axis far field is not all that bright as before. This is not destructive interference ( $\pi$  out of phase). On axis is in between constructive and destructive interference regimes.

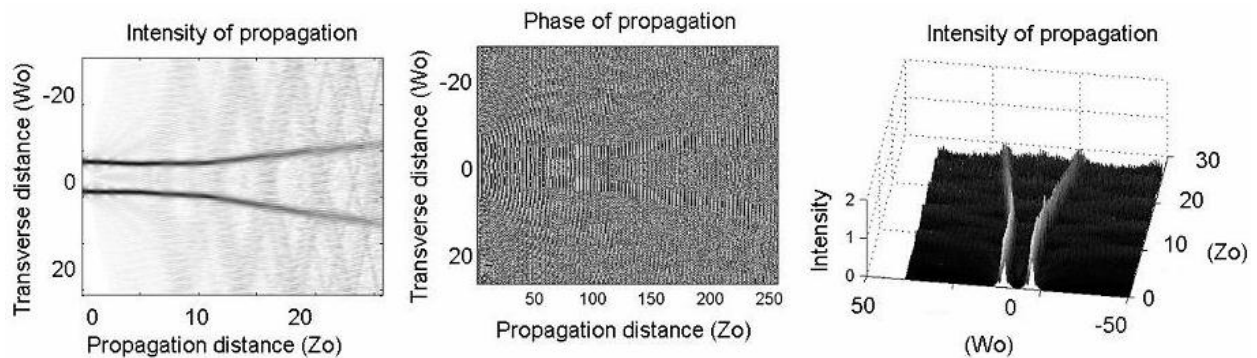


Figure 3.10: Intensity and phase propagation for soliton repulsion.

(Figure Source: Non linear fibre optics by G.P Aggarwal)

Soliton repulsion results are shown above. Clearly, the two solitons start repelling each other at about  $10Z_0$ . As explained earlier, the numerical errors are due to lack of adequate sampling in the propagation ( $z$ ) dimension [computational limitations, as we are propagation until  $25Z_0$ ].

## **Solitons in fiber Optics**

Solitons inherent stability make long –distance transmission possible, without the use of repeaters ,and could potentially double transmission capacity as well.

Optical soliton pulses through optical fiber need no introduction, because of the tremendous potentiality of soliton pulses in digital communication. Similarly the interactions of soliton pulses have also some specific applications. In this paper the authors proposes a new concept of using optical soliton-soliton interaction for switching operation in optical information processing system, where the control signals of this switches may come from a very long distance.

### **3.6 Interaction of Soliton Pulses in Long Distance Switching**

Optical soliton pulses through optical fiber need no introduction, because of the tremendous potentiality of soliton pulses in digital communication. Similarly the interactions of soliton pulses have also some specific applications. In this paper the authors proposes a new concept of using optical soliton-soliton interaction for switching operation in optical information processing system, where the control signals of this switches may come from a very long distance.

Recently optical fiber drawing technology has become so much potential that less than  $10^{-2}$  db / km loss is possible. We know also that the loss depends on the intensity of the input pulse. For lower intensity based input pulse, only the linear refractive index term contributes the loss and dispersion. Optical losses due to many other reasons in the fiber cavity play a major role in the wave propagation. For high intensity coherent pulse, both linear and non-linear refractive index will influence the optical pulse in its propagation[2-6]. In optical fiber an important non-linear effect caused by intensity dependent refractive index goes according to the following equation

$$n = n_0 + n_2 I \quad (3.2)$$

Where  $n_0$  is the linear refractive index of the core medium of the optical fiber and  $n_2$  is the non-linear correction term and I is the effective intensity. The intensity dependent refractive index

leads to the phenomenon known as self-phase modulation and it is the main reason for spectral broadening, which signifies the generation of additional frequencies. Optical pulse propagation through a linear dispersive medium undergoes temporal broadening as well as chirping at wavelength higher than the zero dispersion wavelengths, the instantaneous frequency decreases with increasing time. A pulse propagating through a non-linear non-dispersive medium undergoes no temporal broadening but undergoes only chirping.

A solitary pulse is a pulse that travels without dependence of other pulses and a soliton is the solitary wave pulse whose shape and speed are not altered by a collision. However the term “soliton” indicates in general a peculiar solitary wave whose propagation is framed by non-linear dispersive equation. Here as the non-linearity and dispersion effect balance each other to maintain the temporal and spectral profile unaltered. Such a pulse would broaden neither in the time domain (as in linear dispersion) nor in the frequency domain (as in self-phase modulation) and is called a soliton. Soliton has tremendous potentialities because it does not broaden during its journey through the fiber so it can be used in super high bandwidth and very low loss optical communication system. Thus optical soliton is very much useful in optical fiber based telecommunication system over hundreds of thousands kilometers in reality [7-10].

For a soliton propagating around a 1550 nm wavelength, the peak power  $P_t$  in the pulse (in mw) and pulse duration are related by the equation,

$$P_t \sim 1.5 \times 10^3 D / \tau_f^2 \quad (3.3)$$

Where  $D$  is the dispersion coefficient in ps/Km-nm and  $\tau_f$  is the FWHM (full width half maxima) of the pulse in picoseconds. Thus for a 10 ps soliton operating in a dispersion – shifted fiber with  $D=1$  ps/km-nm the required peak power will be approximately 15 mw. In this communication we propose a new concept of interacting soliton pulses at a long distant point in the fiber to organize logic operation there. This operation is basically controlled from several kilometers of distance from the place of operation.

## Interaction between Two Soliton Pulses

One of the main features in soliton communication system is the interaction between adjacent pulses. To overcome this problem, several effective methods have been proposed. One main factor in limiting the full utilization of bandwidth offered by soliton guided signal system is the soliton-soliton interaction. The interaction occurs due to overlapping of frequency components of either pulse. Depending on the phase difference between the soliton pulses non-linear interaction may be either destructive or constructive. These interactions alter the phases and positions of soliton pulses. While their carrier frequencies and amplitudes remains unaffected. To understand the interactions of soliton pulses, following cases should be studied must where the interaction between the soliton pulses having

- a. Equal amplitude with equal phase
- b. Equal amplitude with unequal phase
- c. Unequal amplitude with equal phase
- d. Unequal frequency with equal phase
- e. Equal frequency with unequal phase

### 3.6.1 Effect of Interaction between Two Soliton Pulses with Different Frequencies but in Same Phase

In a linear dielectric medium the electric polarization is assumed to be linear function of the electric field, that is,

$$P = \epsilon_0 \chi^{(1)} E \quad (3.4)$$

where  $\chi^{(1)}$  is the linear dielectric susceptibility,

E is the electric field and

P is the polarization.

At very high optical field intensity, if the guiding media behave as a non-linear one, then polarization is expressed as,

$$P = \epsilon_0 \chi^{(1)} E_1^{(1)} + \epsilon_0 \chi^{(2)} E_2^2 + \epsilon_0 \chi^{(3)} E_3^3 \quad (3.5)$$

For non-crystalline isotropic media, such as silica-based glass optical fiber,  $\chi^{(2)} = 0$  and lowest order non-linearity arises due to the term  $\chi^{(3)}$ . Now considering two plane optical waves propagating in z direction, the electric field variation of the waves form becomes

$$E_1 = E_0 \cos(w_1 t - kz) \quad (3.5a)$$

$$E_2 = E_0 \cos(w_2 t - kz) \quad (3.5b)$$

Therefore, using equation (3.5a) and (3.5b) in equation (3.5) we can get

$$P = \epsilon_0 \chi^{(1)} \{E_0 \cos(w_1 t - kz) + E_0 \cos(w_2 t - kz)\} + \epsilon_0 \chi^{(3)} \{E_0^3 \{\cos(w_1 t - kz) + E_0 \cos(w_2 t - kz)\}^2\} \quad (3.6)$$

Neglecting second harmonic and third harmonic generation of frequencies due to phase mismatching in optical fiber, equation (3.6) becomes,

$$P = \epsilon_0 E_0 \left\{ \chi^{(1)} + \frac{9}{4} \chi^{(3)} E_0^2 \right\} \{ \cos(w_1 t - kz) + \cos(w_2 t - kz) \} \quad (3.7)$$

Also we know that

$$E_0^2 = (I_1 + I_2)/(c \epsilon_0 n_0) \quad (3.8)$$

where  $I_1$  and  $I_2$  are intensities of the individual waves having the frequencies  $w_1$  and  $w_2$  respectively.

Using equation (3.8) in equation (3.7) we get

$$P = \epsilon_0 \left\{ \chi^{(1)} + \frac{9 \chi^{(3)} (I_1 + I_2)}{4 c \epsilon_0 n_0} \right\} E_0 \cos(w_1 t - kz) + \epsilon_0 \left\{ \chi^{(1)} + \frac{9 \chi^{(3)} (I_1 + I_2)}{4 c \epsilon_0 n_0} \right\} E_0 \cos(w_2 t - kz) \quad (3.9a)$$

$$= P_1 + P_2 \quad (3.9b)$$

where

$$P_1 = \epsilon_0 \left\{ \chi^{(1)} + \frac{9 \chi^{(3)} (I_1 + I_2)}{4 c \epsilon_0 n_0} \right\} E_0 \cos(w_1 t - kz) \quad (3.9c)$$

$$\text{and } P_2 = \epsilon_0 \left\{ \chi^{(1)} + \frac{9 \chi^{(3)} (I_1 + I_2)}{4 c \epsilon_0 n_0} \right\} E_0 \cos(w_2 t - kz) \quad (3.9d)$$

We know general relationship between polarization and refractive index as

$$P = \epsilon_0 (n_i^2 - 1) E_0 \cos(w_1 t - kz) + \epsilon_0 (n_i^2 - 1) E_0 \cos(w_2 t - kz) \quad (3.10)$$

Now comparing equation (3.9a) with equation (3.10) we get,

$$n_i^2 = 1 + \chi^{(1)} + \frac{9\chi^{(3)}(I_1+I_2)}{4c\epsilon_0 n_0} \quad (3.11)$$

or,

$$n_i = \{1 + \chi^{(1)}\}^{\frac{1}{2}} + \frac{9\chi^{(3)}(I_1+I_2)}{8(c\epsilon_0 n_0^2)} \quad (3.12)$$

Therefore refractive index

$$.n=n_i = \{1 + \chi^{(1)}\}^{\frac{1}{2}} + \frac{9\chi^{(3)}(I_1+I_2)}{8(c\epsilon_0 n_0^2)} \quad (3.13)$$

$$=n_0 + n_2(I_1+I_2) \quad (3.14)$$

Where linear refractive index,

$$n_0 = \{1 + \chi^{(1)}\}^{\frac{1}{2}} \quad (3.15a)$$

And non linear correction term

$$n_2 = \frac{9\chi^{(3)}}{8(c\epsilon_0 n_0^2)} \quad (3.15b)$$

Here it can be found that refractive index increases after interaction between two such soliton pulses.

### 3.6.2 Effect of Interaction Among Three Soliton Pulses with Different Frequencies but in Same Phase

Now we consider three plane optical waves propagating in z-direction and their electric field variation of the form of,

$$E = E_0 \cos(\omega_1 t - kz) \quad (3.16a)$$

$$E = E_0 \cos(\omega_2 t - kz) \quad (3.16b)$$

$$E = E_0 \cos(\omega_3 t - kz) \quad (3.16c)$$

Therefore polarization of equation (3.6) becomes

$$P = \epsilon_0 \chi^{(1)} E_0 \{\cos(\omega_1 t - kz) + \cos(\omega_2 t - kz) + \cos(\omega_3 t - kz)\} + \chi^{(3)} E_0^3 \{\cos(\omega_1 t - kz) + \cos(\omega_2 t - kz) + \cos(\omega_3 t - kz)\} \quad (3.17)$$

due to phase mismatching other than the frequencies  $\omega_1, \omega_2$  &  $\omega_3$  are to be neglected and the integrated polarization at the place where the interactions happening, the equation (18) can be written as,

$$P = \epsilon_0 E_0 \left\{ \chi^{(1)} + \frac{15}{4} \chi^{(3)} E_0^2 \right\} \{\cos(\omega_1 t - kz) + \epsilon_0 E_0 \left\{ \chi^{(1)} + \frac{15}{4} \chi^{(3)} E_0^2 \right\} \{\cos(\omega_2 t - kz) + \epsilon_0 E_0 \left\{ \chi^{(1)} + \frac{15}{4} \chi^{(3)} E_0^2 \right\} \{\cos(\omega_3 t - kz)\}\} \quad (3.18)$$

Also we can write equation (3.8) as,

$$E_0^2 = \frac{2}{3} (I_1 + I_2 + I_3) / (c \epsilon_0 n_0) \quad (3.19)$$

Where  $I_1, I_2$  and  $I_3$  are the intensities of the individual waves having the frequencies  $\omega_1, \omega_2$  and  $\omega_3$  respectively.

Now using equation (3.19) in equation (3.18) we get

$$P = \epsilon_0 E_0 \left\{ \chi^{(1)} + \frac{5 \chi^{(3)} (I_1 + I_2 + I_3)}{2 c \epsilon_0 n_0} \right\} \cos(w_1 t - kz) + \epsilon_0 E_0 \left\{ \chi^{(1)} + \frac{5 \chi^{(3)} (I_1 + I_2 + I_3)}{2 c \epsilon_0 n_0} \right\} \cos(w_2 t - kz) + \epsilon_0 E_0 \left\{ \chi^{(1)} + \frac{5 \chi^{(3)} (I_1 + I_2 + I_3)}{2 c \epsilon_0 n_0} \right\} \cos(w_3 t - kz) \quad (3.20a)$$

$$\text{Or, } P = P_1 + P_2 + P_3 \quad (3.20b)$$

where,

$$P_1 = \epsilon_0 E_0 \left\{ \chi^{(1)} + \frac{5 \chi^{(3)} (I_1 + I_2 + I_3)}{2 c \epsilon_0 n_0} \right\} \cos(w_1 t - kz) \quad (3.20c)$$

$$P_2 = \epsilon_0 E_0 \left\{ \chi^{(1)} + \frac{5 \chi^{(3)} (I_1 + I_2 + I_3)}{2 c \epsilon_0 n_0} \right\} \cos(w_2 t - kz) \quad (3.20d)$$

$$P_3 = \epsilon_0 E_0 \left\{ \chi^{(1)} + \frac{5 \chi^{(3)} (I_1 + I_2 + I_3)}{2 c \epsilon_0 n_0} \right\} \cos(w_3 t - kz) \quad (3.20e)$$

We can rewrite equation (3.10) as the form of

$$P = \epsilon_0 (n_i^2 - 1) E_0 \cos(w_1 t - kz) + \epsilon_0 (n_i^2 - 1) E_0 \cos(w_2 t - kz) + \epsilon_0 (n_i^2 - 1) E_0 \cos(w_3 t - kz) \quad (3.21)$$

Now comparing equation (22) with equation (21a) one may get,

$$n_i^2 = 1 + \chi^{(1)} + \frac{5 \chi^{(3)} (I_1 + I_2 + I_3)}{2 c \epsilon_0 n_0} \quad (3.22)$$

Or,

$$n_i = \{1 + \chi^{(1)}\}^{\frac{1}{2}} + \frac{5 \chi^{(3)}(I_1 + I_2 + I_3)}{4 (c\epsilon_0 n_0^2)} \quad (3.23)$$

$$n = n_i = n_0 + n_2(I_1 + I_2 + I_3) \quad (3.24)$$

Here non-linear correction term becomes

$$n_2 = \frac{5 \chi^{(3)}}{4 (c\epsilon_0 n_0^2)} \quad (3.25)$$

Here also the refractive index of the media increases with increasing intensity (that is with the number of increasing interacting soliton pulses having same phase).

## CHAPTER 4

# OPTISYSTEM SIMULATION RESULTS

---

Optical communication systems are becoming increasingly complex. The design and analysis of these systems, which normally involves multiple signal channels, different topologies, nonlinear devices, and non-Gaussian noise sources, is highly complex and labor-intensive. Advanced software tools make the design and analysis of these systems quick and efficient.

OptiSystem is an innovative optical communication system simulation package for the design, testing, and optimization of virtually any type of optical link in the physical layer of a broad spectrum of optical networks, from long-haul systems to LANs and MANs. A system level simulator based on the realistic modeling of fiber-optic communication systems, OptiSystem possesses a powerful new simulation environment and a truly hierarchical definition of components and systems. Its capabilities can be easily expanded with the addition of user components and seamless interfaces to a range of widely used tools.

A comprehensive Graphical User Interface controls the optical component layout, component models, and presentation graphics. An extensive library of active and passive components includes realistic, wavelength-dependent parameters. Parameter sweeps and optimizations allow you to investigate the effect of particular device specifications on system performance. Created to address the needs of system integrators, optical telecom engineers, research scientists, and academia, OptiSystem satisfies the demand of the booming photonics market for a powerful yet easy to use optical system design tool.

### **Benefits of Using Optiwave System Simulation Software**

- Dramatic reduction of investment risk and time-to-market
- Rapid, low-cost prototyping
- Global insight into system performance
- Assessment of parameter sensitivities aiding design tolerance specifications
- Direct visual presentation of design options and scenarios to prospective customers
- Straightforward access to extensive sets of system characterization data
- Automatic parameter sweeping and optimization
- Dispersion map design
- Estimation of BER and system penalties with different receiver models
- Amplified System BER and link budget calculations.

This section contains the following advanced and illustrative simulation projects.

- Fundamental and higher order solitons.
- Interactions of optical solitons.
- Decay of higher order solitons in the presence of third-order dispersion.
- Stability of solitons in birefringent optical fibers.
- SOA as in-line amplifier in soliton communication systems.
- Decay of higher order solitons in the presence of intrapulse Raman scattering.
- Decay of higher order solitons in the presence of self-steepening.

## 4.1 Fundamental and Higher Order Solitons

This lesson demonstrates that the exact balance between the effects of SPM and GVD leads to the formation of a fundamental soliton - a light pulse that propagates without changing its shape and spectrum, and shows some basic features of the higher-order solitons.

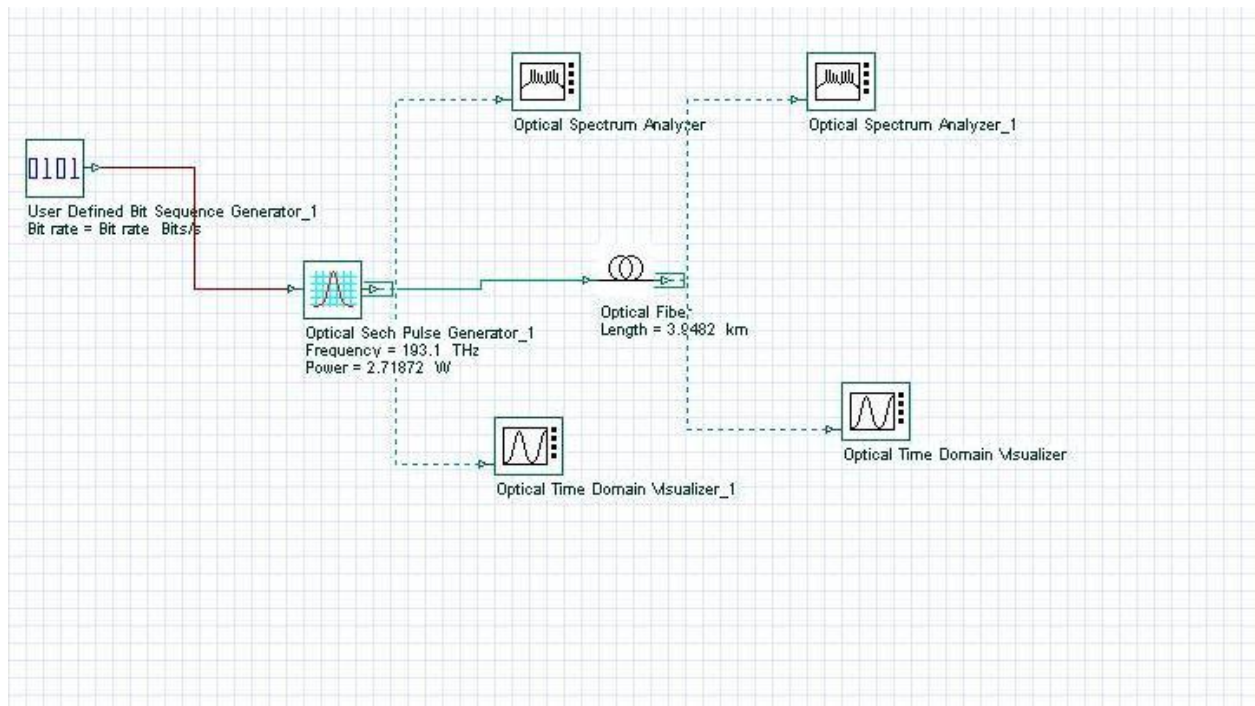


Figure 4.1.1: System Layout

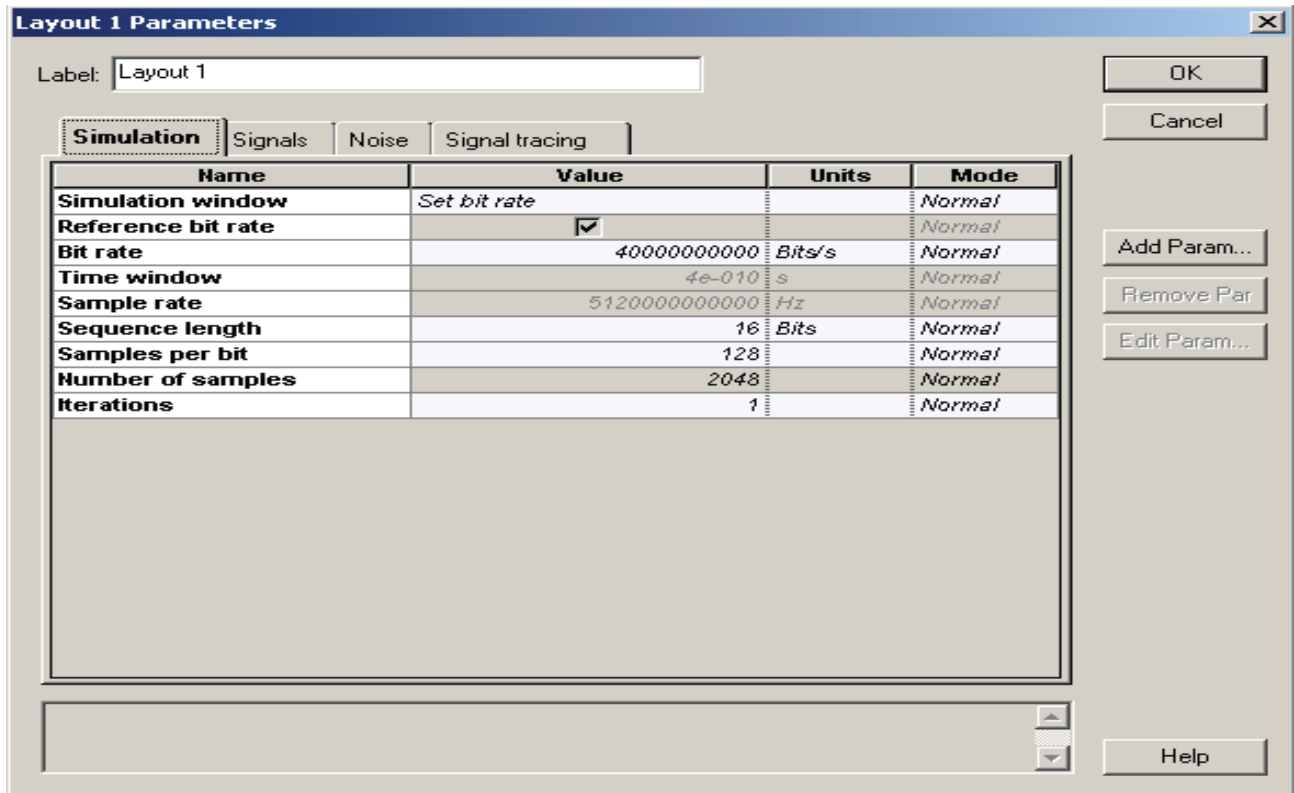


Figure 4.1.2: System Parameters

The compensation between the effects of SPM and GVD is not complete for Gaussian pulses since the SPM induced chirp is different from that induced by the GVD. The exact compensation occurs when the pulse shape is that of a fundamental soliton.

## Input Pulses Shapes

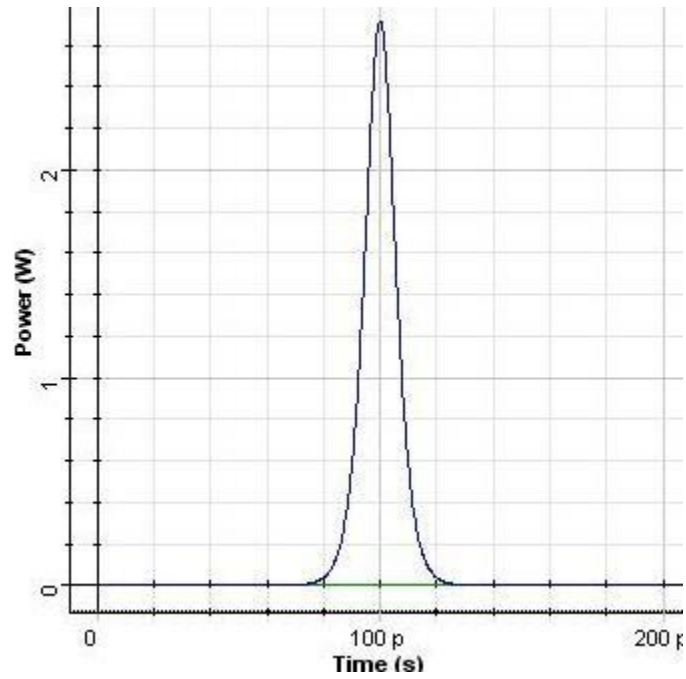


Figure 4.1.3: Input pulse shape(optical time domain visualize)

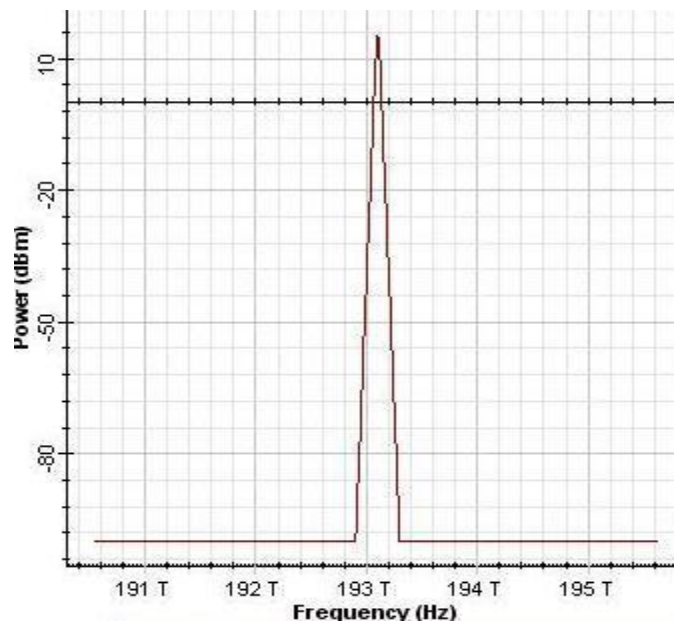


Figure 4.1.4: Input pulse shape (optical spectrum analyzer)

**Output Pulse Shapes corresponding to the fundamental (N=1) soliton over one soliton period.**

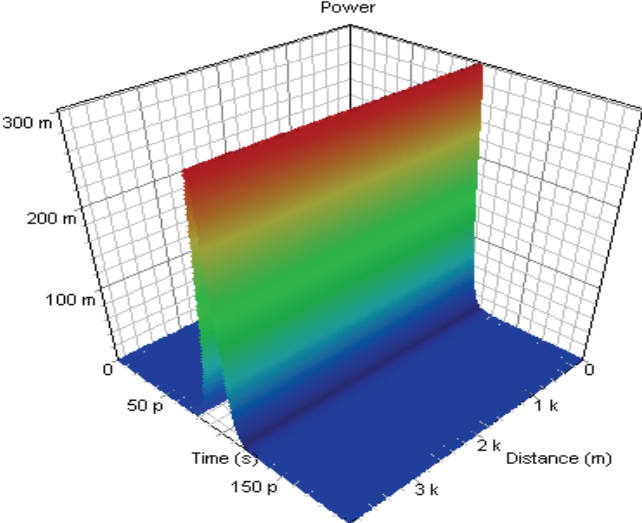


Figure 4.1.5: Output pulse shape(optical time domain visualize)

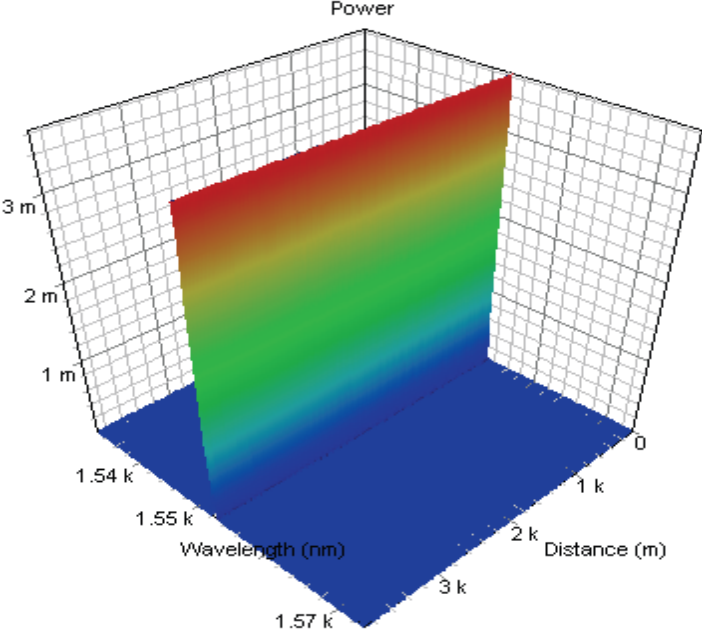


Figure 4.1.6: Output pulse shape (optical spectrum analyzer)

**Output Pulse Shapes Corresponding to the Fundamental (N=1) Soliton over One Soliton Period.**

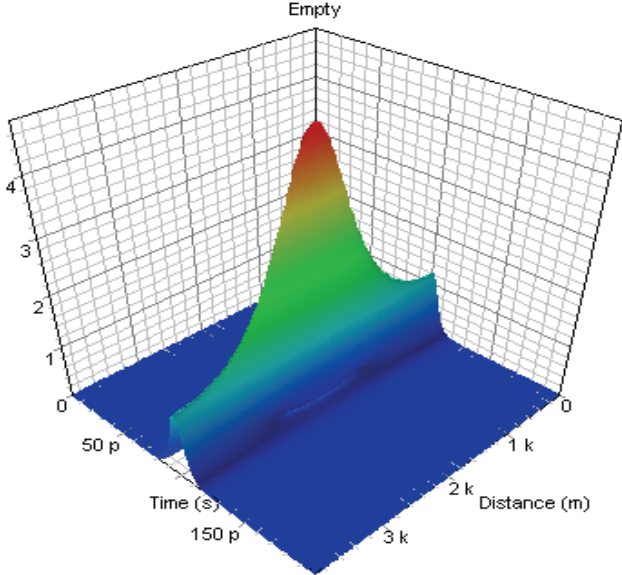


Figure 4.1.6: Output pulse shape(optical time domain visualize)

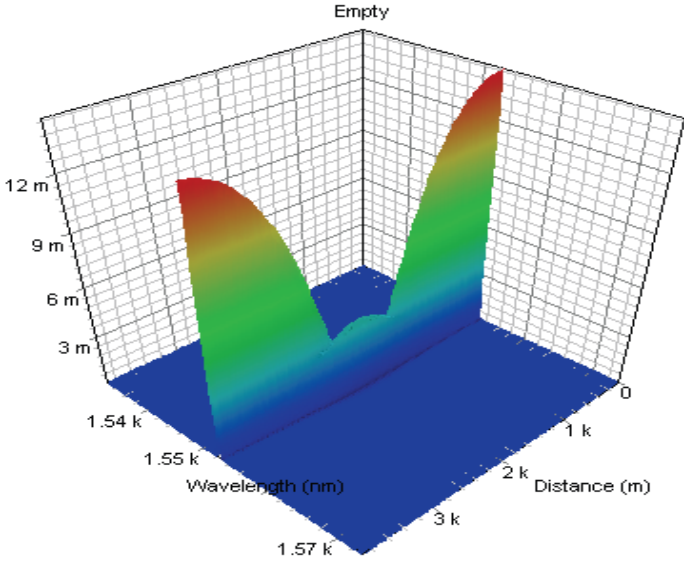


Figure 4.1.7: Output pulse shape (optical spectrum analyzer)

## 4.2 Interaction of Optical Solitons

This lesson demonstrates the particle-like nature of the solitons through some basic features of their interactions. The fundamental optical soliton propagates (see "Self-phase modulation and group velocity dispersion" from the Tutorials) undistorted due to the exact balance between the nonlinear (SPM) and dispersive (GVD) effects. Thus the soliton propagates as a "particle" (i.e. maintains its shape) rather than as a linear wave packet.

The particle-like nature of solitons manifests itself clearly through the interactions between neighboring solitons. Soliton pulses remain unaffected after interacting with each other. Besides, soliton interaction is phase-sensitive. In-phase solitons "attract"  $\pi$  - but out-of-phase ones repel each other. The intermediate cases (phase difference between zero and  $\pi$ ) pertain to an initial attraction followed by repulsion.

When two identical, in-phase solitons, separated in time by  $T$ , interact with each other, the time separation between them evolves periodically and the period (the collision length) given by the inverse scattering theory [55] is:

$$L_{coll} = L_D \frac{\pi \sinh \frac{T}{T_0} \cosh \frac{T}{2T_0}}{\frac{T}{T_0} + \sinh \frac{T}{T_0}} \quad (4.2.1)$$

In equation 4.2.1,  $L_D$  is the dispersion length, and  $T_0$  is the pulse width. At 40 Gb/s, and 0.5 bit pulse width for sech pulses,  $T_0 = 7.0902 ps$ .

The dispersion length is then:

$$L_D = \frac{T_0^2}{|\beta_2|} = \frac{(7.0902)^2}{20} = 2.513 km \quad (4.2.2)$$

With time separation of 75 ps chosen here from Equation 1, we see that the collision length is  $L_{coll} \approx 782 \text{ km}$ . To demonstrate the periodic behavior of soliton interactions we create the following layout.

### 4.2.1 Interaction between Identical, In-Phase Solitons

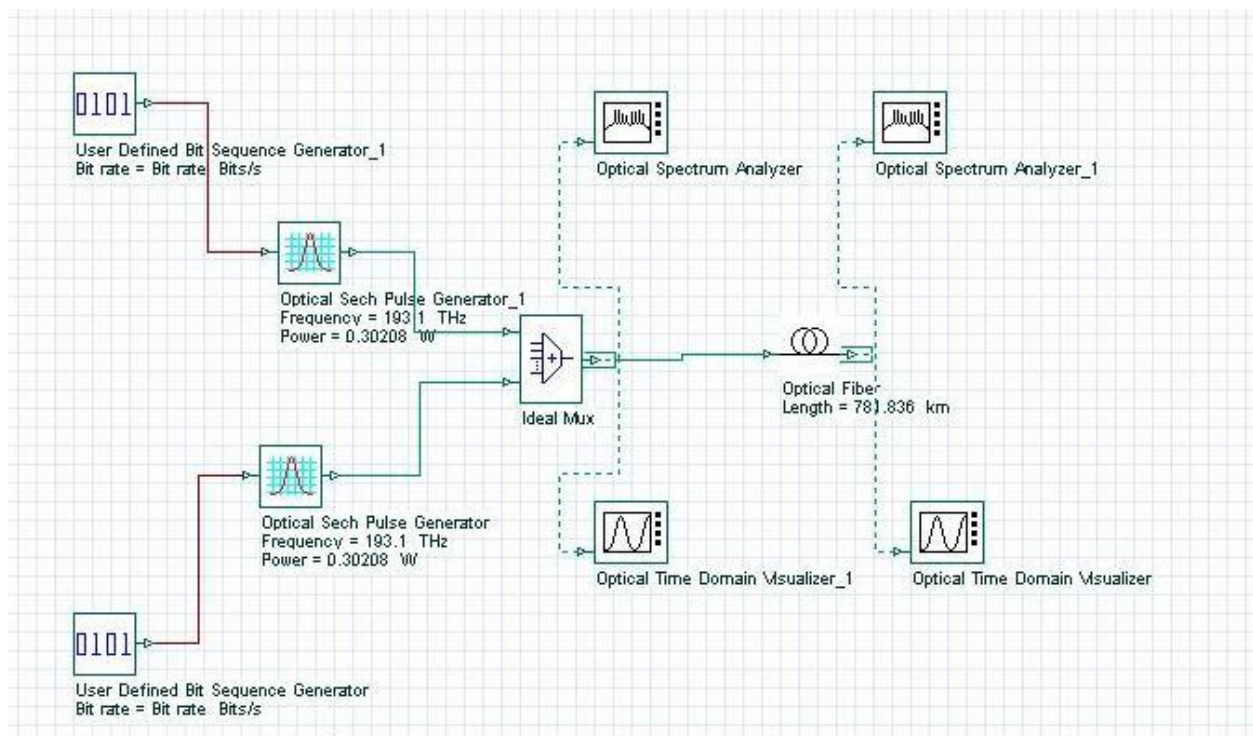


Figure 4.2.1: System Layout

**Sequence Generator/CW Laser:** It is commonly used as optical source.

**Pulse Generator:** It is commonly used to convert the sequence generated sequence into pulse.

**Optical Spectrum Analyzer:** It is used to show where the highest energy of the signal exists, i.e. fundamental frequency region.

**Optical Time Domain Visualizer:** A scope to visualize electrical signals in time domain. When you connect a visualizer to a component output port, OptiSystem inserts a default data monitor to the component output port. You can then connect the component to the visualizer. Visualizers always connect to monitors. You can have multiple visualizers attached to the same component output port, because they are actually attached to the monitor, not to the component. Data monitors are represented by a rectangle around the component output port.

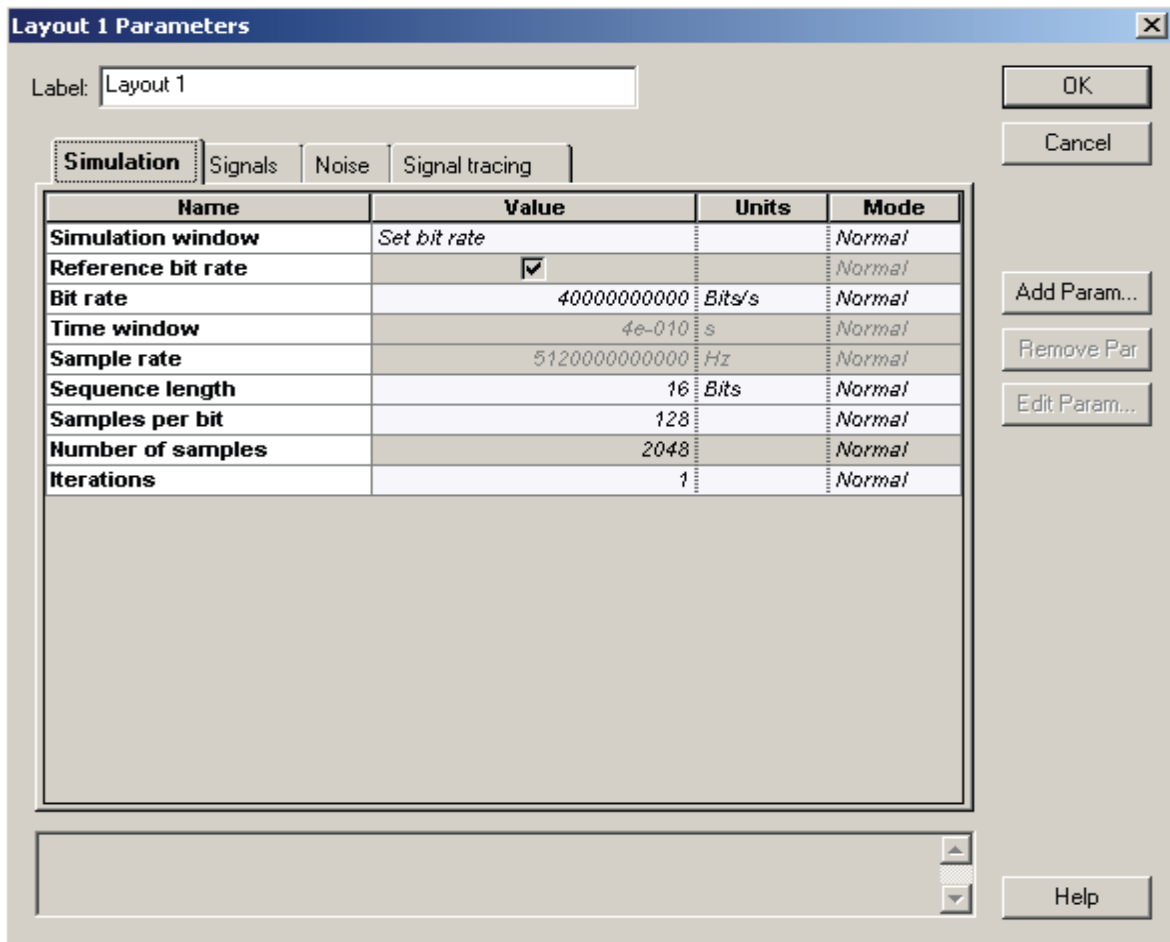


Figure 4.2.2: Layout Parameters

To achieve the necessary accuracy we use the iterative implementation of the split-step Fourier method.

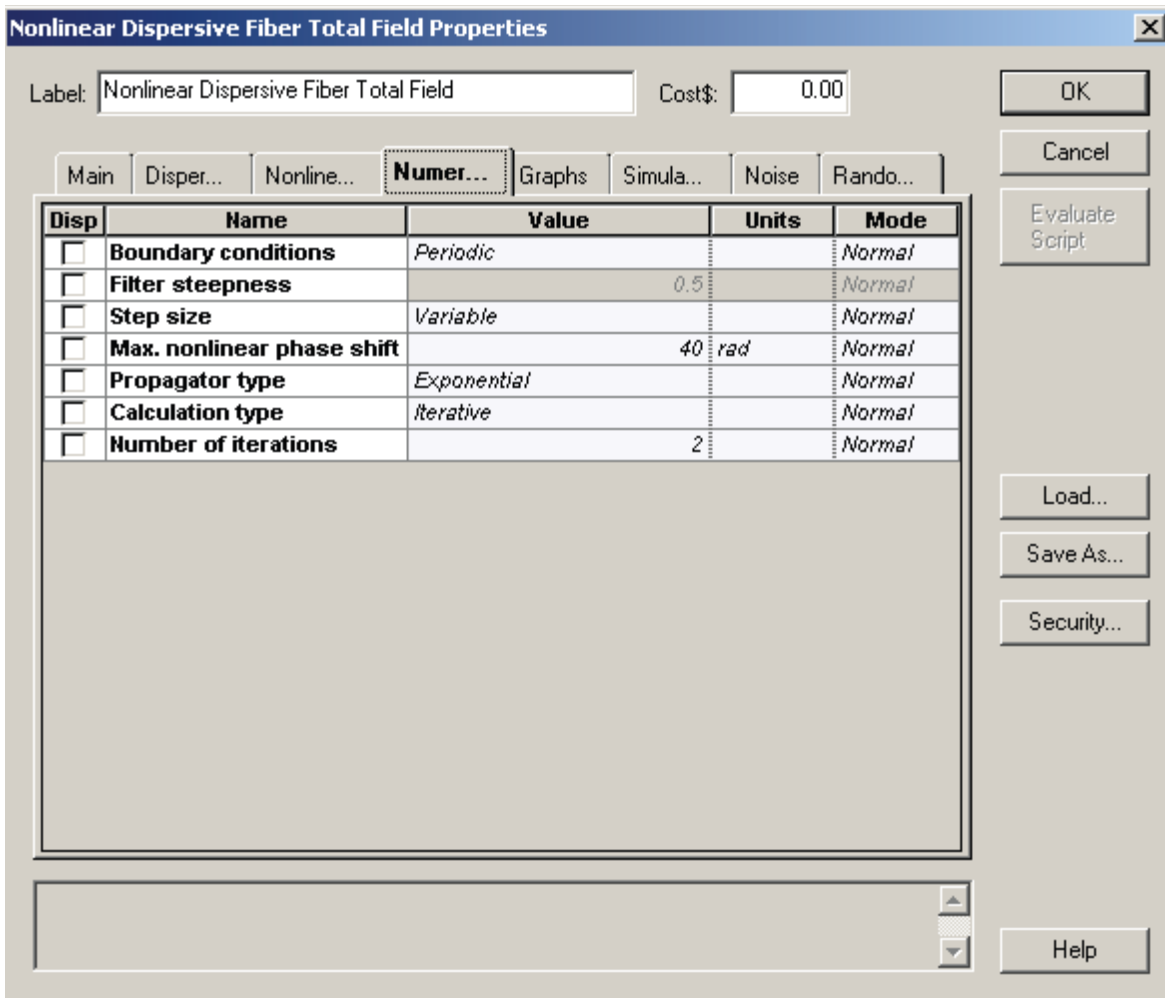


Figure 4.2.3: Iterative implementation of the split-step Fourier method

At first we consider interaction between two identical in-phase solitons. In this case they form a bound pair. Figure 4 shows the evolutions of the soliton pair separated initially by 75 ps within one collision length (782 km in this case). The solitons attract each other and become superimposed at a distance equal to half the collision length. Then at a distance equal to the collision length, the initial configuration is restored completely (the pulses are again separated by 75 ps in time).

This picture repeats itself with further propagation with the initial configuration being restored at fiber length equal to multiples of the collision length.

# Pulse Shapes for Interaction between Identical, In-Phase Solitons within One Collision Length.

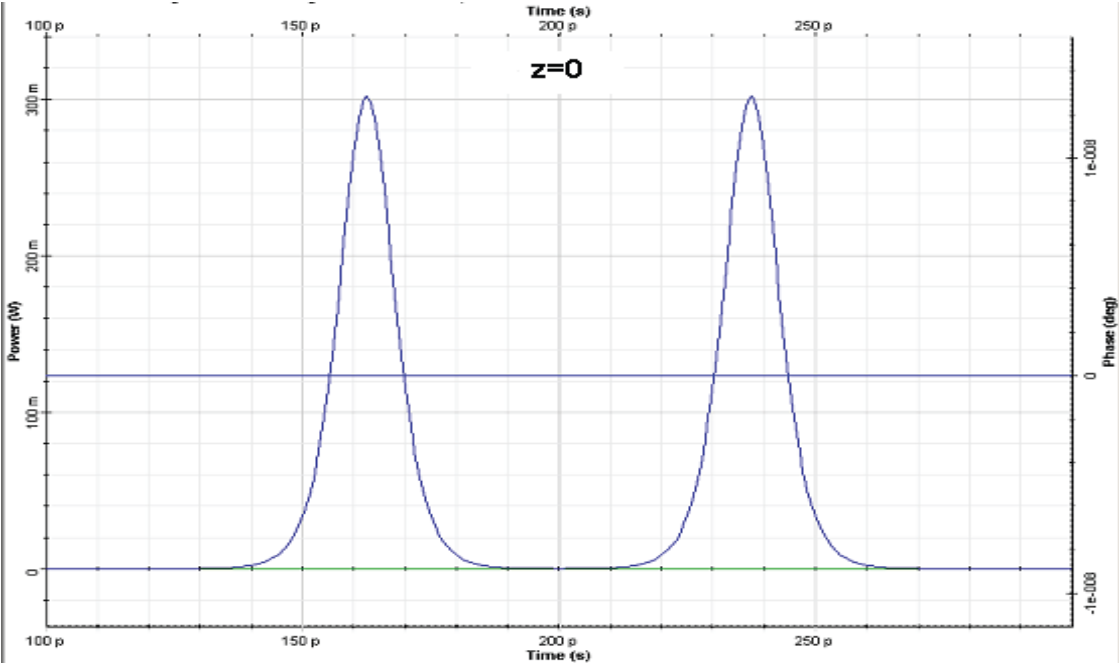


Figure 4.2.4: Pulse shape(optical time domain visualizer)

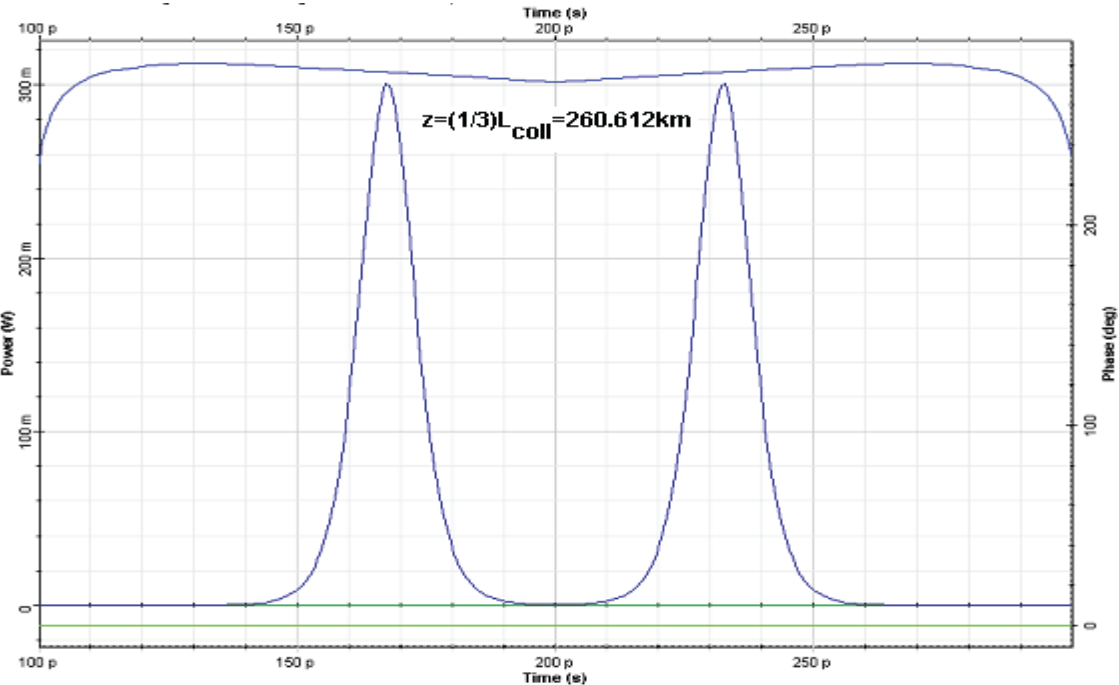


Figure 4.2.5: Input pulse shape(optical time domain visualize)

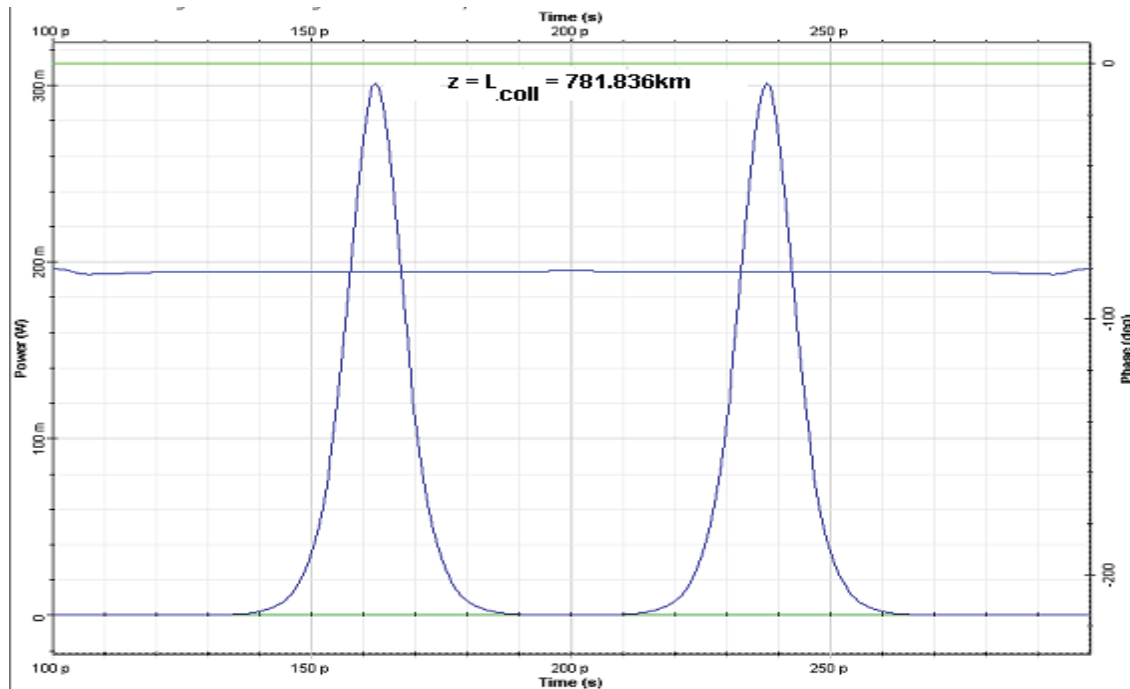


Figure 4.2.6: Input pulse shape(optical time domain visualizer)

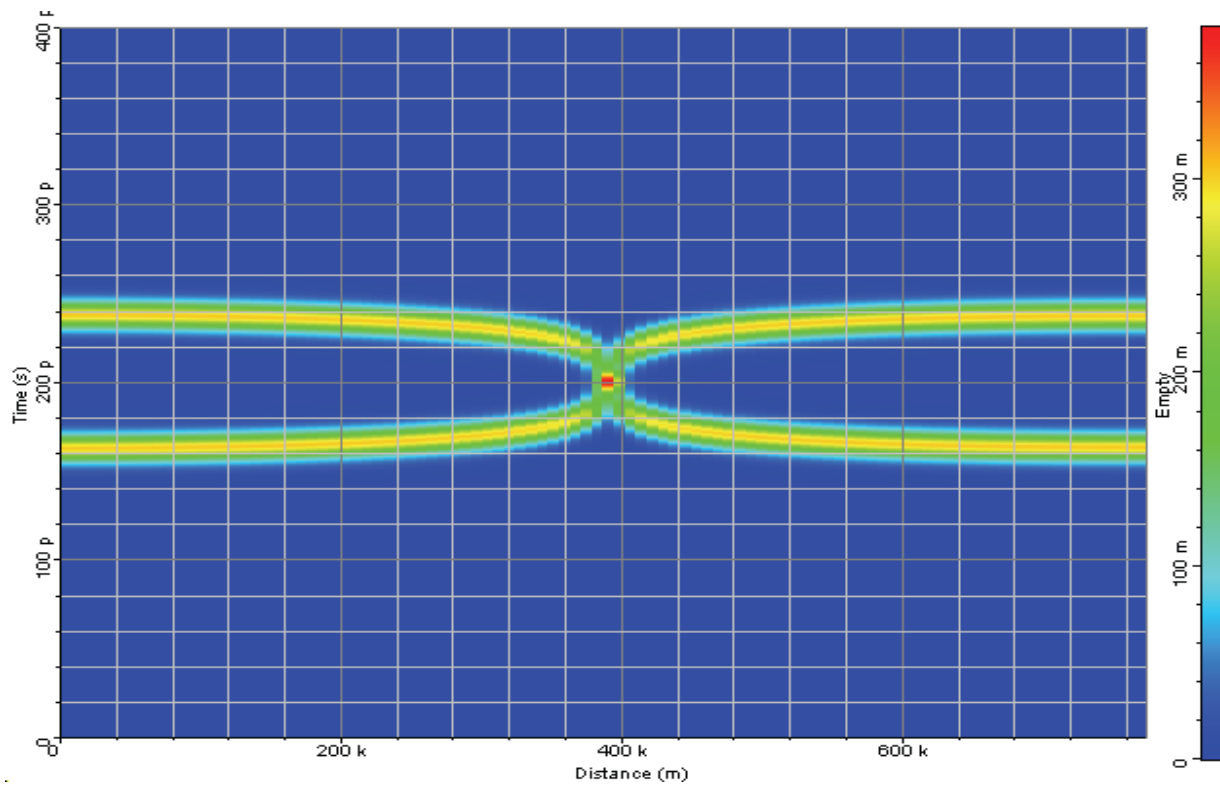


Figure 4.2.7: Interaction between identical, in-phase solitons within one collision length.

(Figure Source:G. P. Agrawal Nonlinear Fiber Optics, Academic Press (2001).)

## 4.2.2 Interaction between Identical, $\pi$ -out of Phase Solitons within one Collision Length. Repulsion is Evident.

The second case we consider is an interaction of an  $\pi$  out-of-phase soliton pair. In this case the time separation  $T_z$  after propagation in a fiber with length equal to can be obtained by treating the interaction as a perturbation, an assumption that is valid in the case of weak overlap between the neighboring solitons [55]. The result is:

$$T_z = T(z = 0) + 2T_0 \ln \left( \cosh \left( \frac{2z}{L_D} \exp \left( -\frac{T(z=0)}{2T_0} \right) \right) \right) \quad (4.2.3)$$

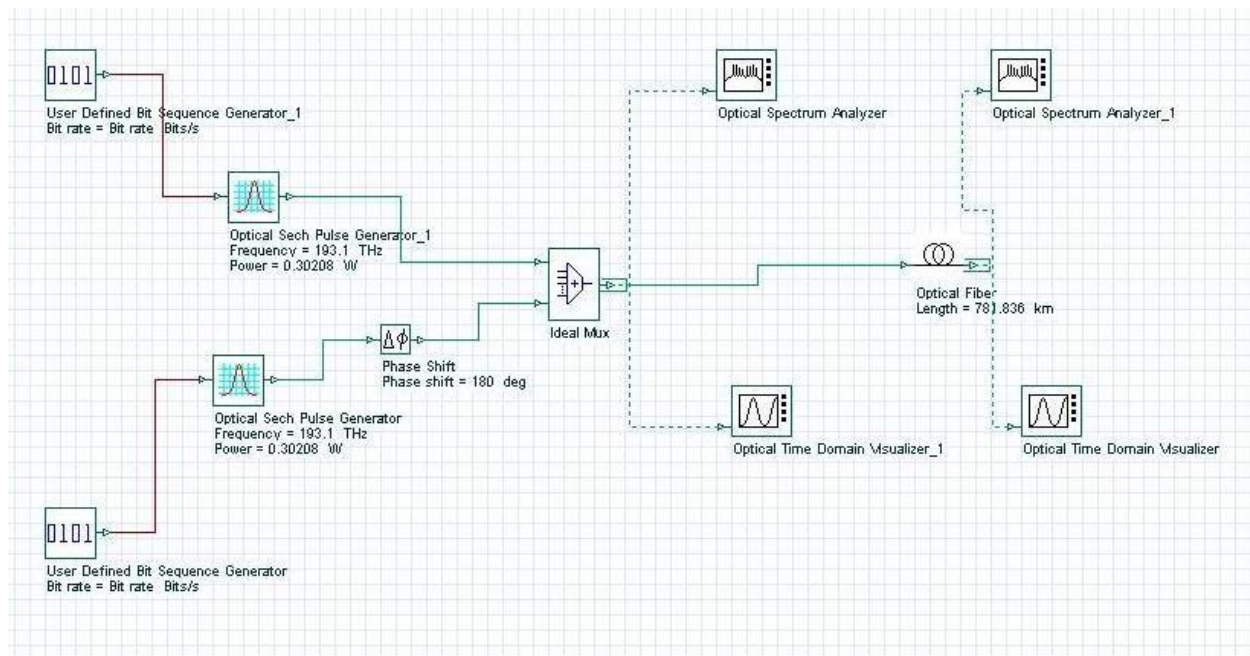


Figure 4.2.8: System Layout

## Pulse shapes:

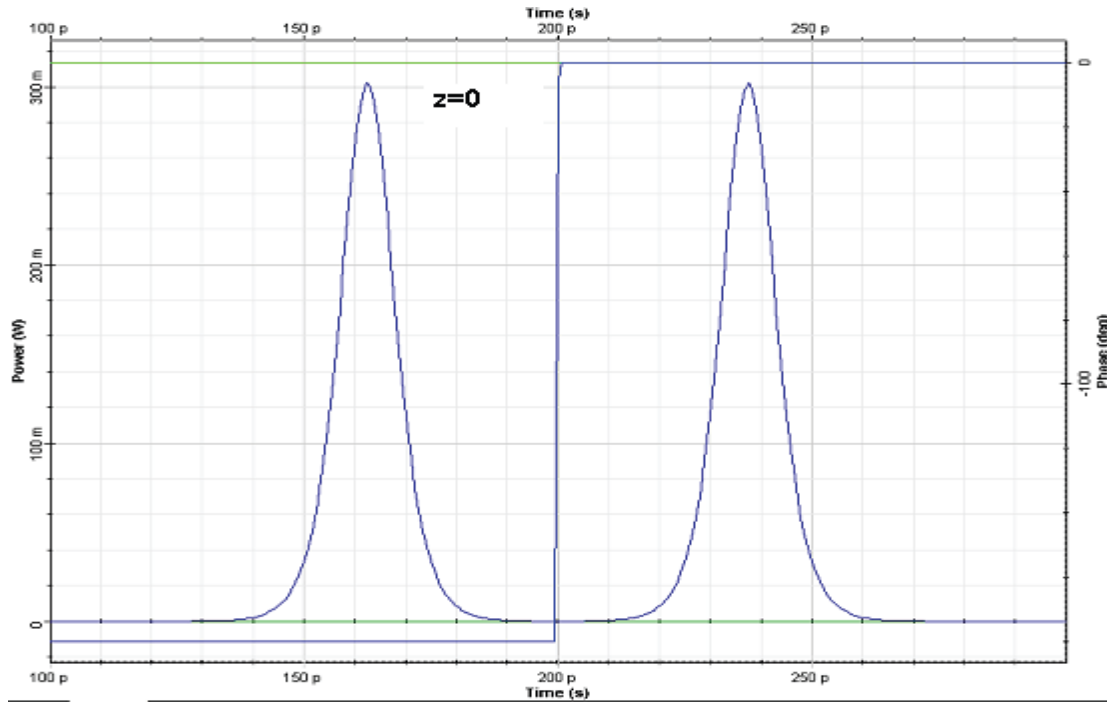


Figure 4.2.9: Input pulse shape(optical time domain visualize)

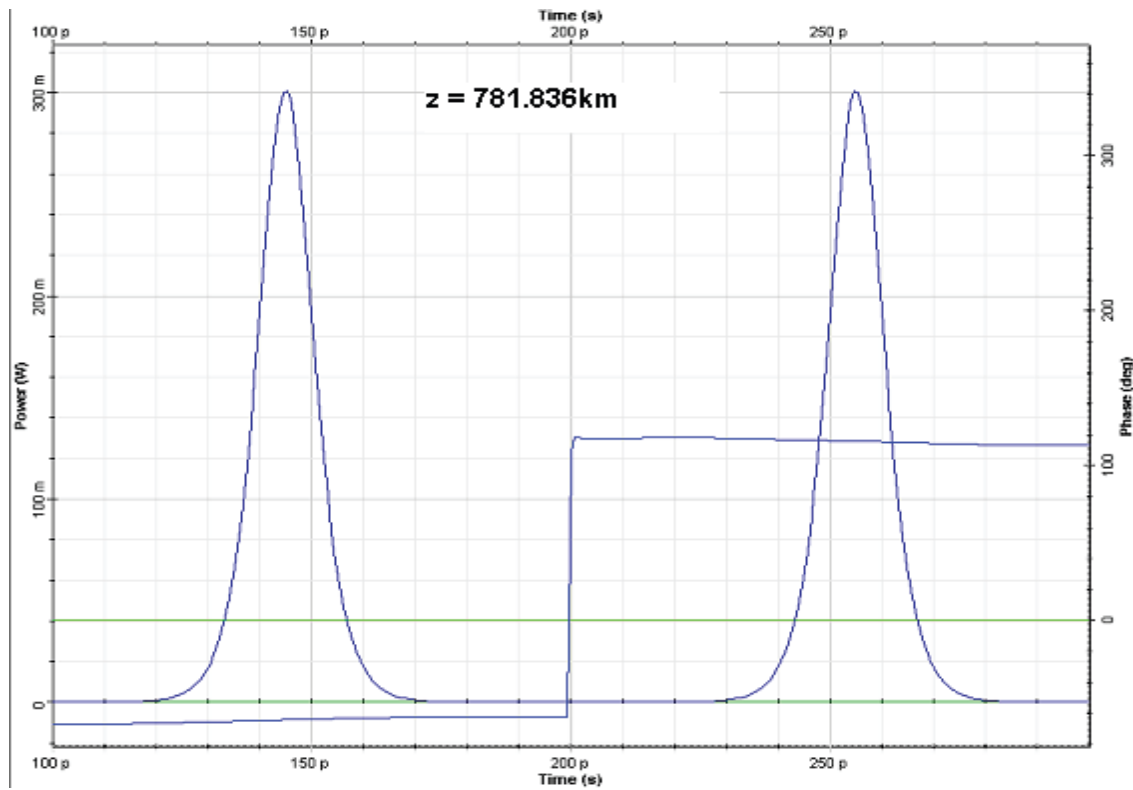


Figure 4.2.10: Input pulse shape(optical time domain visualizer)

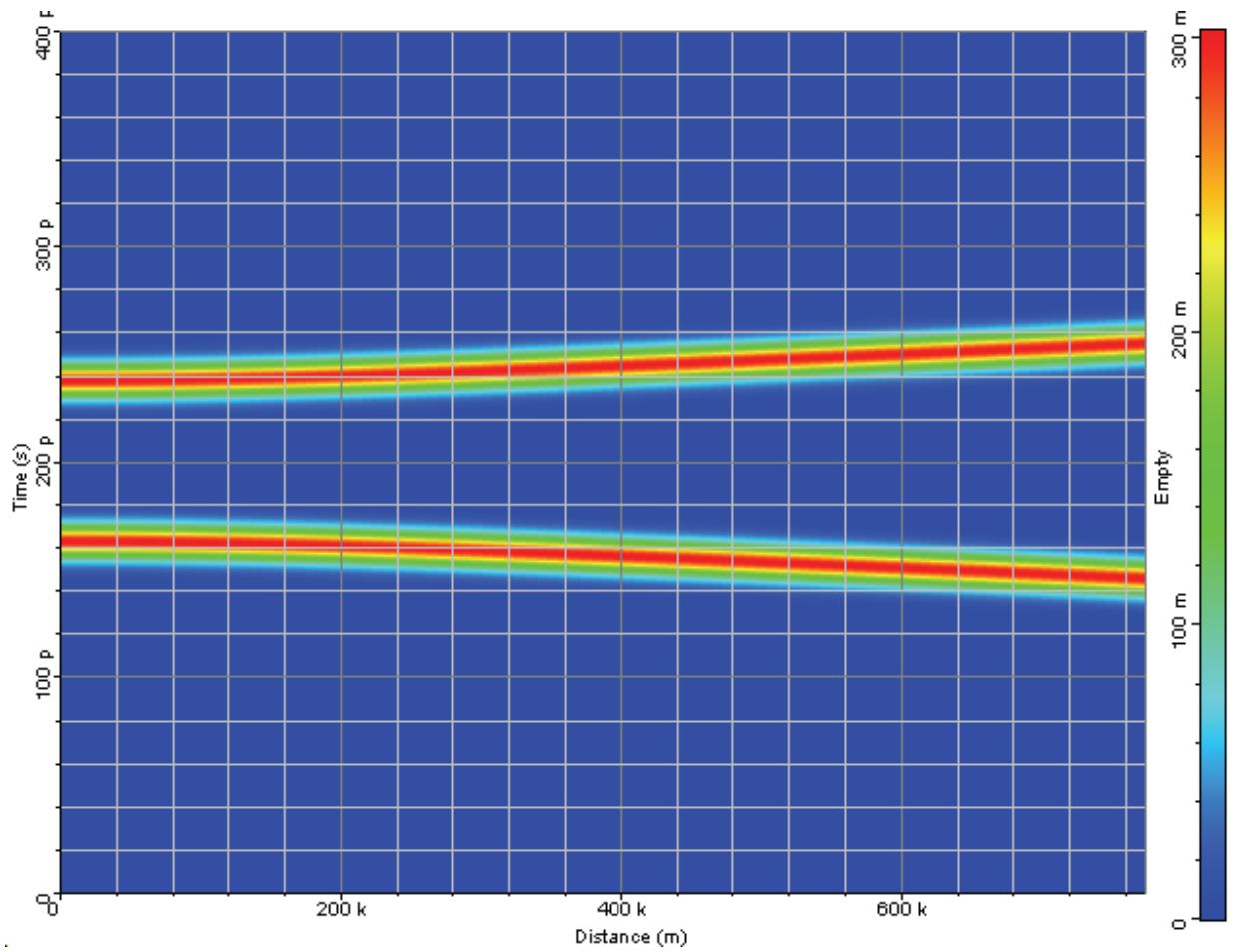


Figure 4.2.11: Interaction between identical,  $\pi$ -out of phase solitons within one collision length. Repulsion is evident.

(Figure Source: G. P. Agrawal Nonlinear Fiber Optics, Academic Press (2001).)

### 4.3 Decay of Higher order Solitons in the Presence of Third-Order Dispersion(TOD)

This lesson demonstrates the effect of third-order dispersion on the fundamental and higher-order solitons. The layout that we use and its global parameters are shown in Figure 1.

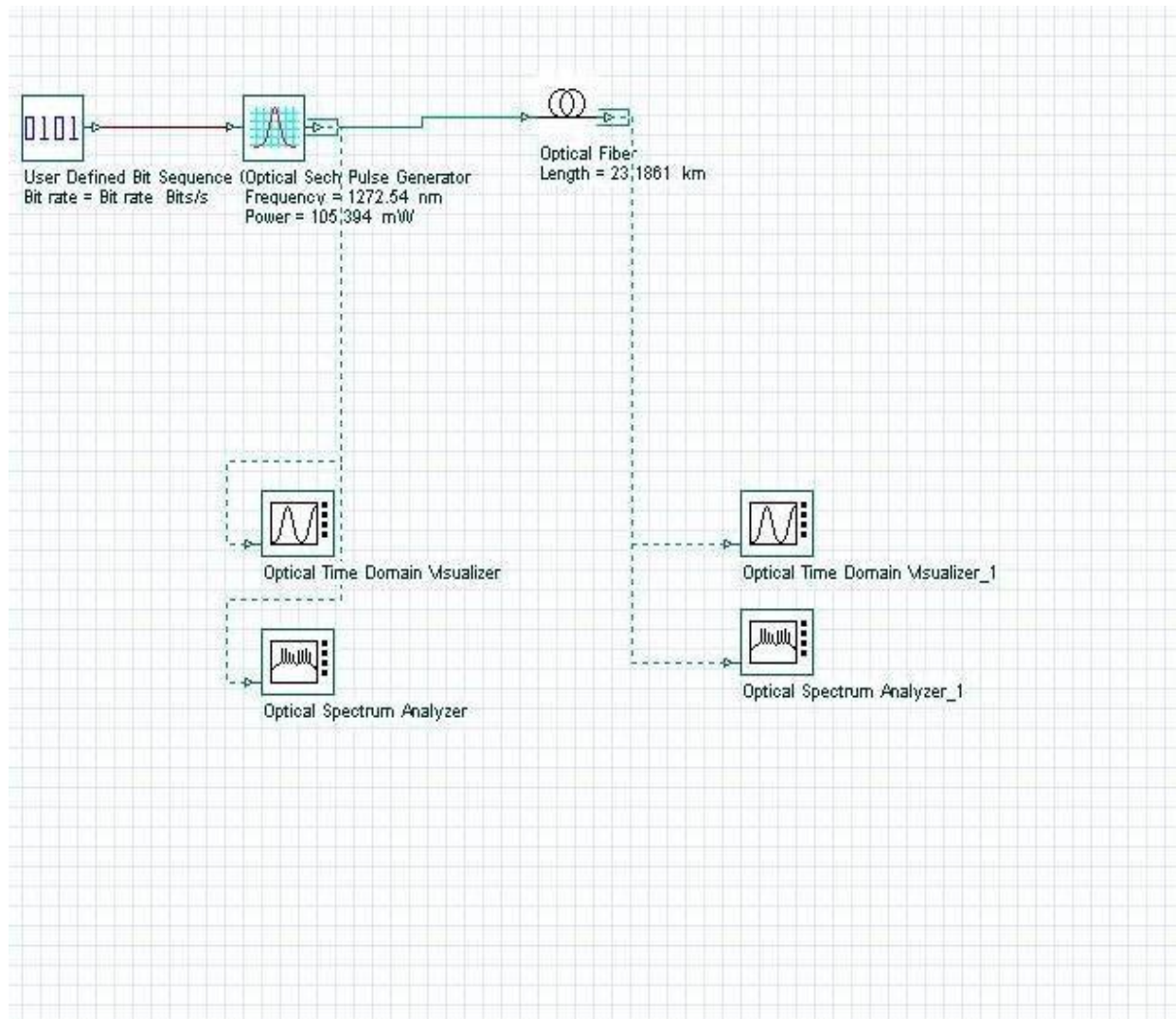


Figure 4.3.1 System layout

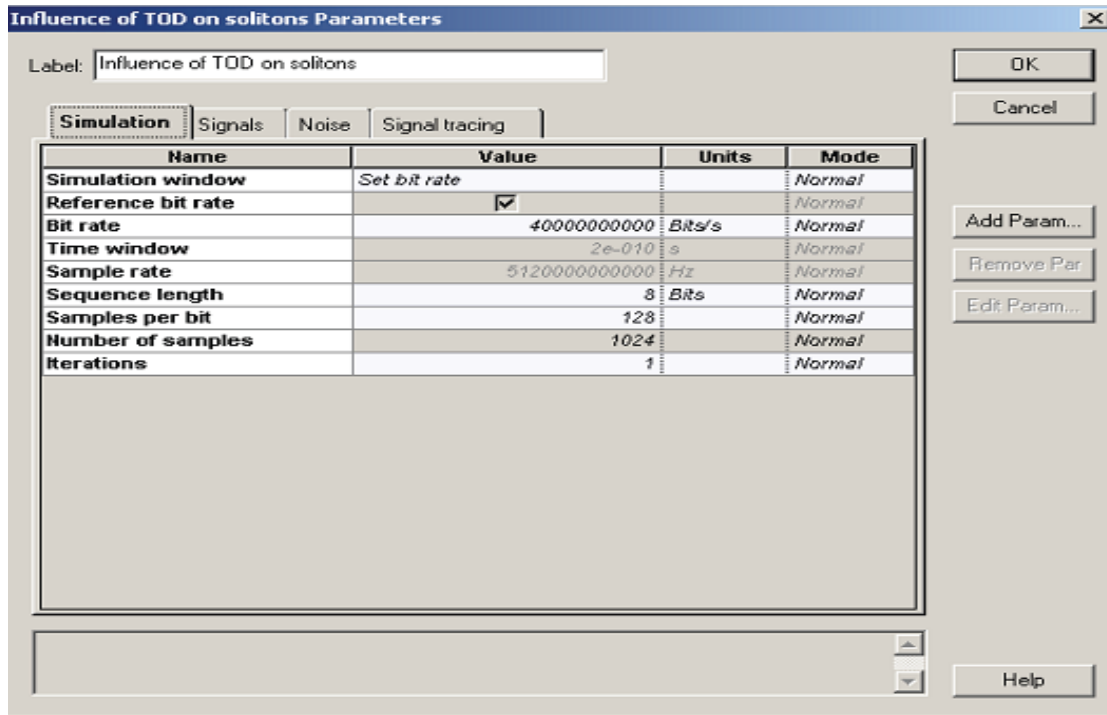


Figure 4.3.2: System parameters

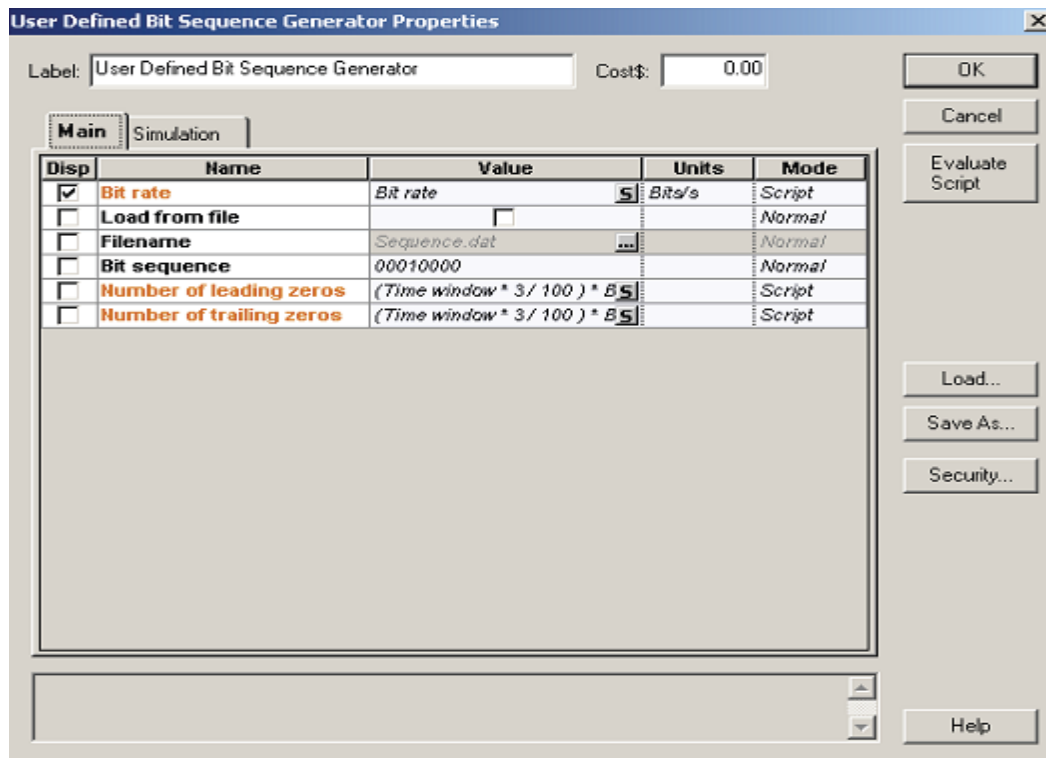


Figure 4.3.3: Setup for the bit sequence generator

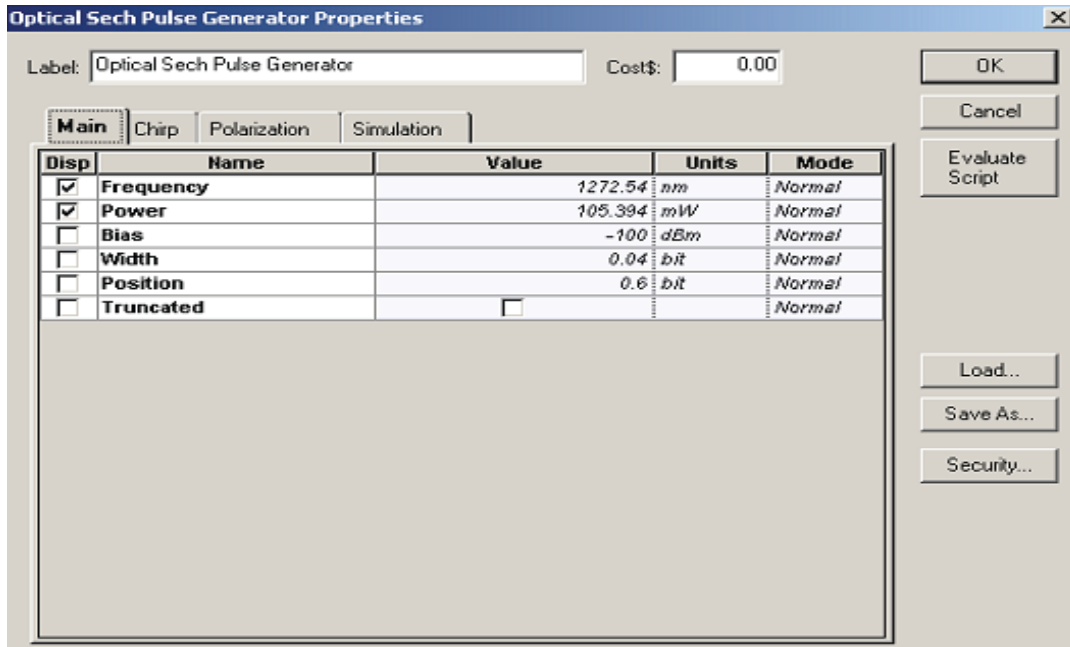
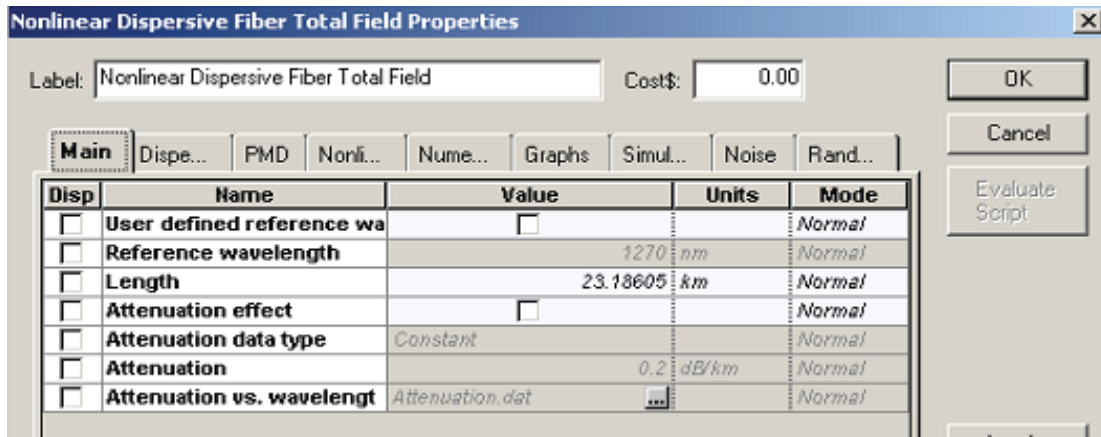


Figure 4.3.4: Setup for the sech-pulse generator.



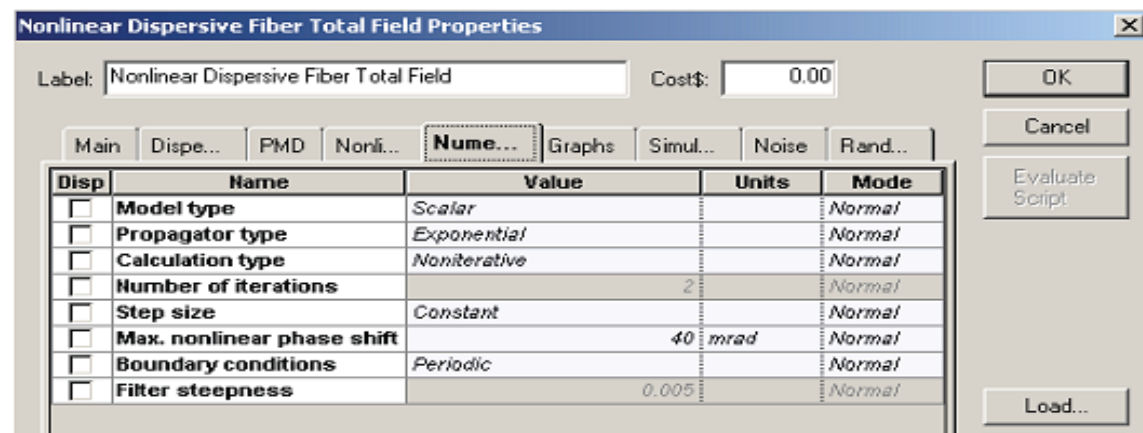
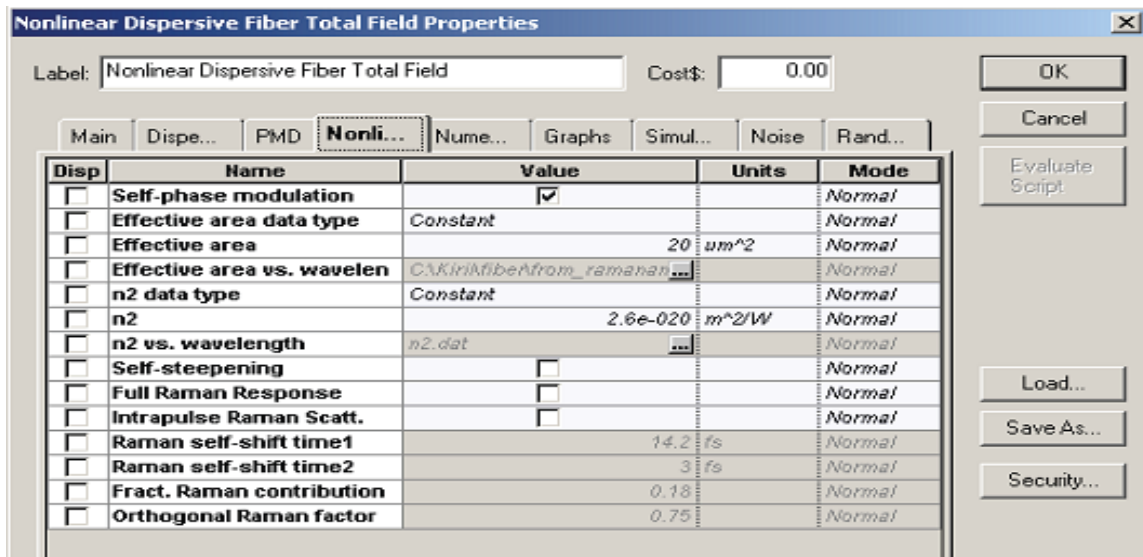
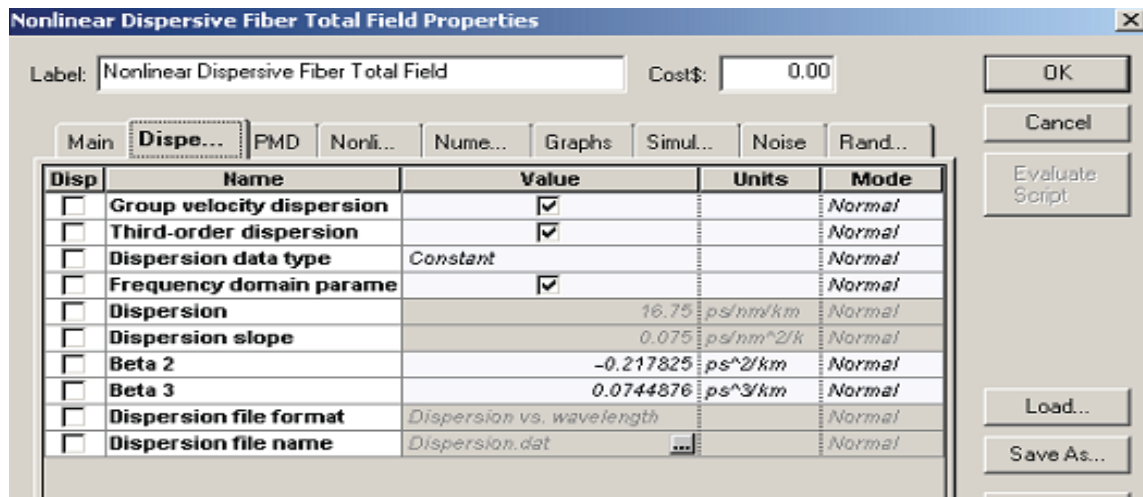


Figure 4.3.5: Setup for the nonlinear dispersive fiber component

## Input Pulse Shapes:

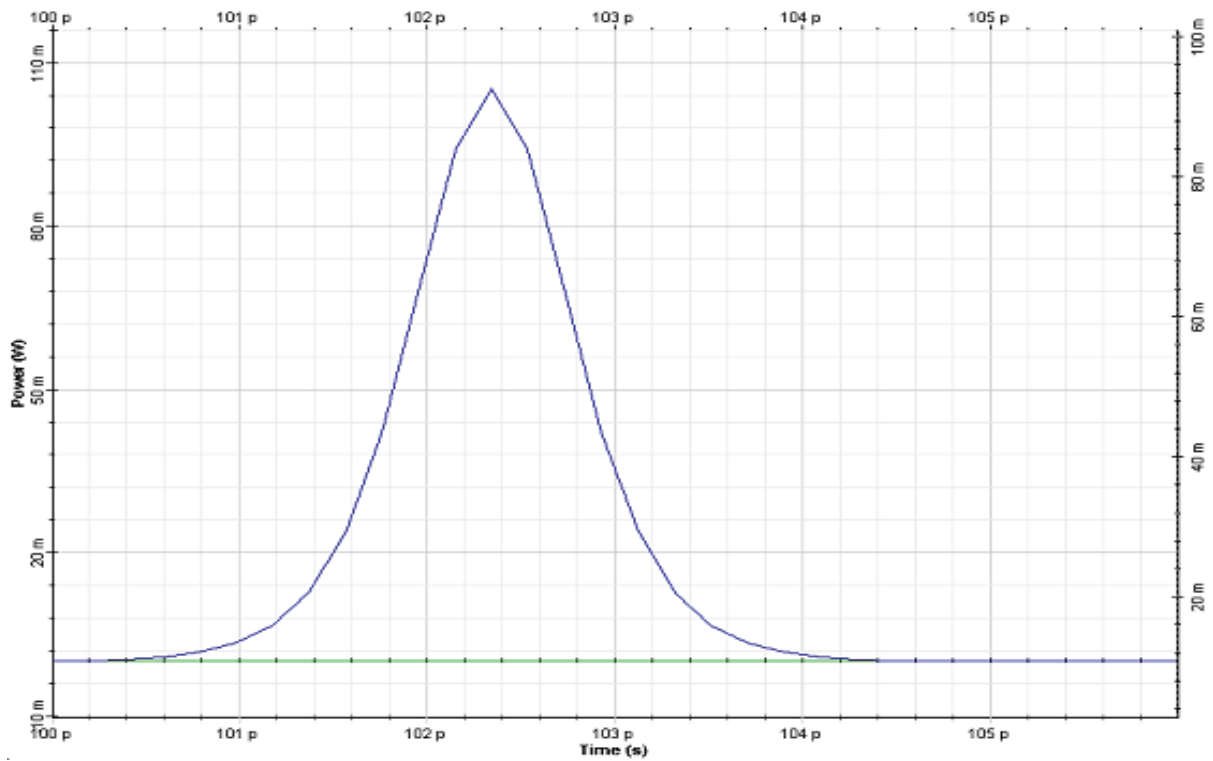


Figure 4.3.6: Input pulse shape(optical time domain visualizer)

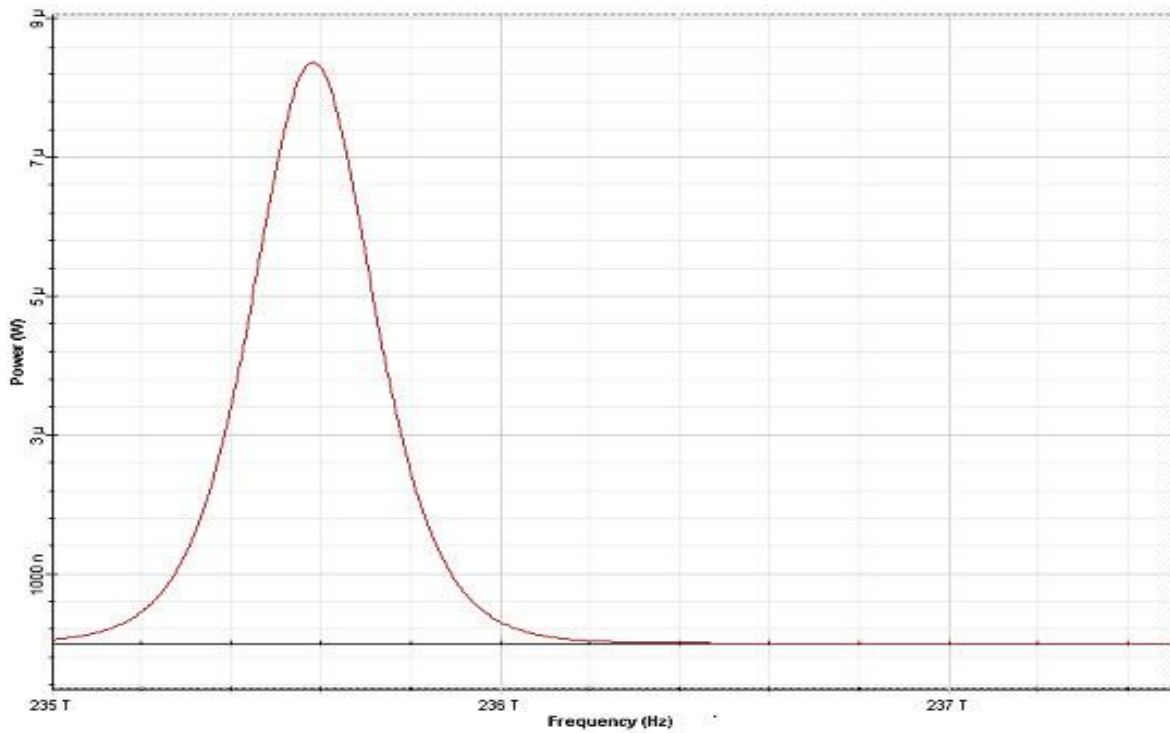


Figure 4.3.7: Input pulse shape (optical spectrum analyzer)

The input pulse (Figure 4.3.1) is a 1 ps wide (FWHM) fundamental soliton propagating near the zero dispersion wavelength [1]. The output pulse shape and spectrum are shown in Figure 4.3.8.

The principal effect of the third-order dispersion term is to stimulate radiation resonantly at a frequency:

$$\omega - \omega_0 = \frac{|\beta_2|}{\beta_3} \quad (4.3.1)$$

## Output Pulses Shape

Output (at 10 soliton periods or 23.18 km) . Resonance radiation peak is evident

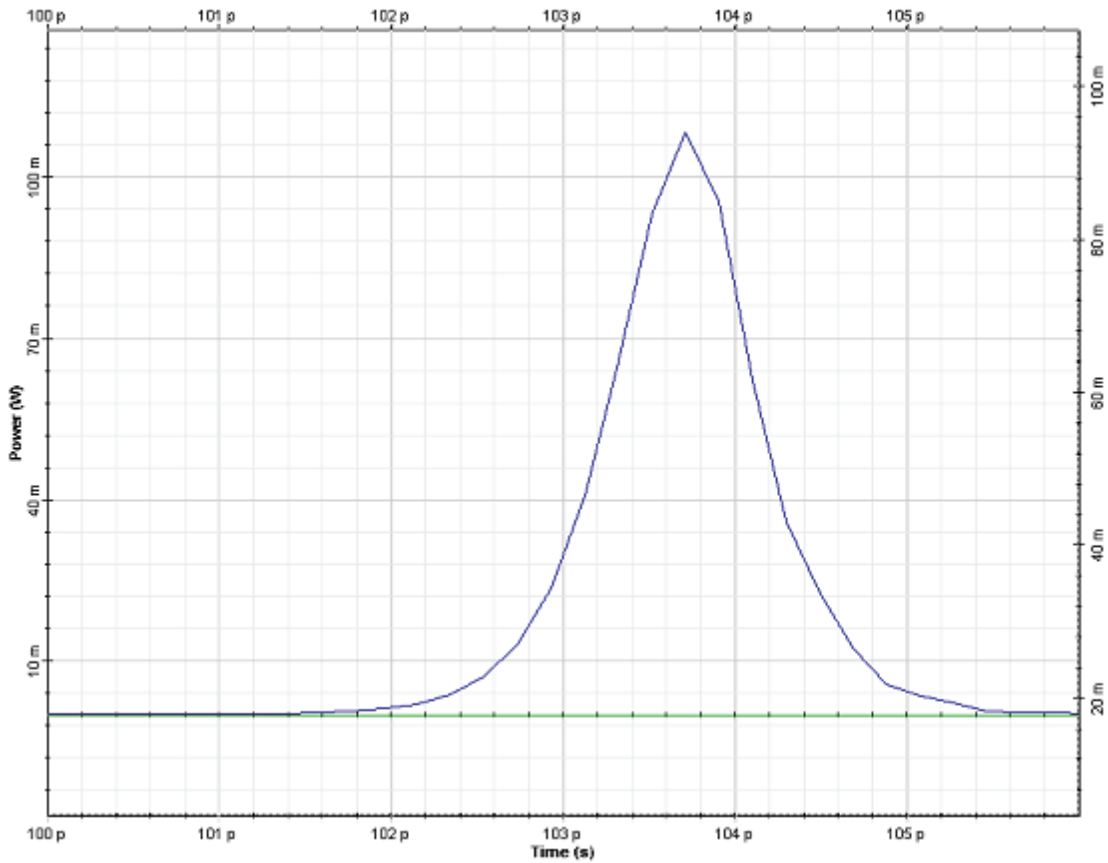


Figure 4.3.8: Output pulse shape(optical time domain visualize)

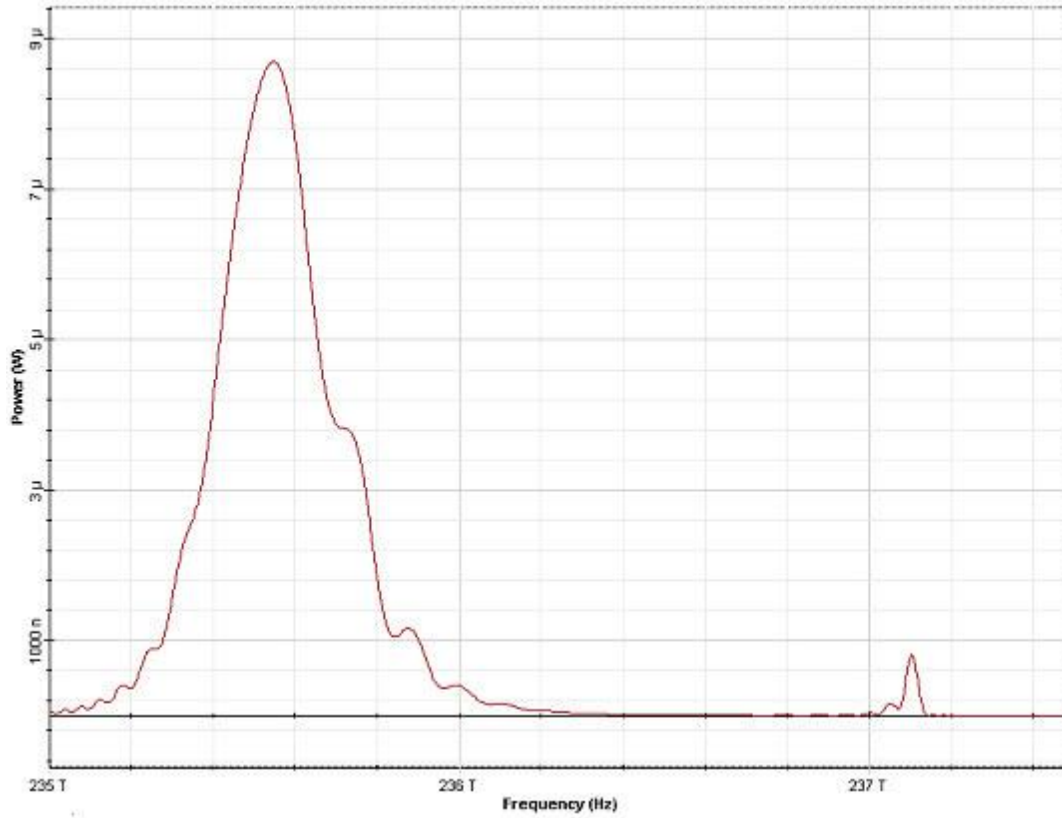


Figure 4.3.9: Output pulse shape (optical spectrum analyzer)

Good agreement can be seen between the results presented in [A] and in Figure 4.3.8 & 4.3.9.

Output pulse shape after 11.6 km (or 5 soliton periods) of propagation. Second order soliton has been split into its constituents by the effect of TOD [A]

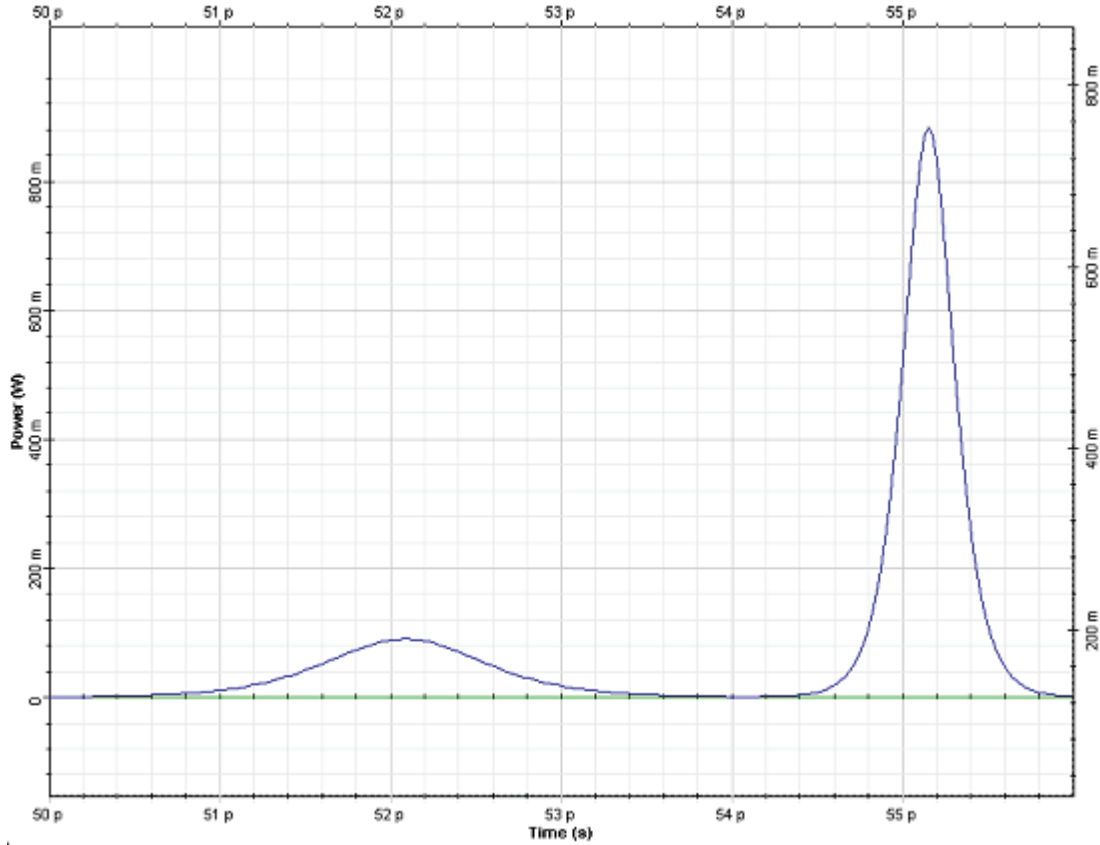


Figure 4.3.10: Output pulse shape after 11.6 km (or 5 soliton periods) of propagation.

The second part of this tutorial considers TOD-induced decay of  $N=2$  soliton. To simulate this phenomenon, the following changes of the parameters are applied. The sequence length is set to four bits and the samples per bit parameter is set to 1024. The bit sequence in the user defined bit sequence generator is changed to "0100". The power of the sech-pulse generator is set to  $421.576\text{mW}$  (corresponding to second order soliton). The fiber length is changed to  $11.593\text{km}$ , which corresponds to five soliton periods. Beta 3 dispersion parameter in the optical fiber component is set to  $0.019366776\text{ps}^3/\text{km}$ . The output pulse shape is presented in Figure 4.3.10.

The second-order soliton has been split into its constituents by the effect of TOD [1].

## 4.4 Stability of Solitons in Birefringent Optical Fibers

This lesson demonstrates that the Kerr nonlinearity, which stabilizes solitons against spreading due to GVD, also stabilizes them against splitting due to birefringence [55]

The "single-mode" fibers are actually bimodal because of the presence of birefringence. This means that the group velocity is different for pulses polarized along the two principal axes. If the pulse contains both polarization components, in addition to spreading due to GVD, the partial pulses will tend to split apart because of birefringence [55].

In the anomalous GVD regime, the Kerr nonlinearity can compensate the spreading due to GVD, leading to formation of a soliton. The similar fact is true for the birefringent walk-off. Above a certain soliton number, which increases with the strength of the linear birefringence, the two polarizations interact to form a soliton consisting of both polarizations. The physical effect responsible for this type of behavior is the cross-phase modulation between the two polarization components.

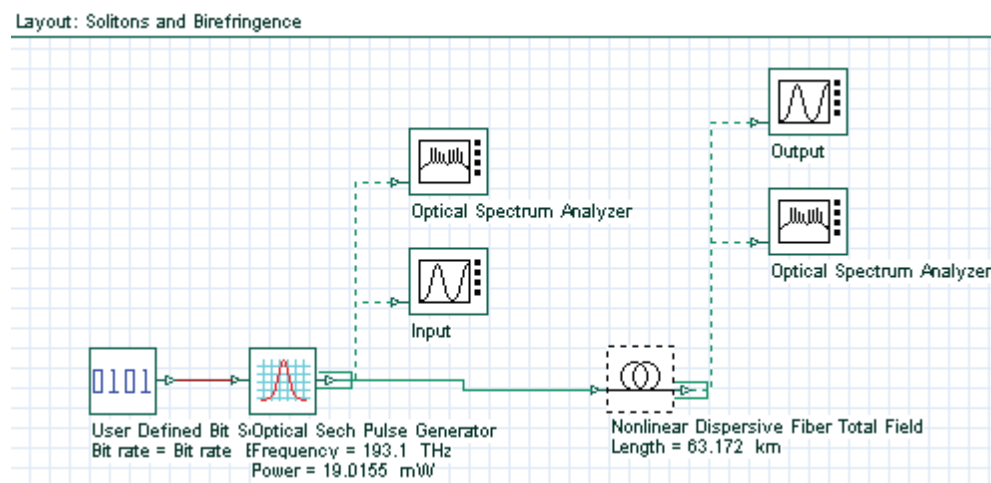


Figure 4.4.1: System layout

To see the birefringence-induced time delay between both polarization components, we set azimuth in the optical sech pulse generator equal to 45 degree, fiber length to 631.72 km (10 soliton periods) and switch the nonlinear effects OFF.

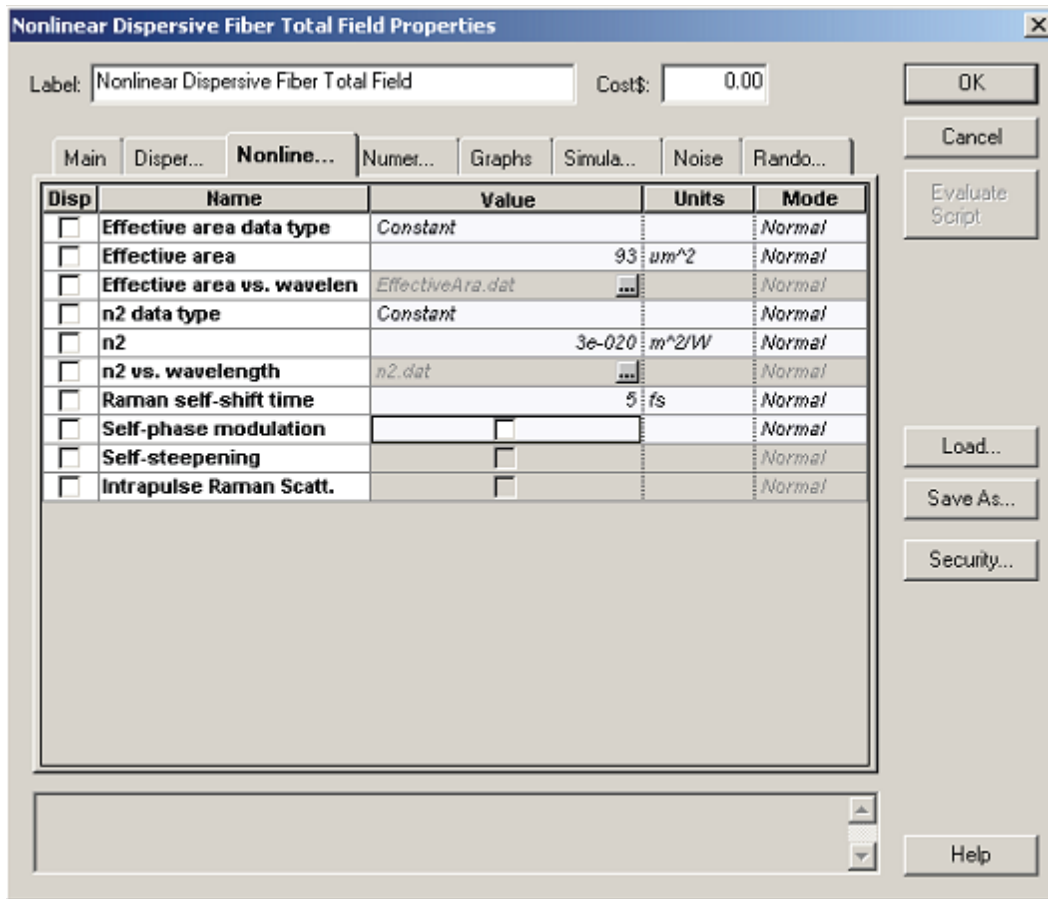


Figure 4.4.2:Layout Parameters

## Input and Output Pulse Shapes without Nonlinearity Effect

Figures below, shows the input & output partial pulse after 631.72 km propagation in a loss-free fiber. Both partial pulses are broadened by GVD and shifted in time by 440 ps with respect to each other, which corresponds to a difference in the arrival times of 0.7 ps for 1 km of fiber length. This shift can be attributed to the birefringence.

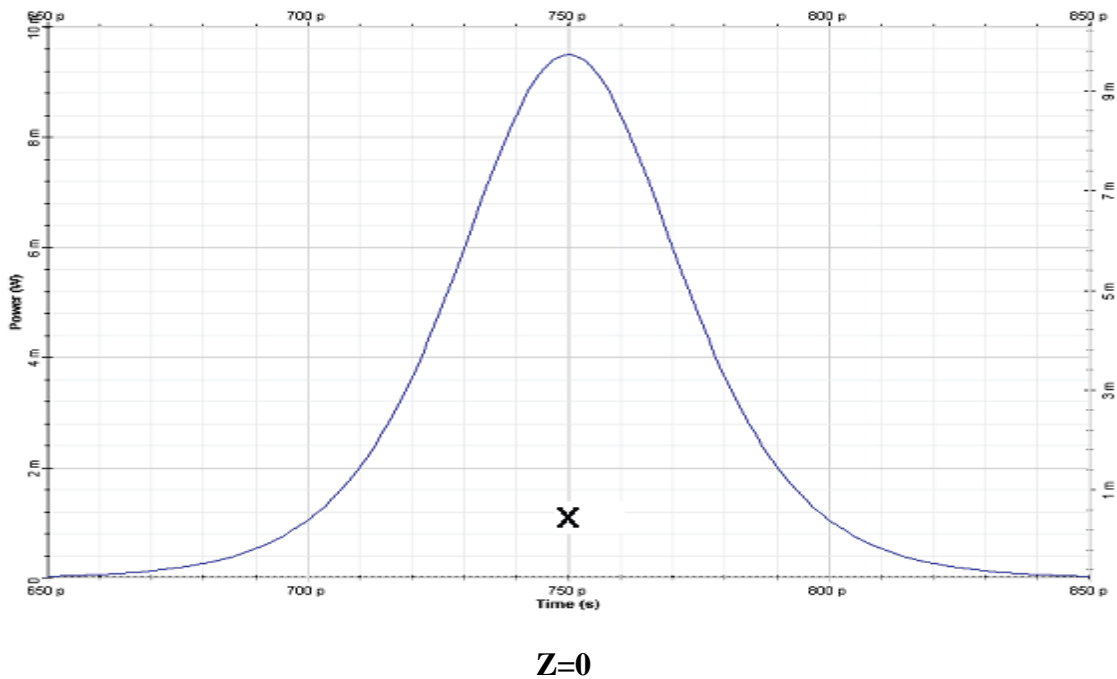
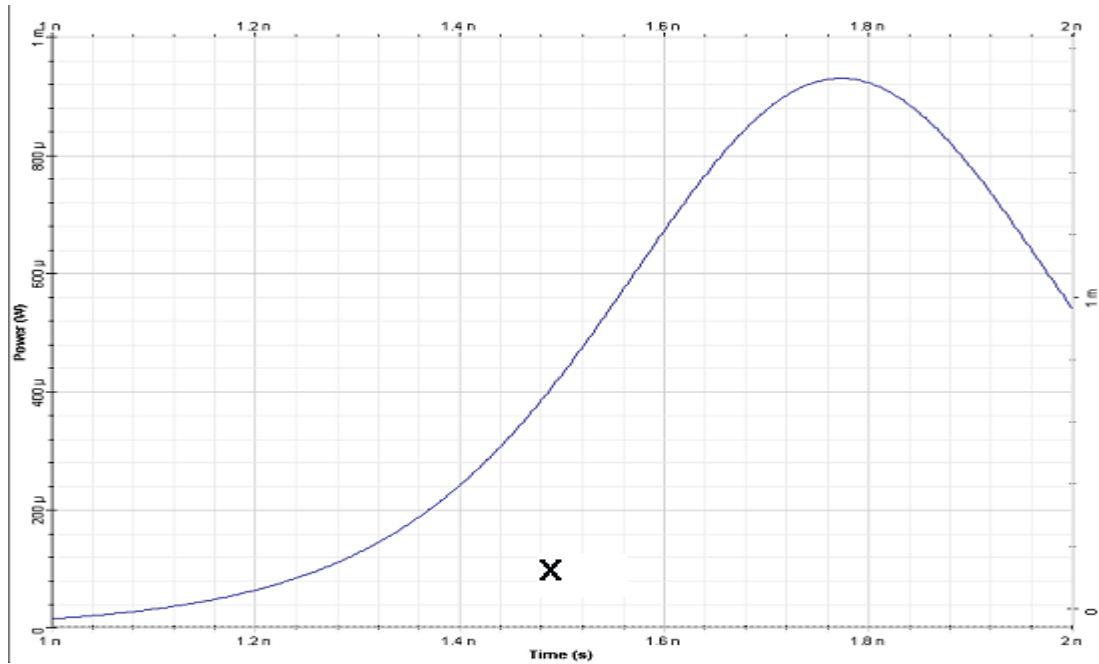


Figure 4.4.3: Input polarization components x for a sech-pulse in linear regime



**Z= 631.72 km**

Figure 4.4.4: Output polarization components x for a sech-pulse in linear regime

When the nonlinearity is taken into account, the two polarization components remain bound together if  $N$  exceeds some critical value that increases with the increase .

To see this, we switch the nonlinear effects ON in the fiber component. The output pulses for 631.72 km of propagation are shown in Figure 4.4.5.

## Output Pulse Shape with Nonlinearity Effect

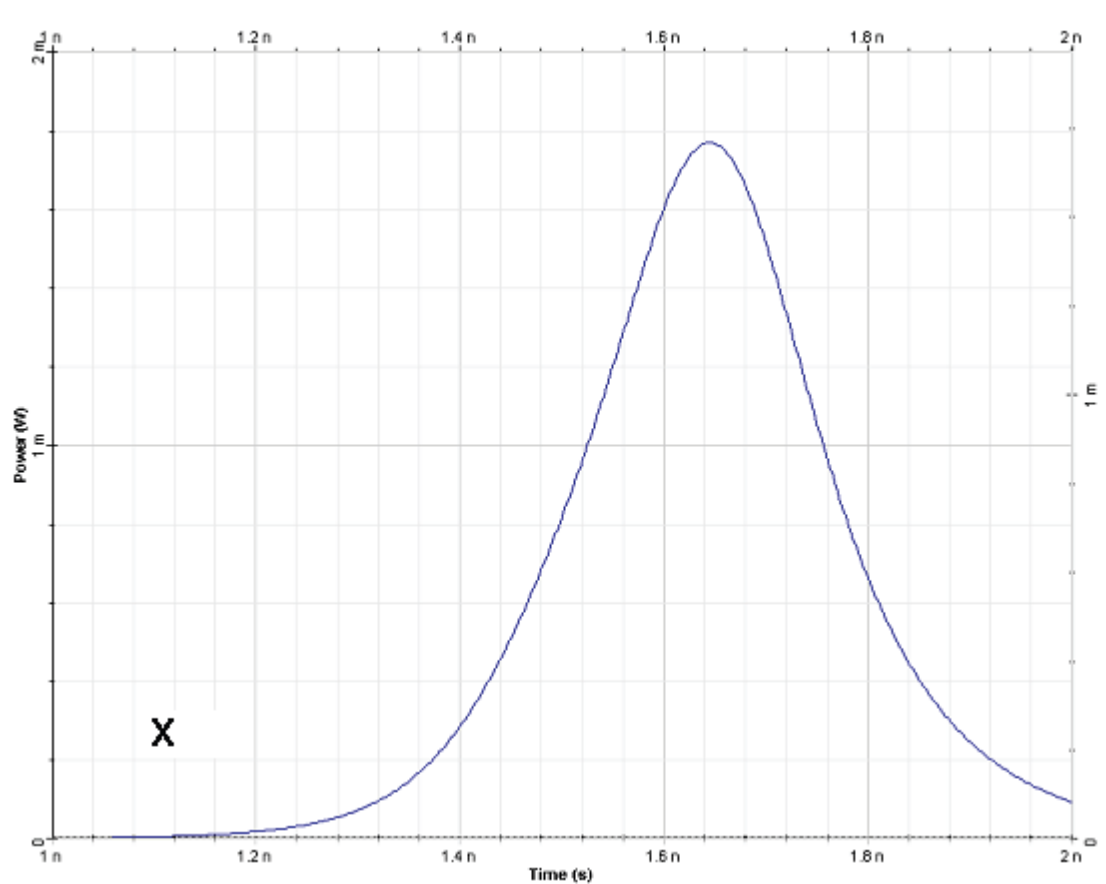
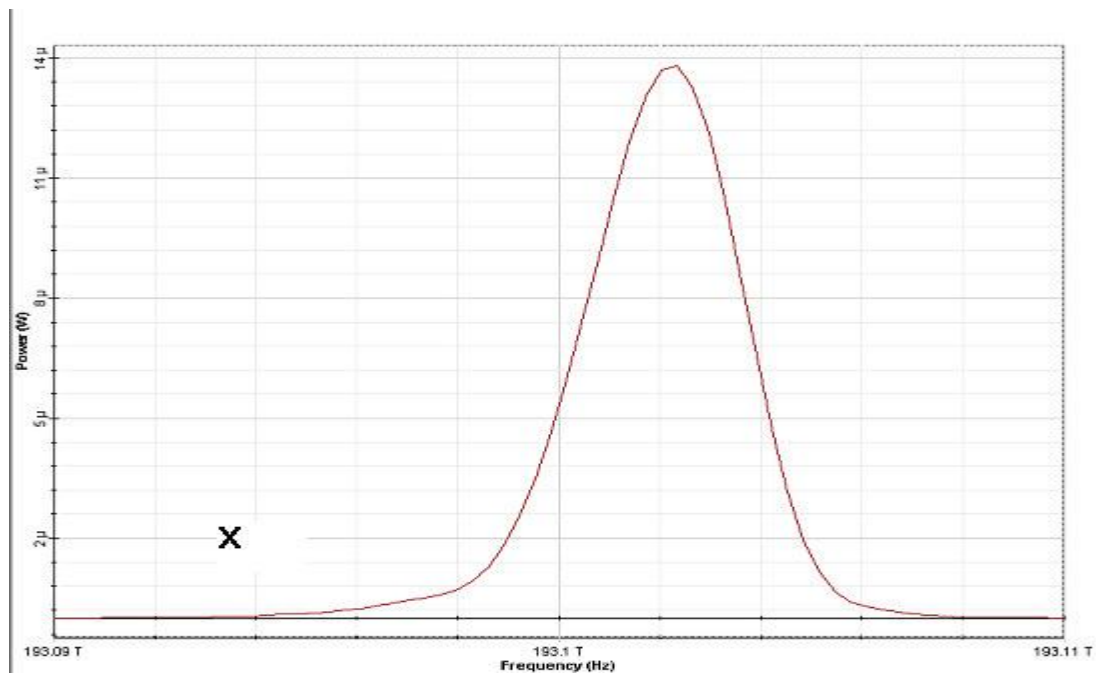


Figure 4.4.5: Partial pulses after propagating in 631 km of fiber taking into account the nonlinear effect

Comparing Figure 4.4.5 and Figure 4.4.3, we can see that the impact of the nonlinearity is twofold: Nonlinear effects reduce the GVD induced pulse broadening for each of the polarization components, and the time delay between both is reduced with respect to case of linear propagation (i.e. neglecting the nonlinear effects, Figure 4.4.3).

## Input Pulse Shapewith Nonlinearity Effect



$$Z = 0$$

Figure 4.4.6: Input pulse spectra evolution over 10 soliton periods  $x$  (slow axis)

## Output Pulse shape

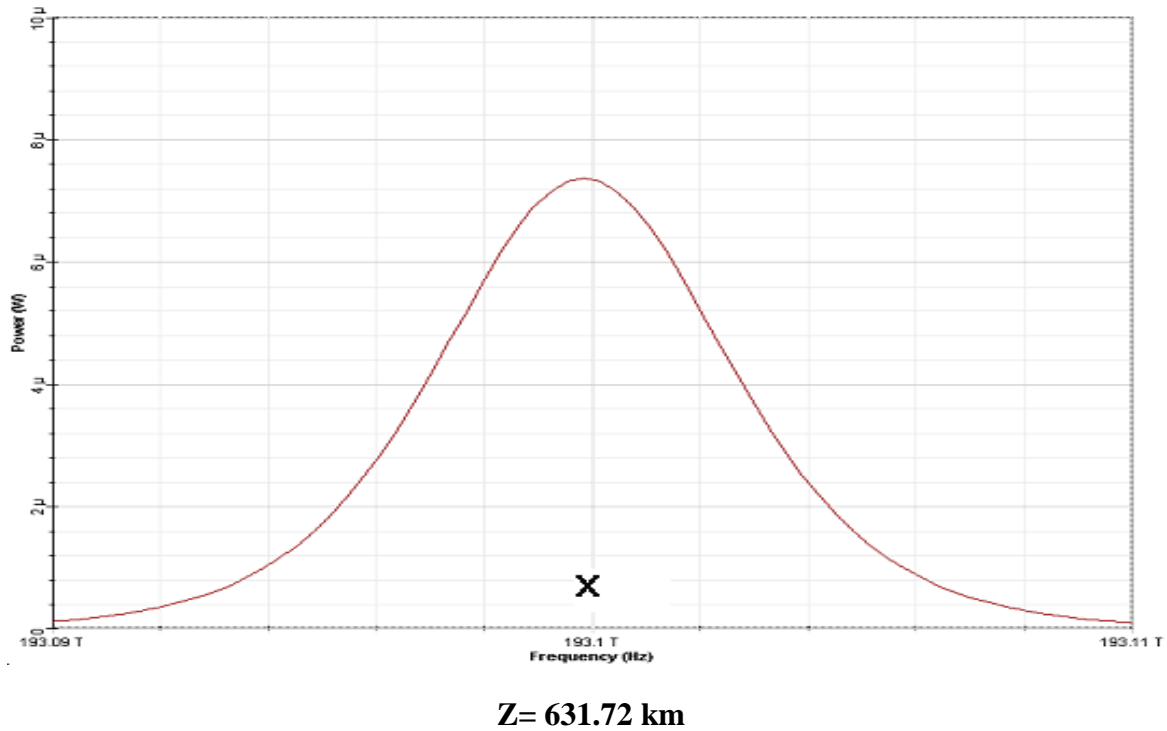


Figure 4.4.7: Output pulse spectra evolution over 10 soliton periods  $x$  (slow axis)

When the nonlinear effects are taken into account, the time delay is roughly 200 ps, which is more than a factor of two smaller compared to the case of linear-regime propagation. It can be concluded that Kerr nonlinearity reduces the birefringent walk-off [2].

## 4.5 Soliton Amplifier(SOA) as In-Line Amplifier in Soliton Communication Systems

One possible way to upgrade an existing network from previously installed standard optical fibers is to exploit the 1.3  $\mu\text{m}$  optical window, where the step index fibers have a zero-dispersion wavelength using SOA.

The **advantages** of using SOA as in-line single-channel optical amplifiers are:

- 1.Low dispersion of the SMF at this carrier wavelength
- 2.Attractive features of semiconductor optical amplifiers

Two **disadvantages** of using SOA as in-line single-channel optical amplifiers are:

- 1.Gain-saturation effects, which lead to non-equal amplification of pulses in the pattern (so called pattern effect)
- 2.Chirp that the pulse acquires after amplification

This lesson demonstrates the pattern effect at 10 Gb/s transmission over a 500 km optical link consisting of SMF and in-line SOA's [1]. We will try to use parameters similar to the parameters in [55].

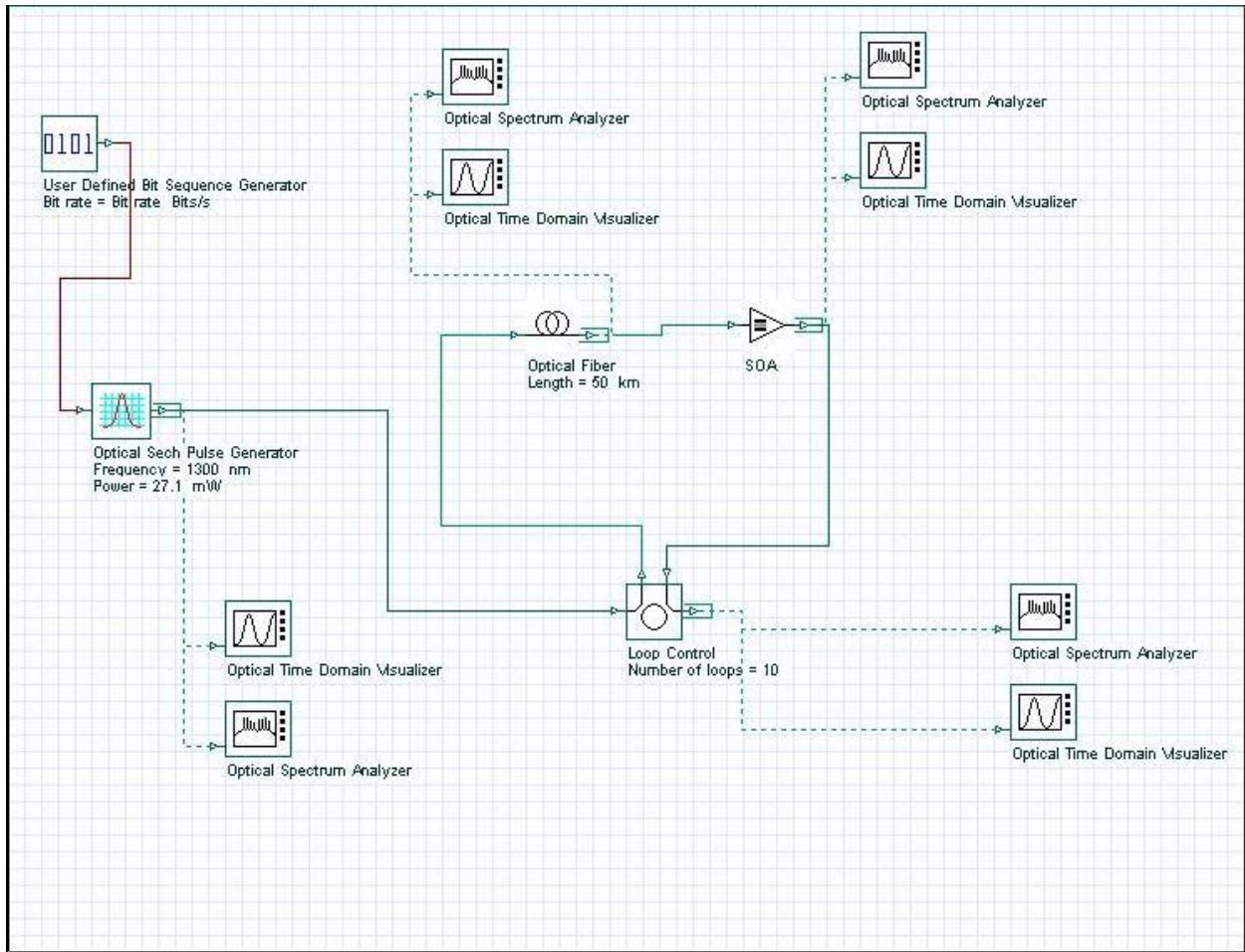


Figure 4.5.1: System Layout

SOA Soliton System Parameters

Label: SOA Soliton System

Simulation Signals Spatial effects Noise Signal tracing

Name	Value	Units	Mode
Simulation window	Set bit rate		Normal
Reference bit rate	<input checked="" type="checkbox"/>		Normal
Bit rate	10000000000	Bits/s	Normal
Time window	1.6e-009	s	Normal
Sample rate	640000000000	Hz	Normal
Sequence length	16	Bits	Normal
Samples per bit	64		Normal
Number of samples	1024		Normal

OK  
Cancel  
Add Param...  
Remove Par  
Edit Param...

Figure 4.5.2: Simulation parameters for transmission at 10 Gb/s

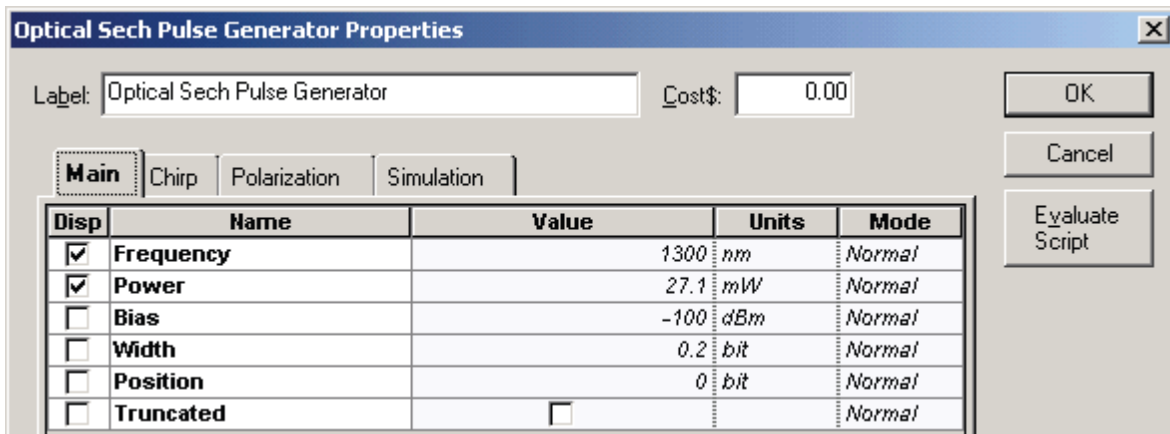
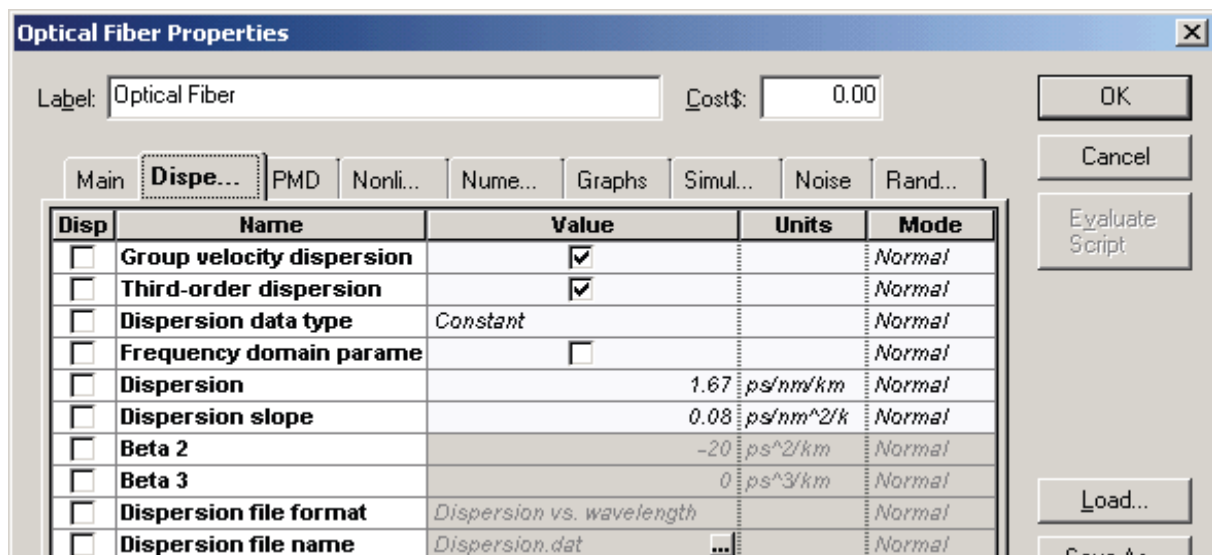
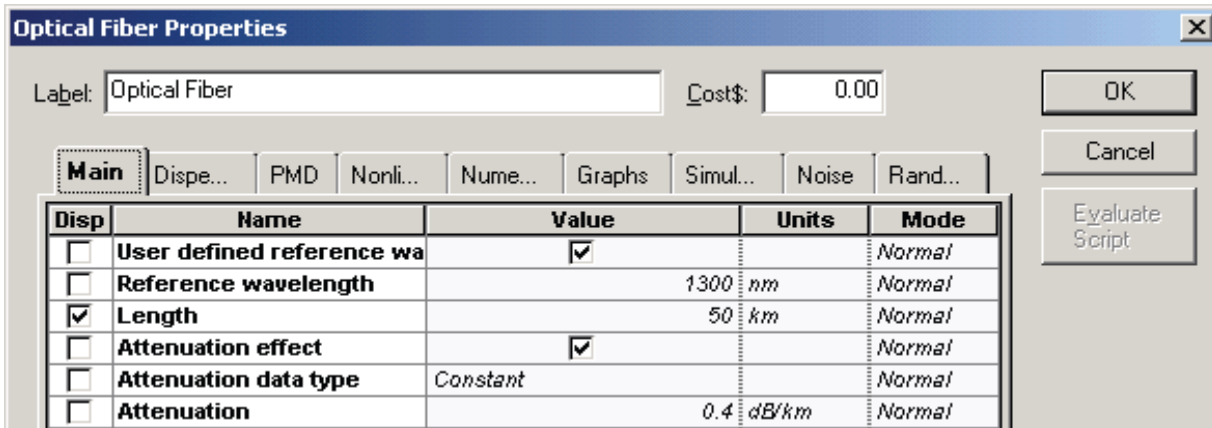


Figure 4.5.3: Optical Sech Pulse Generator Main parameters for transmission at 10 Gb/s



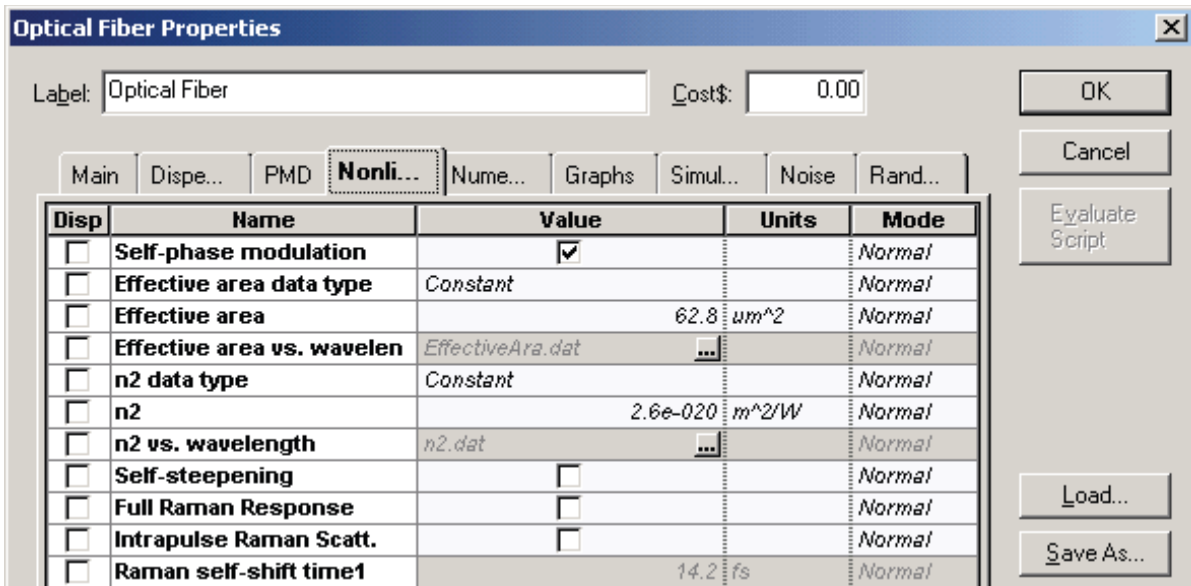


Figure 4.5.4: Optical fibre parameters

The Kerr nonlinearity coefficient

$$\gamma = \frac{n_2 \omega_0}{c A_{eff}} \quad (4.5.1)$$

for the fixed values of nonlinear refractive index.

This is unsaturated single pass gain required from SOA. To obtain this gain, the following parameters have been used (see Figure 4.5.5 and Figure 4.5.6).

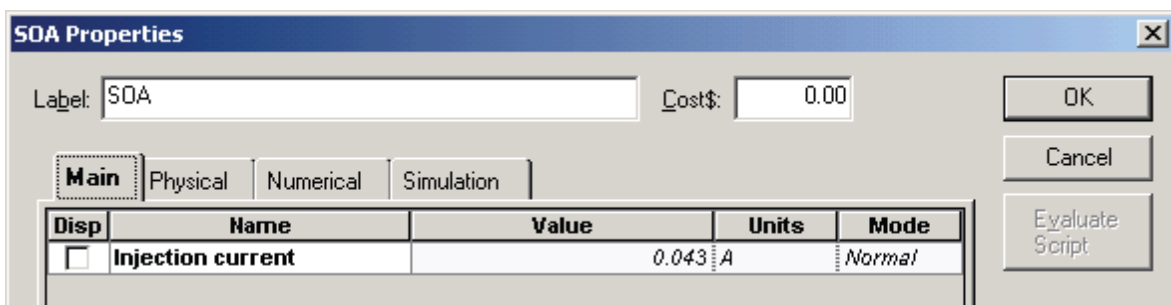


Figure 4.5.5: SOA Main parameters

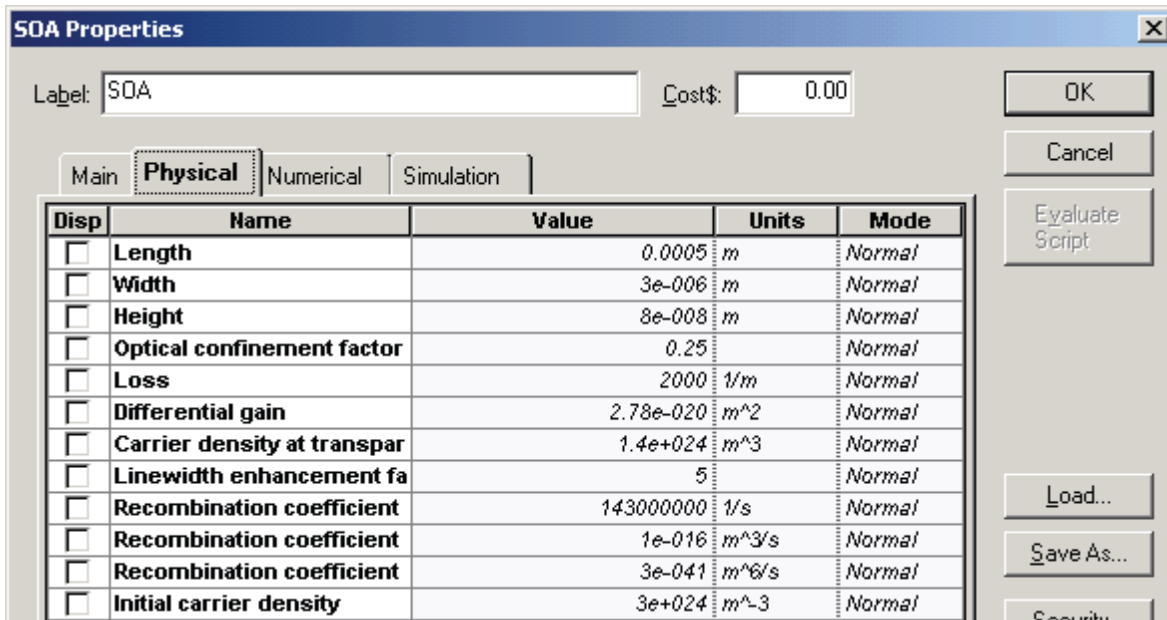
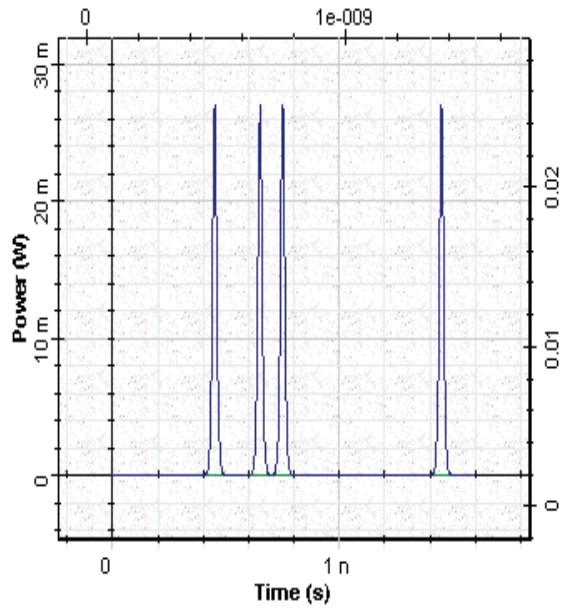


Figure 4.5.6:SOA Physical parameters

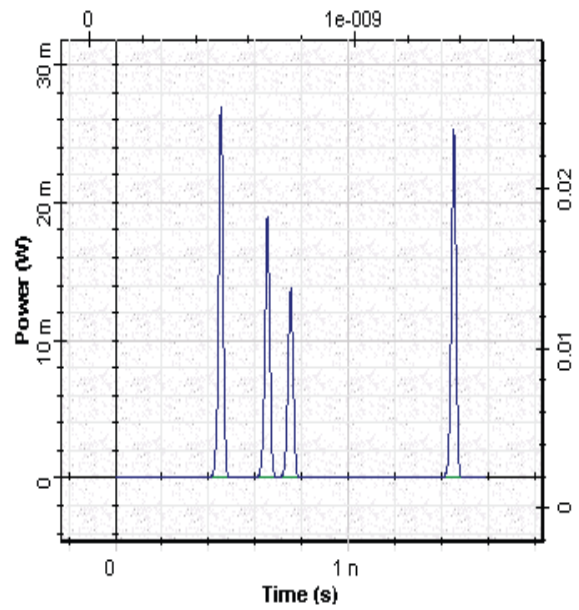
Figure 4.5.7 shows the initial pattern of pulses, and the same pattern of pulses after 200, 350, and 500 km transmission in SMF and periodic amplification with SOA at every 50 km.

Optical Time Domain Visualizer



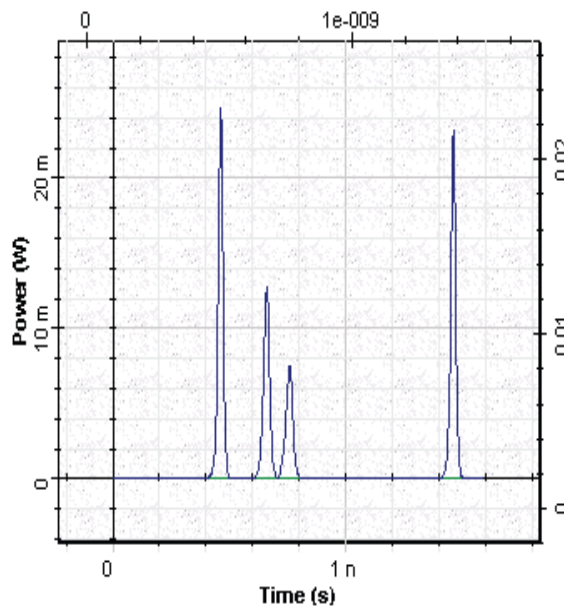
Initial pulse pattern

Optical Time Domain Visualizer



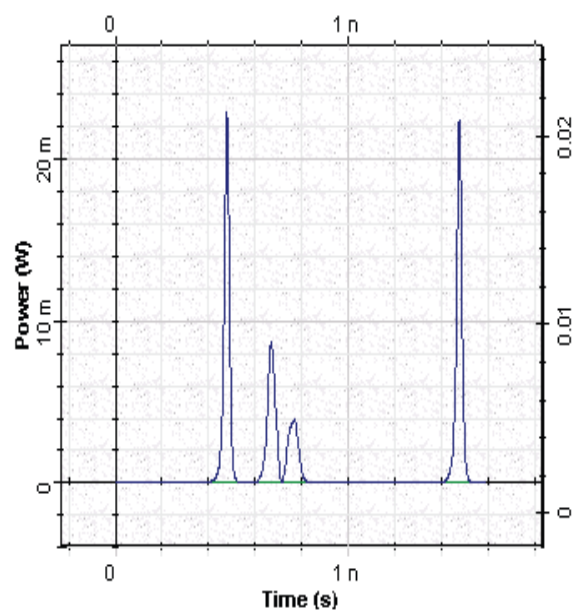
Pulse pattern after 200 km transmission in SMF

Optical Time Domain Visualizer



Pulse pattern after 350 km transmission in SMF

Optical Time Domain Visualizer



Pulse pattern after 500 km transmission in SMF

Figure 4.5.7 SOA pulse patterns

In this figure, we can see the pattern effect that leads to a reduction in the gain of the pulses after the first one in the first group. Regarding our default parameters, the carrier lifetime is approximately 1.4 ns even for the last pulse, which is at a distance of approximately 1 nm from the first one. There is not enough time for the gain to recover completely.

This lesson demonstrated two basic problems associated with using the SOA as an in-line amplifier:

1. Pattern effect, which is a consequence of the gain saturation properties of the SOA
2. Nonlinear crosstalk [3]

## 4.6 Decay of Higher order Solitons in the presence of Intrapulse Raman(IR) Scattering

This lesson demonstrates the influence of stimulated Raman scattering on short soliton pulses.

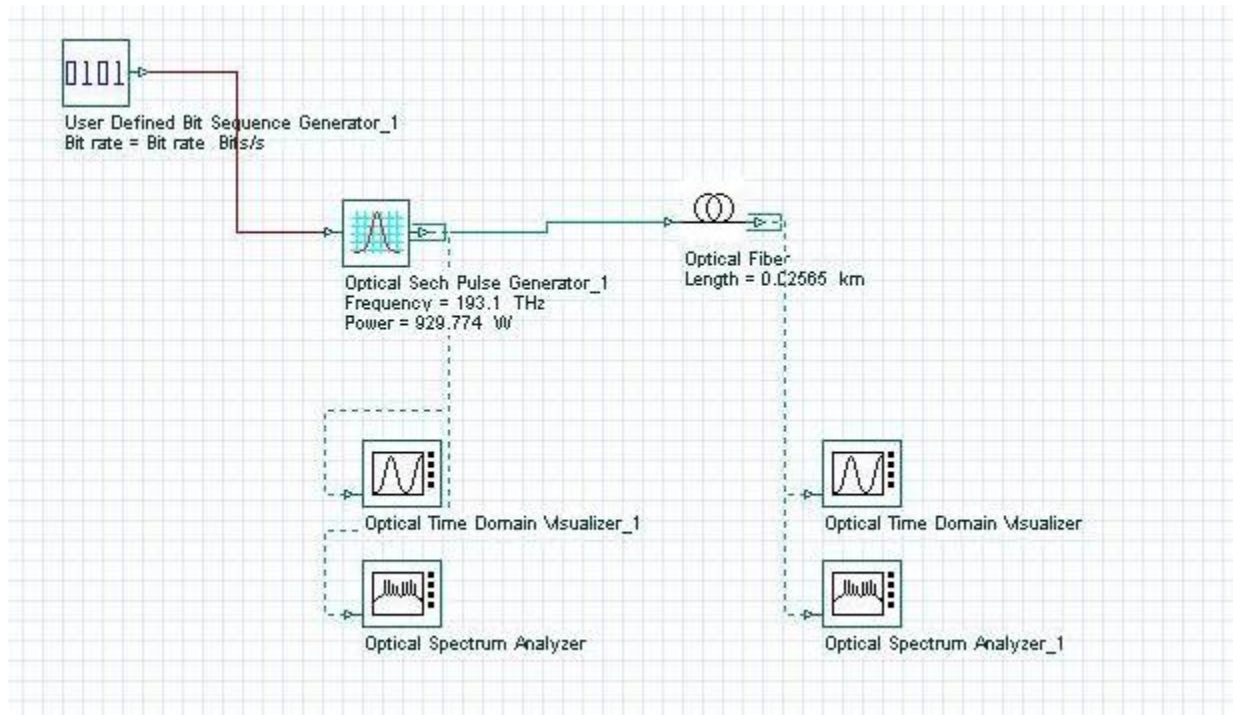


Figure 4.6.1: System Layout

SRS induced soliton decay Parameters

Label: SRS induced soliton decay

Simulation Signals Noise Signal tracing

Name	Value	Units	Mode
Simulation window	Set bit rate		Normal
Reference bit rate	<input checked="" type="checkbox"/>		Normal
Bit rate	40000000000	Bits/s	Normal
Time window	5e-011	s	Normal
Sample rate	8.192e+013	Hz	Normal
Sequence length	2	Bits	Normal
Samples per bit	2048		Normal
Number of samples	4096		Normal
Iterations	1		Normal

OK  
Cancel  
Add Param...  
Remove Par...  
Edit Param...

Figure 4.6.2: System Parameters

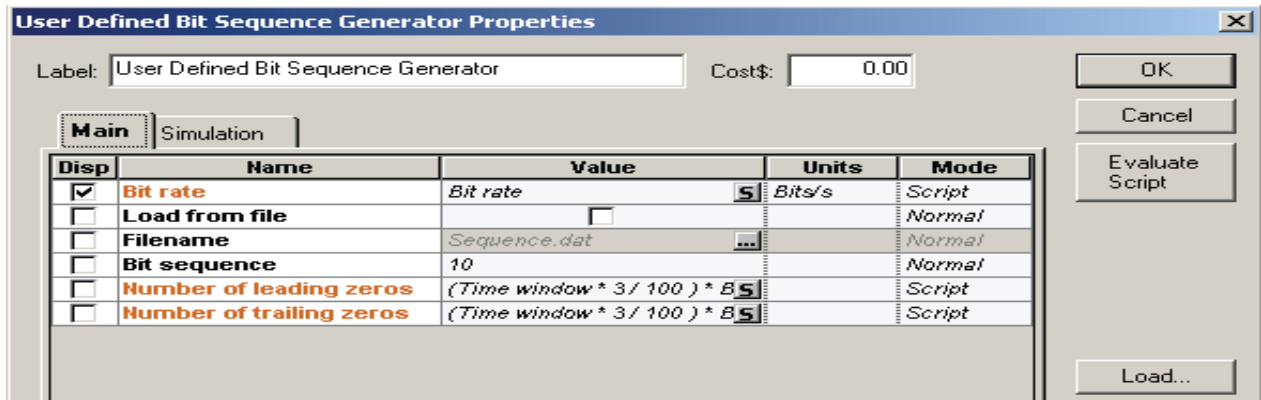


Figure 4.6.3: Setup for the Bit sequence generator

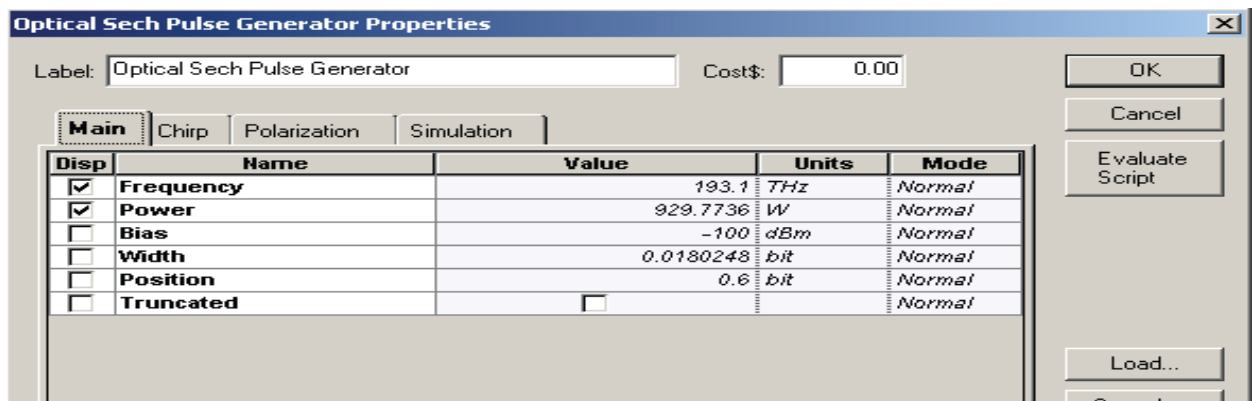


Figure 4.6.4: Setups for the Sech-pulse generator

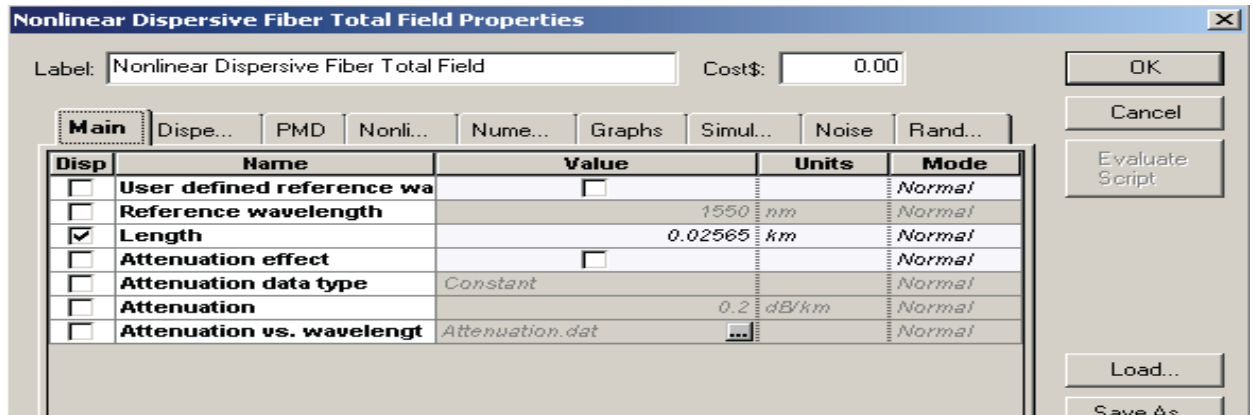


Figure 4.6.5: Parameters of the nonlinear dispersive fiber component

## Input Pulse Shapes

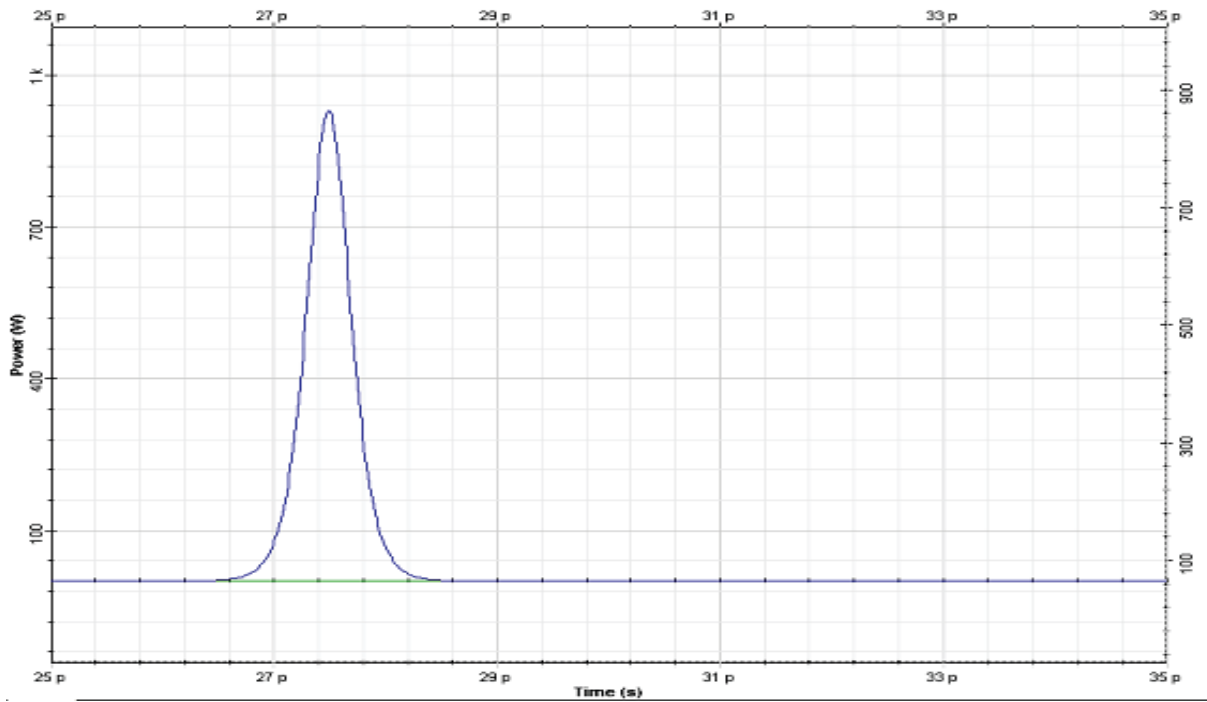


Figure 4.6.6: Input pulse shape(optical time domain visualize)

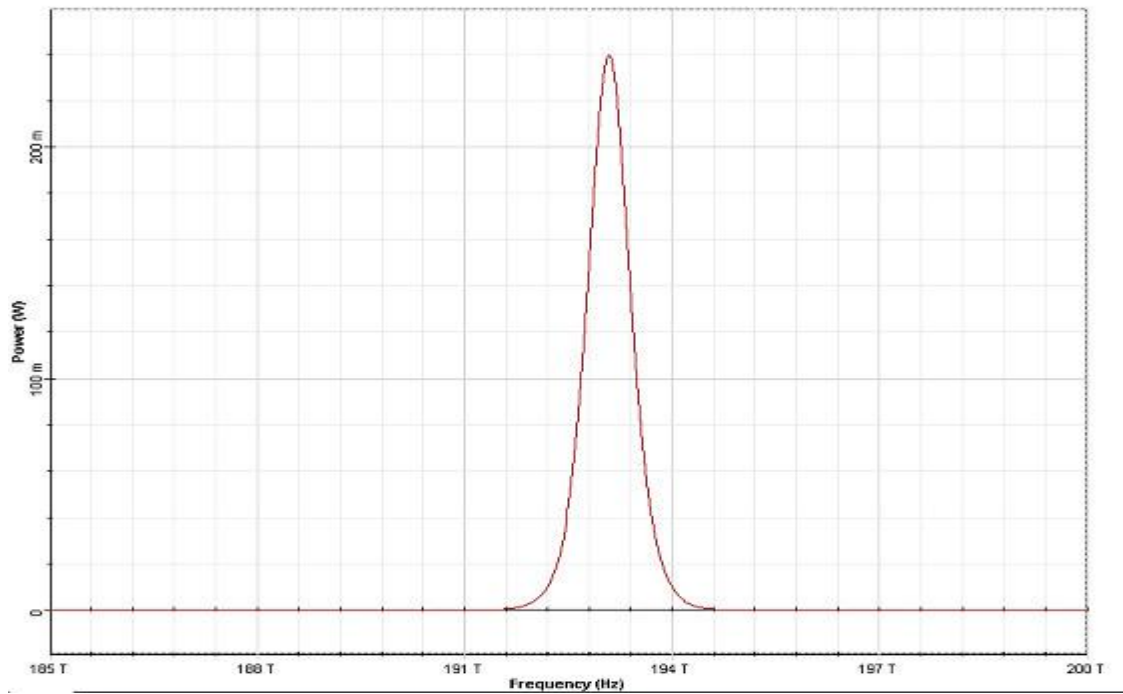


Figure 4.6.7: Input pulse shape (optical spectrum analyzer)

## Output Pulse Shapes

It can be seen that the effect of stimulated Raman scattering on the higher-order soliton is to split it into its constituents. Moreover, the frequency domain manifestation of this effect (soliton self-frequency shift) can be clearly seen upon comparing the input and output pulse spectrum.

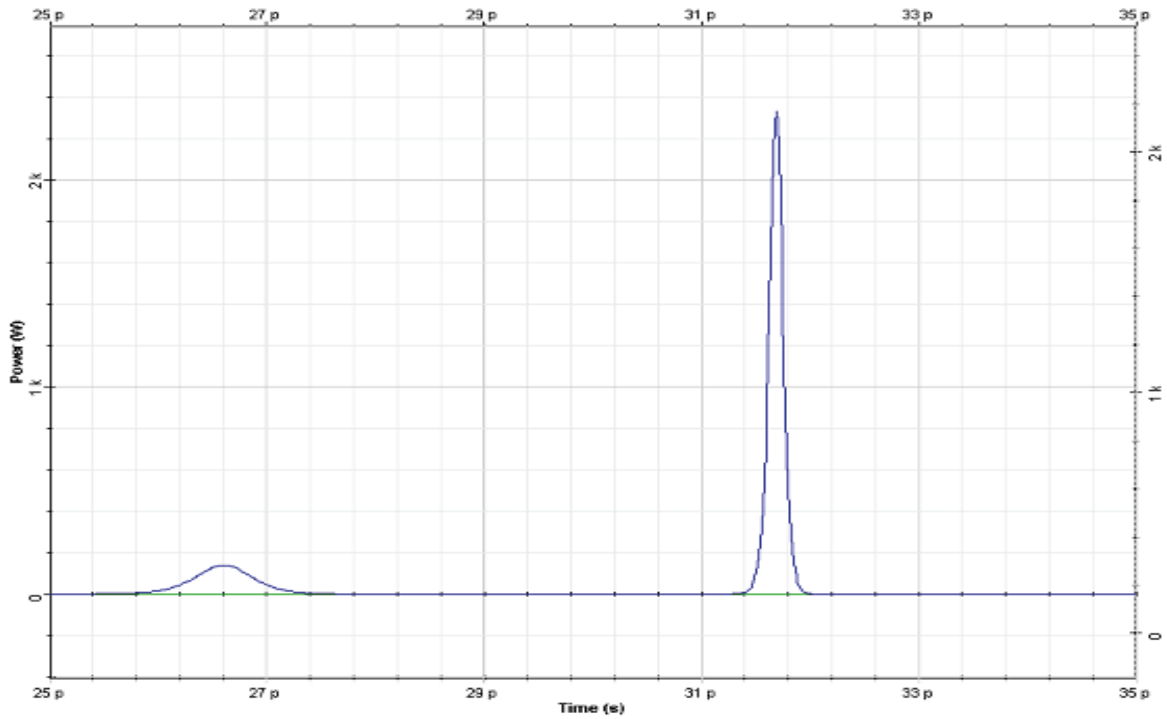


Figure 4.6.8: Output pulse shape(optical time domain visualize)

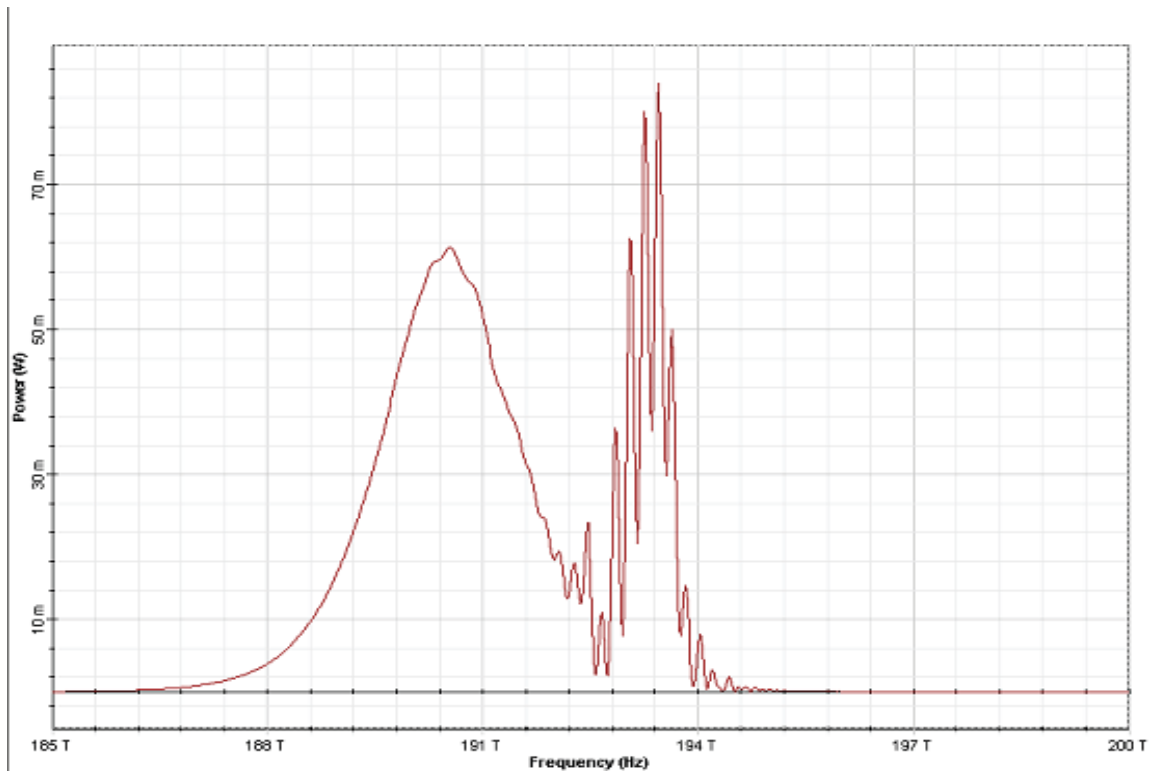


Figure 4.6.9: Output pulse shape (optical spectrum analyzer)

The same layout can be used to demonstrate the applicability of the approximation of the full Raman response of the material with the intrapulse Raman scattering in the case when the signal bandwidth is much narrower compared to the Raman gain spectrum [1], which is the case considered here.

## Full Raman Response in the Nonlinear Dispersive Fiber

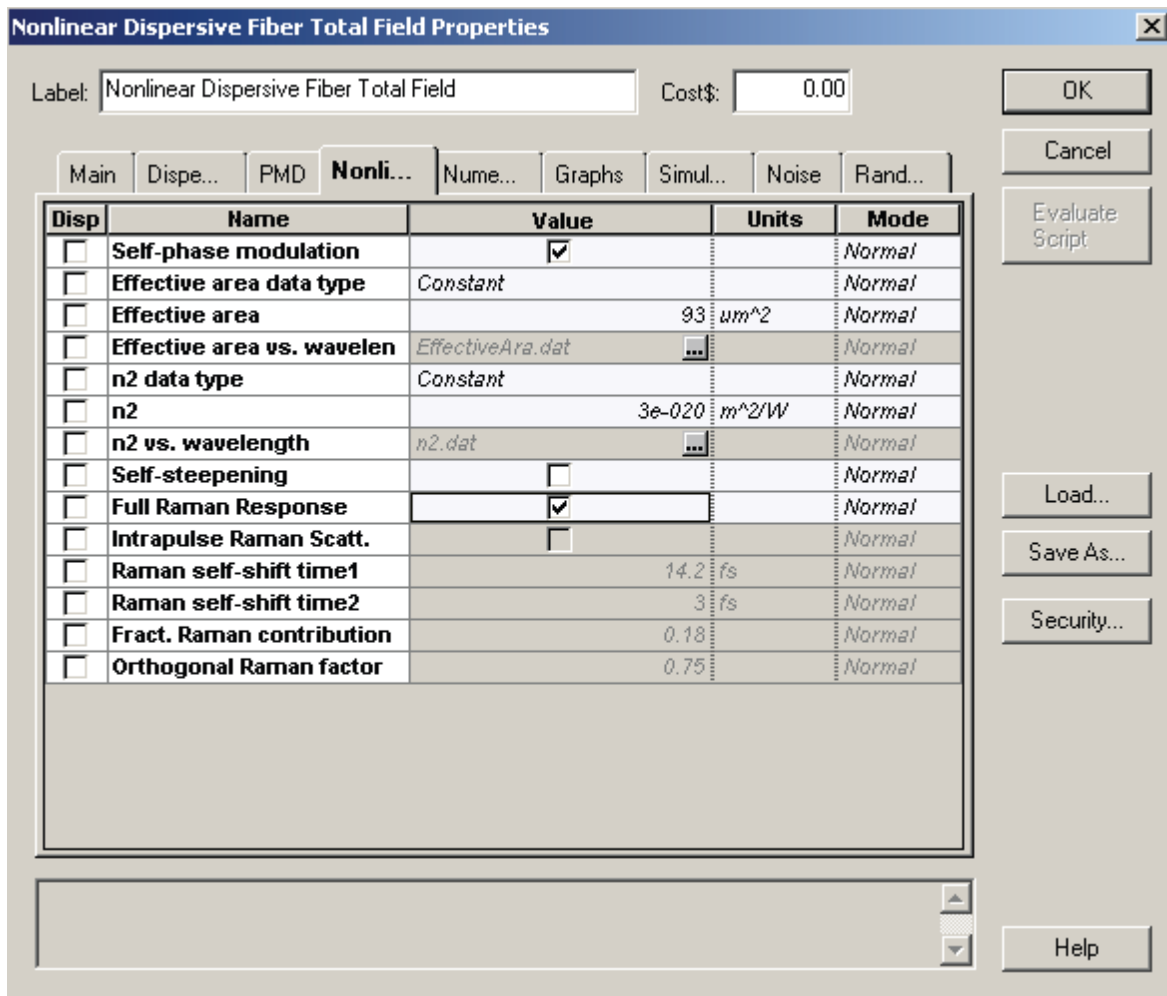


Figure 4.6.10: Full Raman response in the nonlinear dispersive fiber

The rest of the setup remains unchanged.

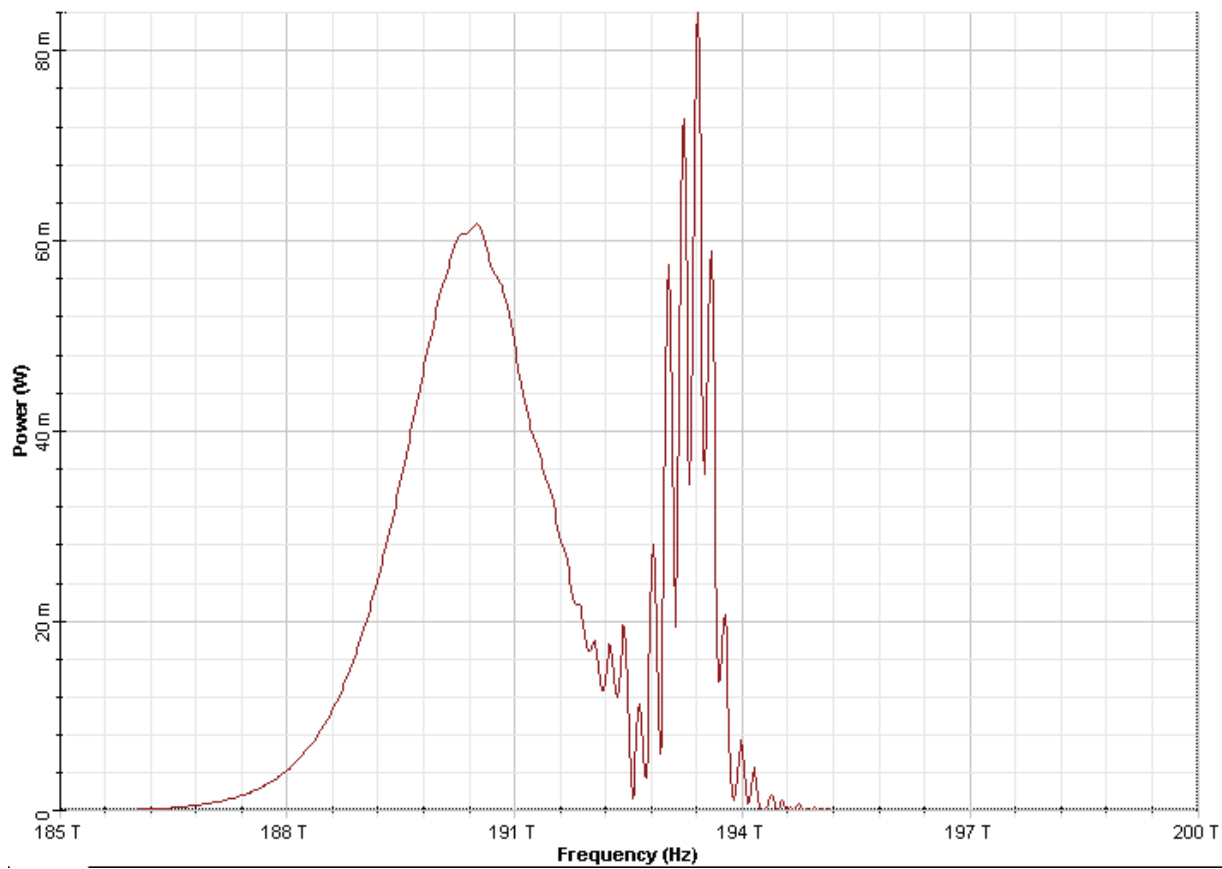


Figure 4.6.11: Output pulse spectrum at five soliton periods. "Full Raman response" is used in the nonlinear dispersive fiber.

The remainder of this lesson demonstrates a phenomenon known as soliton self-frequency shift.

**Input and output pulse shape at 50 soliton periods pulse spectrum**

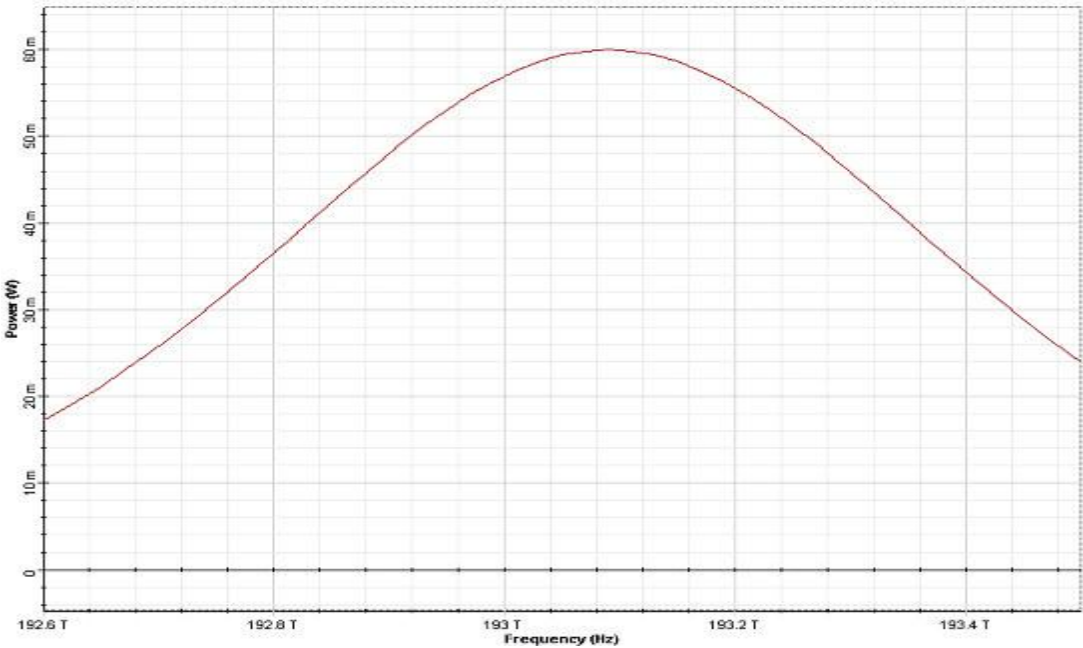


Figure 4.6.12: Input at 50 soliton periods (right) pulse spectrum

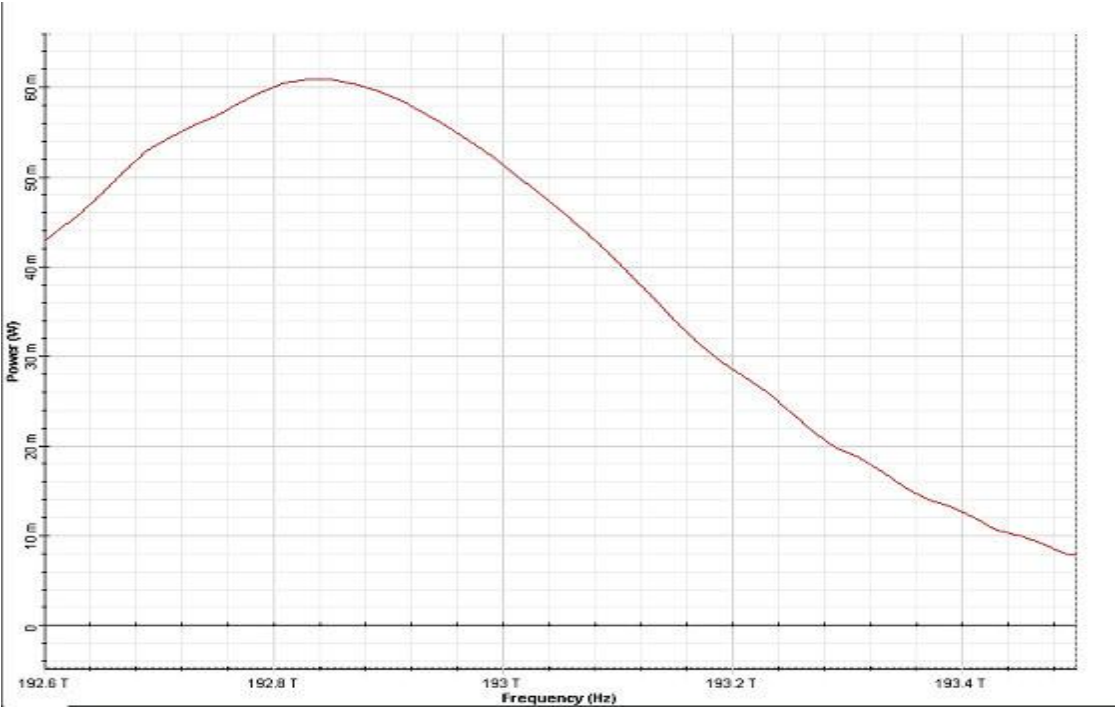


Figure 4.6.13: Output at 50 soliton periods (right) pulse spectrum

## 4.7 Decay of Higher order Solitons in the presence of Self-Steepening

This lesson demonstrates the influence of self-steepening effect on short soliton pulses

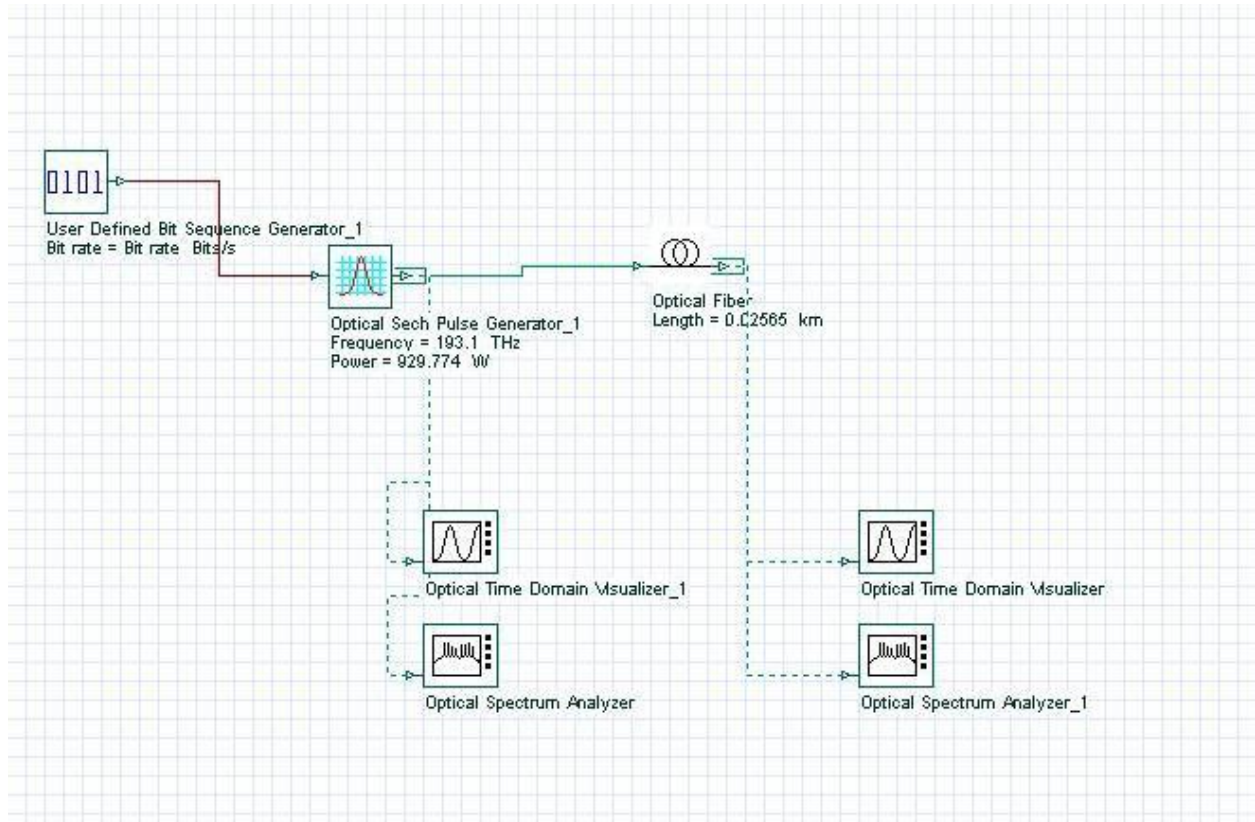


Figure 4.7.1: System Layout

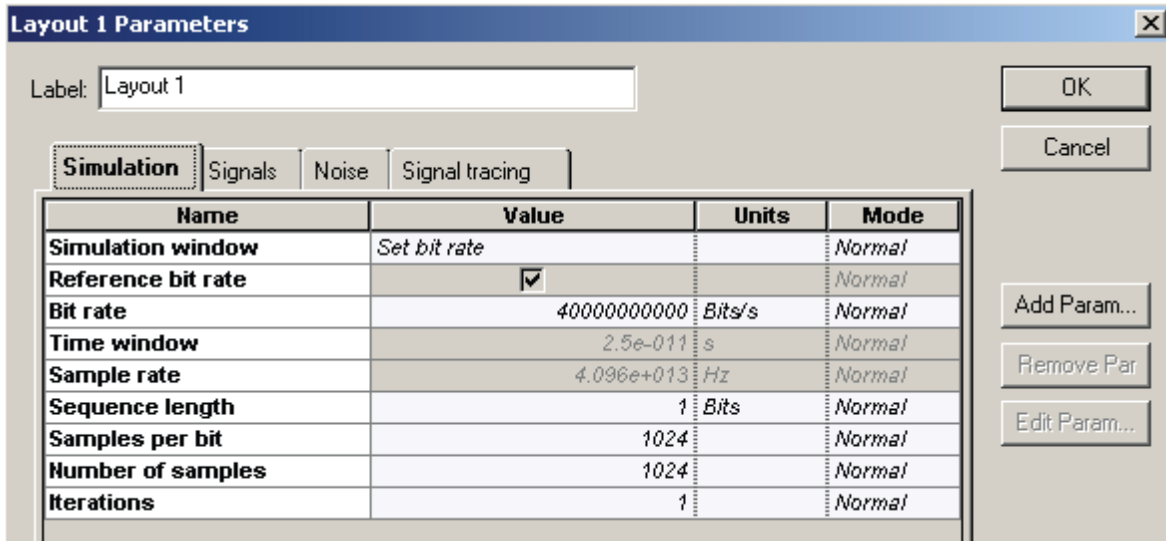


Figure 4.7.2:Layout parameters

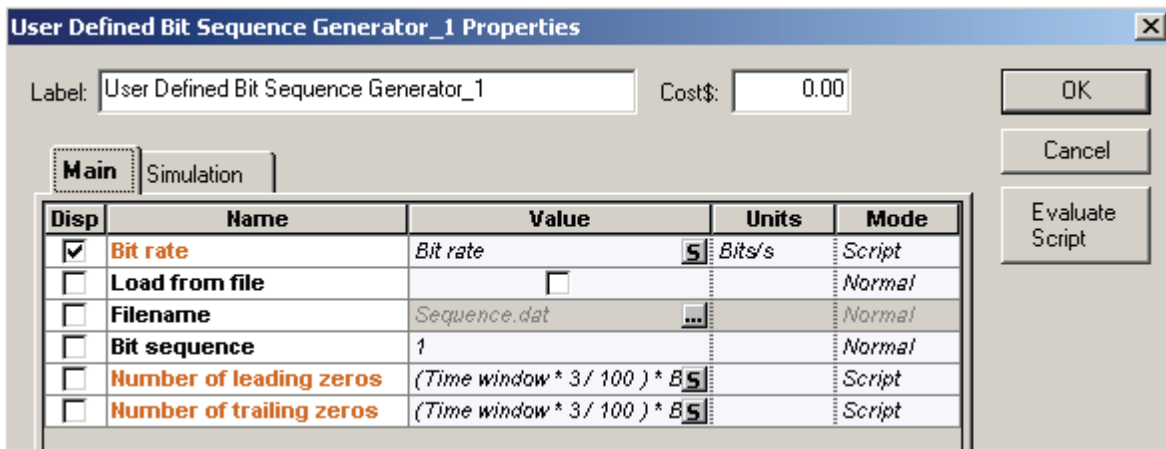


Figure 4.7.3: Bit sequence generator parameters

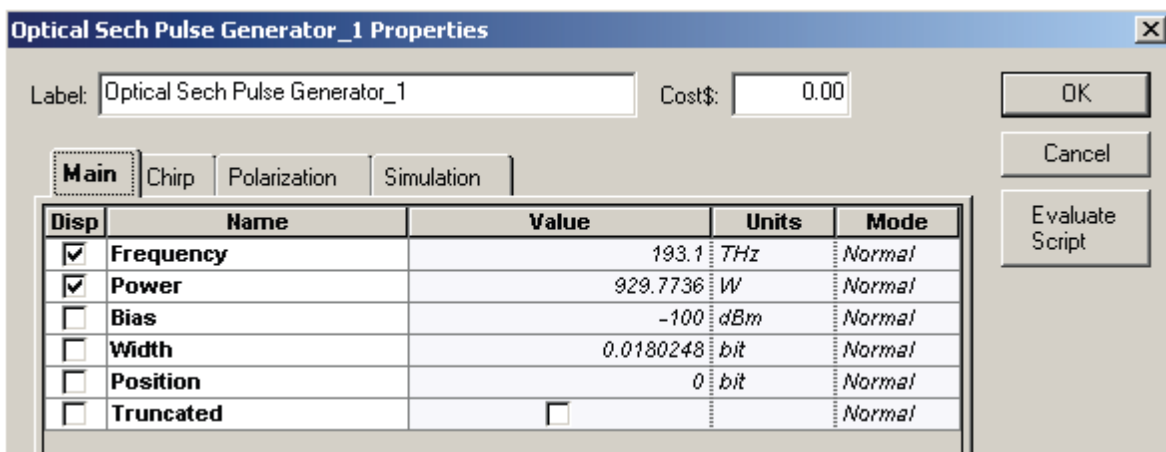


Figure 4.7.4:Sech-pulse generator parameters

**Nonlinear Dispersive Fiber Total Field Properties**

Label:  Cost\$:

Main
  Dispe...
  PMD
  Nonli...
  Nume...
  Graphs
  Simul...
  Noise
  Rand...

Disp	Name	Value	Units	Mode
<input type="checkbox"/>	User defined reference wa	<input type="checkbox"/>		Normal
<input type="checkbox"/>	Reference wavelength	1550	nm	Normal
<input checked="" type="checkbox"/>	Length	0.02565	km	Normal
<input type="checkbox"/>	Attenuation effect	<input type="checkbox"/>		Normal
<input type="checkbox"/>	Attenuation data type	Constant		Normal
<input type="checkbox"/>	Attenuation	0.2	dB/km	Normal
<input type="checkbox"/>	Attenuation vs. wavelengt	Attenuation.dat		Normal

OK  
Cancel  
Evaluate Script

Main
  Dispe...
  PMD
  Nonli...
  Nume...
  Graphs
  Simul...
  Noise
  Rand...

Disp	Name	Value	Units	Mode
<input type="checkbox"/>	Group velocity dispersion	<input checked="" type="checkbox"/>		Normal
<input type="checkbox"/>	Third-order dispersion	<input type="checkbox"/>		Normal
<input type="checkbox"/>	Dispersion data type	Constant		Normal
<input type="checkbox"/>	Frequency domain parame	<input checked="" type="checkbox"/>		Normal
<input type="checkbox"/>	Dispersion	16.75	ps/nm/km	Normal
<input type="checkbox"/>	Dispersion slope	0.075	ps/nm <sup>2</sup> /k	Normal
<input type="checkbox"/>	Beta 2	-20	ps <sup>2</sup> /km	Normal
<input type="checkbox"/>	Beta 3	0	ps <sup>3</sup> /km	Normal
<input type="checkbox"/>	Dispersion file format	Dispersion vs. wavelength		Normal
<input type="checkbox"/>	Dispersion file name	Dispersion.dat		Normal

Cancel  
Evaluate Script  
Load...  
Save As...

Main
  Dispe...
  PMD
  Nonli...
  Nume...
  Graphs
  Simul...
  Noise
  Rand...

Disp	Name	Value	Units	Mode
<input type="checkbox"/>	Model type	Scalar		Normal
<input type="checkbox"/>	Propagator type	Exponential		Normal
<input type="checkbox"/>	Calculation type	Noniterative		Normal
<input type="checkbox"/>	Number of iterations	2		Normal
<input type="checkbox"/>	Step size	Constant		Normal
<input type="checkbox"/>	Max. nonlinear phase shift	20	mrad	Normal
<input type="checkbox"/>	Boundary conditions	Periodic		Normal
<input type="checkbox"/>	Filter steepness	0.005		Normal
<input type="checkbox"/>	Lower calculation limit	1000	nm	Normal
<input type="checkbox"/>	Upper calculation limit	2000	nm	Normal

Cancel  
Evaluate Script  
Load...  
Save As...

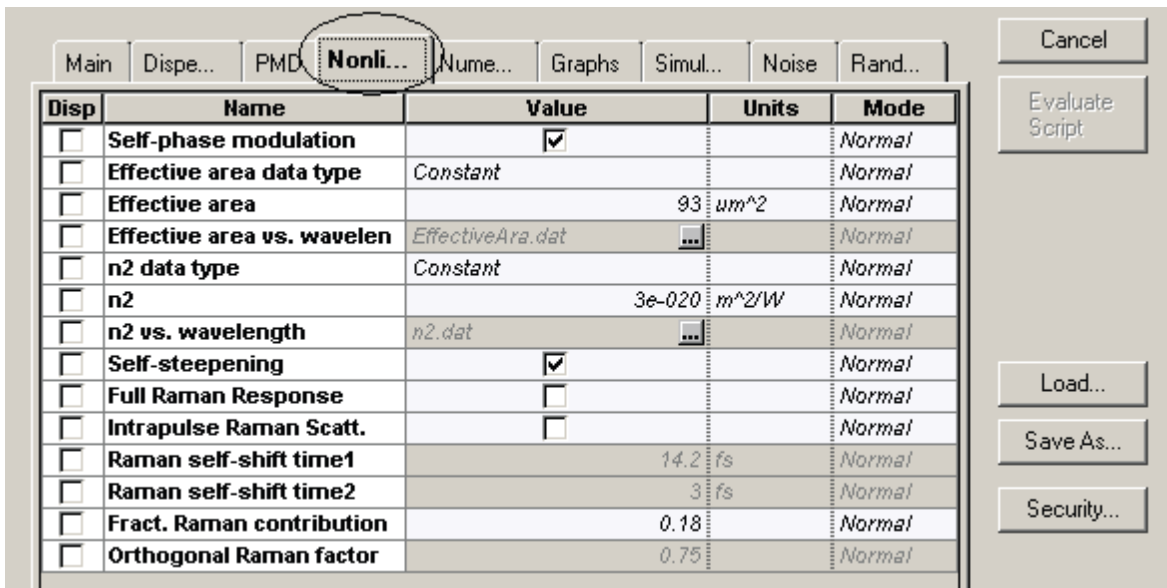


Figure 4.7.5:Fibreparameters

## Input pulse shape

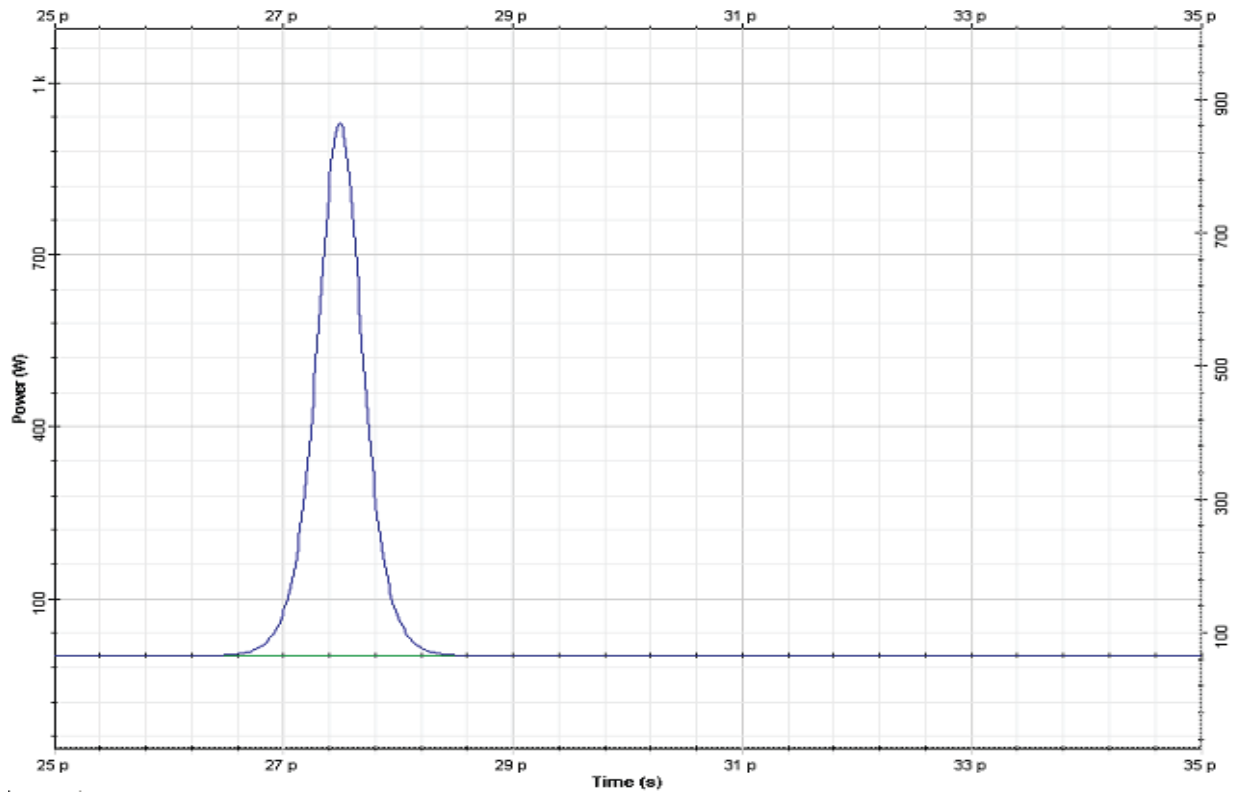


Figure 4.7.6: Input pulse shape

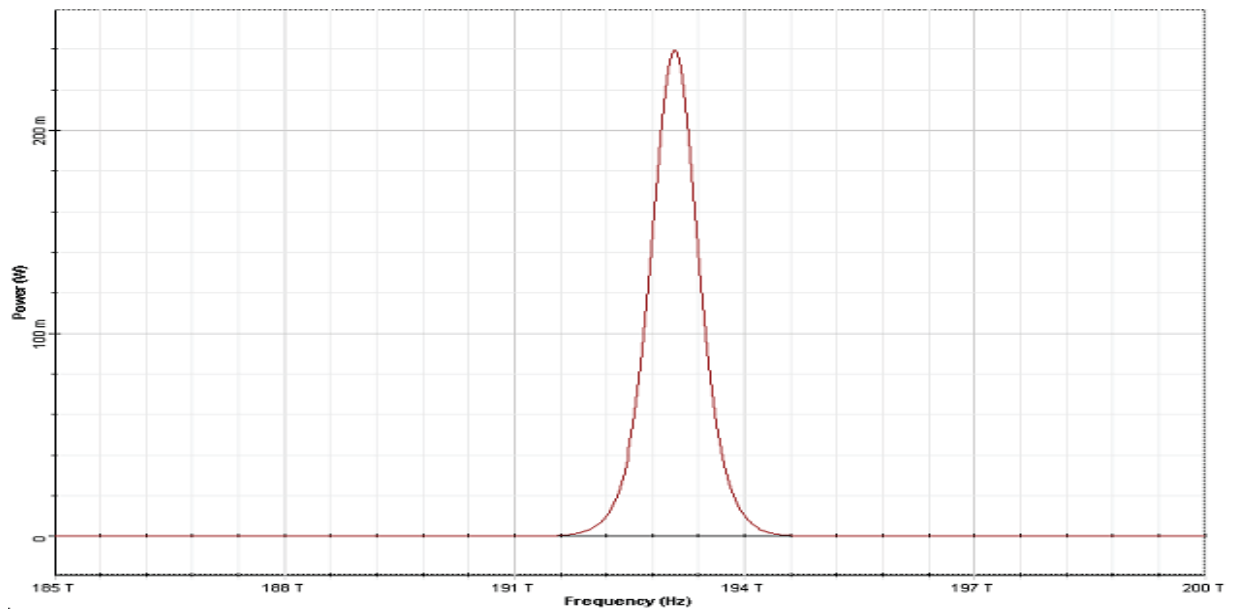


Figure 4.7.7: Input pulse shape at spectrum

### Output pulse shape

The output pulse shape after five and ten soliton periods of propagation are shown in Figure 4.7.8 and 4.7.9. It can be seen that the effect of self-steepening on the higher-order soliton is to split it into its constituents [1].

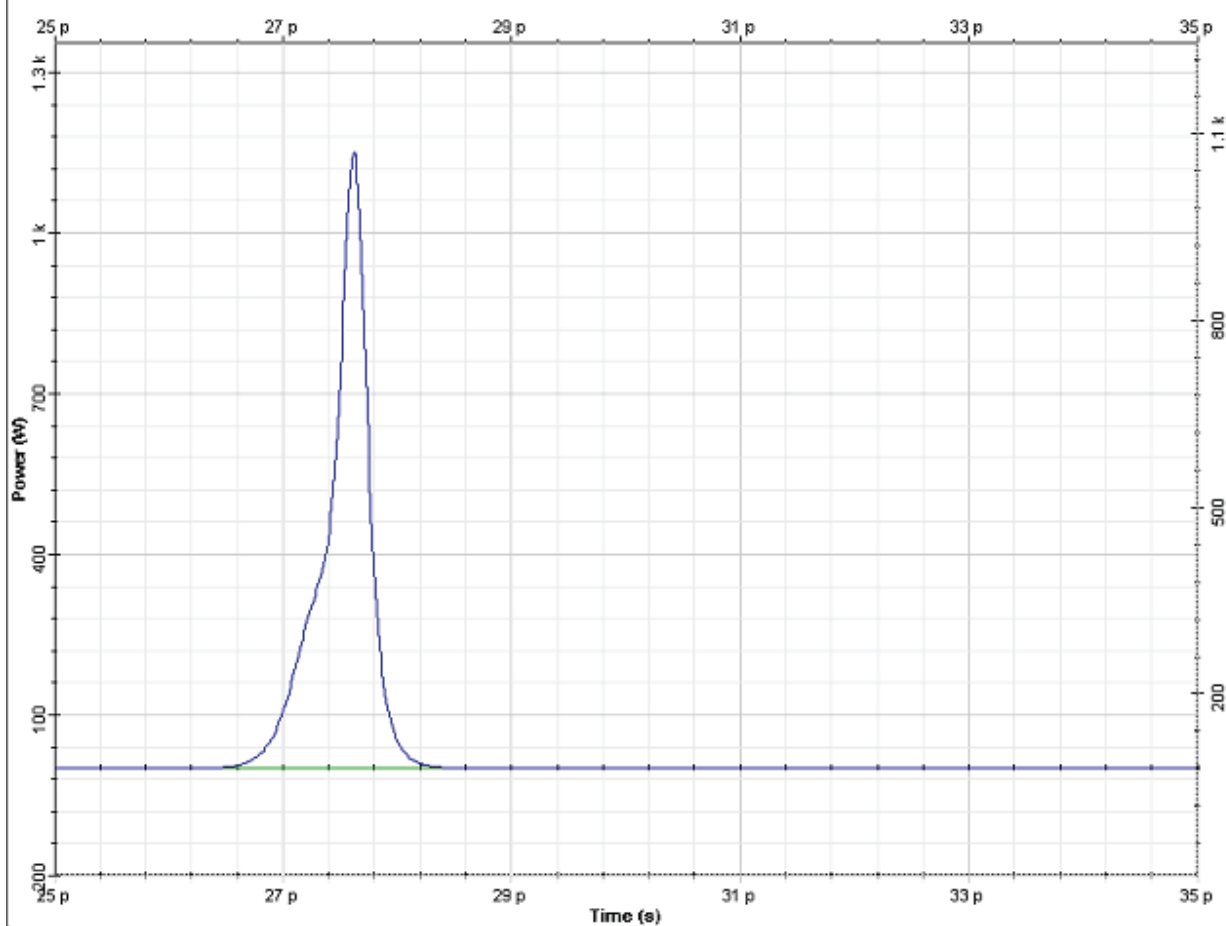


Figure 4.7.8: Output pulse shape at five soliton periods

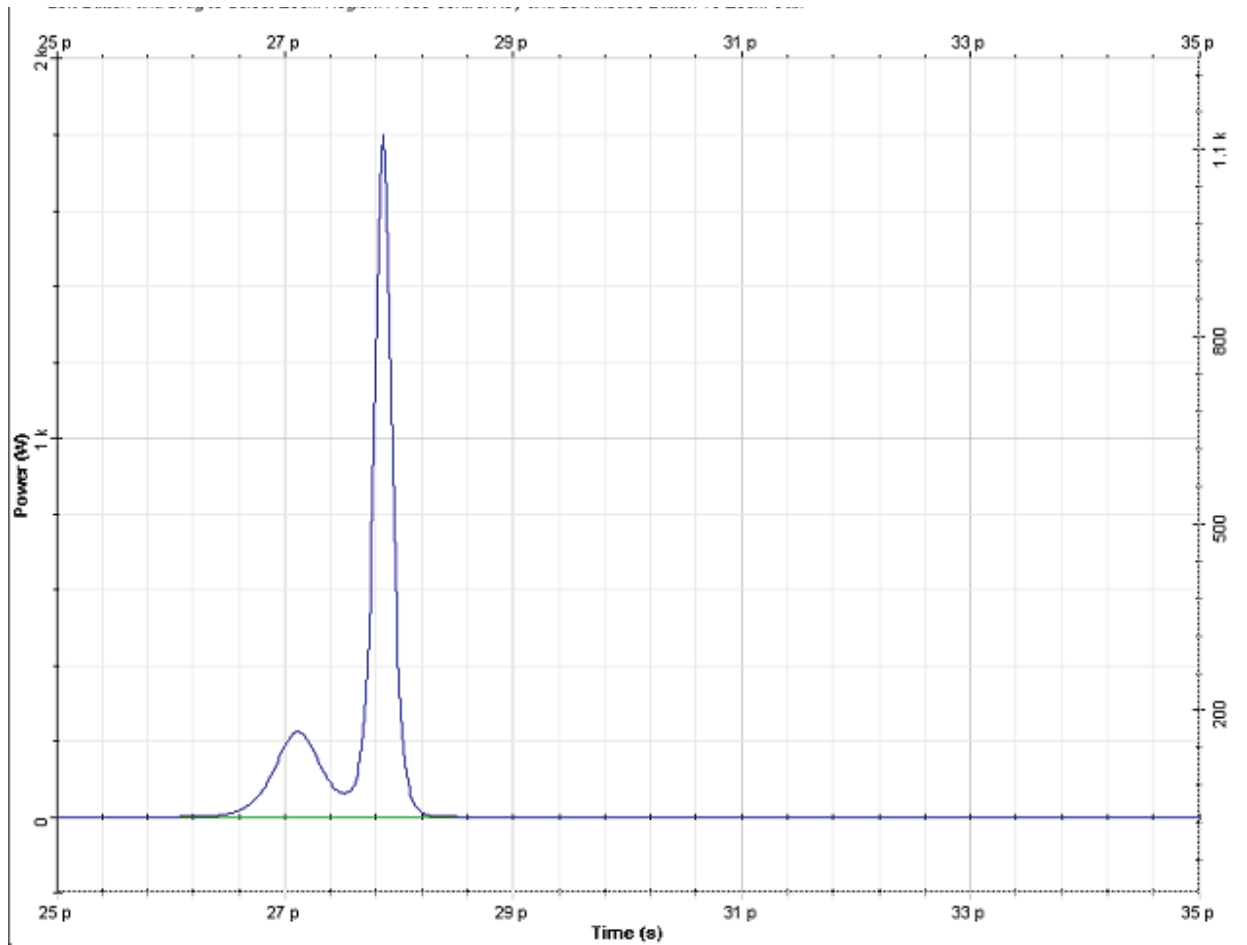


Figure 4.7.9: Output pulse shape at ten soliton periods

While the soliton splitting has occurred within a distance of five soliton periods in the case when the intrapulse Raman scattering acts as a perturbing effect, the splitting is still in its initial stage (for the same input configuration) in the case considered here. This shows that the self-steepening effect is weaker than the stimulated Raman scattering [1].

## CHAPTER 5

### CONCLUDING REMARKS AND FUTURE SCOPE

---

It is established in the above THESIS that when number of soliton pulses having same phases interact with each other the interaction enhances the refractive index at the point where they meet. This enhancement depends on the intensities of the participating pulses individually. This character can be exploited very nicely in long distance remote switching through optical fiber. The change of refractive index in optical fiber media by interaction between two or among more numbers of soliton pulses can lead leakage of light from the fiber at the interaction point. Many other similar incidences can be organized by this interaction and these can be directly utilized in long distance switching. Optical logic operation can be conducted from a long distance if the interaction can be organized properly. We can see also from the above discussion that the change of refractive index will not depend at all of the frequencies of the carrier waves of the interacting soliton pulses.

We studied solitons & soliton systems in the above thesis and get the results through Optisystem simulation software and compared all the obtained experimental results with the theoretical results.

Lot of research is going in the field of optical solitons to explore the properties of soliton for pattern formation. Everyone in America knows what a fractal is. Take a stroll around any college campus and you will pass by young computer scientists wearing T-shirts emblazoned with brightly colored spiraling patterns. In the corporate world, fractals thrive in the after hours as screen-savers come to life on cubicle workstations. Similarly, pattern formation has also captured the imagination of the media. Coffee-table picture books and websites abound showing images of zebras next to striped tropical fish, or brains compared to coral. But while these familiar images surround us in nature and on computer screens, something of a gap remains. Although truly a breakthrough in many respects, the ability to generate a fractal picture of a leaf on a computer screen does not necessarily enhance our understanding of the physical mechanisms that

actually caused the leaf to form in the manner that it did. Too often the dynamics of pattern formation are no less mysterious than they ever were.

## **REFERENCES**

- [1] J. S. Russell, in *14<sup>th</sup> Meeting of the British Association Reports* (York, 1844).
- [2] K. E. Lonngren, *Plasma Phys.* **25**, 943 (1983).
- [3] E. Polturak, P. G. N. deVegvar, E. K. Zeise, D. M. Lee, *Phys. Rev. Lett.* **46**, 1588 (1981).
- [4] A. Hasegawa and F. Tappert, *Appl. Phys. Lett.* **23**, 142 (1973).
- [5] A. Barthelemy, S. Maneuf, C. Froehly, *Opt. Commun.* **55**, 201 (1985).
- [6] J. S. Aitchison, *et al.*, *Opt. Lett.* **15**, 471 (1990).
- [7] J. S. Aitchison, K. Al-Hemyari, C. N. Ironside, R. S. Grant, W. Sibbett, *Electron. Lett.* **28**, 1879 (1992).
- [8] U. Bartuch, U. Peschel, Th. Gabler, R. Waldhaus and H.-H. Horhold, *Opt. Commun.* **134**, 49 (1997).
- [9] V.E Zarkarov and A.B Shabat, *Sovt.Phys.* **34**62(1972).
- [10] G. I. Stegeman and M. Segev, *Science* **286**, 1518 (1999).
- [11] N. J. Zabusky and M. D. Kruskal, *Phys. Rev. Lett.* **15**, 240 (1965).
- [12] M. Hercher, *J. Opt. Soc. Amer.* **54**, 563 (1964).
- [13] L. F. Mollenauer, R. H. Stolen, and J. P. Gordon, *Phys. Rev. Lett.* **45**, 1095 (1980).
- [14] G. P. Agrawal, in *Nonlinear Fiber Optics*, Academic Press, San Diego, CA, 1989, Chap. 5.
- [15] A. Hasegawa, *Solitons in Optical Fibers*, Springer-Verlag, Berlin, 1989.
- [16] M. Nakazawa, *Proc. Eur. Conf. Opt. Commun.*, Paris, Sept. 9-12, 1991, pp. 150-164.
- [17] A. Hasegawa and W. F. Brinkman, *Quant. Elec. Lett.* **Q1-16**, 694 (1980).
- [18] I. H. Malitson, *J. Opt. Soc. Am.* **55**, 1205 (1965).

- [19] G. Duree, J. L. Shultz, G. Salamo, M. Segev, A. Yariv, B. Crosignani, P. DiPorto, E. Sharp, R. Neurgaonkar, *Phys. Rev. Lett.* **71**, 533 (1993).
- [20] A. W. Snyder, D. J. Mitchell, L. Polodian, and F. Ladouceur, *Opt. Lett.* **16**, 21 (1991); A. W. Snyder and A. P. Sheppard, *Opt. Lett.* **18**, 482 (1993); A. W. Snyder, S. J. Hewlett, and D. J. Mitchell, *Phys. Rev. Lett.* **72**, 1012 (1994).
- [21] A. Ashkin, G. D. Boyd, J. M. Dziedzic, R. G. Smith, A. A. Ballman, J. J. Levinstein, and K. Nassau, *Appl. Phys. Lett.* **9**, 72 (1966).
- [22] P. Yeh, in *Introduction to Photorefractive Nonlinear Optics*, Wiley, New York, 1993, Chapter 3.
- [23] A. Barthelemy, S. Maneuf, and C. Froehly, *Opt. Comm.* **55**, 201 (1985); J. S. Aitchison, A.M. Weiner, Y. Silberberg, M. K. Oliver, J. L. Jackel, D. E. Leaird, E. M. Vogel, and P. W. E. Smith, *Opt. Lett.* **15**, 471 (1990).
- [24] Y. N. Karamzin and A. P. Sukhorukov, *Sov. Phys. JETP* **41**, 414 (1976).
- [25] W. E. Torruellas, Z. Wang, D. J. Hagan, E. W. Van Stryland, G. I. Stegeman, L. Torner, and C. R. Menyuk, *Phys. Rev. Lett.* **74**, 5036 (1995); R. Schiek, Y. Baek.
- [26] M. Mitchell, Z. Chen, M. Shih, and M. Segev, *Phys. Rev. Lett.* **77**, 490 (1996).
- [27] D. N. Christodoulides, T. H. Coskun, M. Mitchell, and M. Segev, *Phys. Rev. Lett.* **78**, 646 (1997); **80**, 2310 (1998).
- [28] E. M. Dianov, P. V. Mamyshev, A. M. Prokhorov, and S. V. Chernikov, *Opt. Lett.* **14**, 1008 (1989).
- [29] P. V. Mamyshev, C. Bosshard, and G. I. Stegeman, *J. Opt. Soc. Am. B* **11**, 1254 (1994).
- [30] M. D. Iturbe-Castillo, M. Torres-Cisneros, J. J. Sanchez-Mondragon, S. Chavez-Cerda, S. I. Stepanov, V. A. Vysloukh, and G. E. Torres-Cisneros, *Opt. Lett.* **20**, 1853 (1995).
- [31] M. I. Carvalho, S. R. Singh, and D. N. Christodoulides, *Opt. Comm.* **126**, 167 (1996).
- [32] A. Hasegawa, *Opt. Lett.* **9**, 288 (1984).

- [33] M. Artiglia, E. Ciaramella, and P. Gallina, *Trends in Optics and Photonics* **12**, 305 (1997).
- [34] M. Soljacic, M. Segev, T. Coskun, D. N. Christodoulides, and A. Vishwanath, *Phys. Rev. Lett.* **84**, 467 (2000).
- [35] D. Kip, M. Soljacic, M. Segev, E. Eugenieva, and D. N. Christodoulides, *Science* **290**, 495 (2000); J. Klinger, H. Martin, and Z. Chen, *Opt. Lett.* **26**, 271 (2000).
- [36] G. B. Whitham, *J. Fluid Mech.* **22**, 273 (1965).
- [37] A. Hasegawa, *Phys. Fluids* **15**, 870 (1972).
- [39] M. Segev, B. Crosignani, A. Yariv, and B. Fischer, *Phys. Rev. Lett.* **68**, 923 (1992).
- [40] G. Duree, J. L. Shultz, G. Salamo, M. Segev, A. Yariv, B. Crosignani, P. DiPorto, E. Sharp, and R. R. Neurgaonkar, *Phys. Rev. Lett.* **71**, 533 (1993).
- [41] Y. N. Karamzin and A. P. Sukhorukov, *Sov. Phys. JETP*, **41**, 414 (1976).
- [42] W. E. Torruellas, Z. Wang, D. J. Hagan, E. W. VanStryland, G. I. Stegeman, L. Torner, and C. R. Menyuk, *Phys. Rev. Lett.* **74**, 5036 (1995).
- [43] M. Shalaby and A. J. Barthelemy, *IEEE J. Quantum Electron.* **28**, 2736 (1992).
- [44] M. Mitchell, Z. Chen, M. Shih, and M. Segev, *Phys. Rev. Lett.* **77**, 490 (1996).
- [45] M. Mitchell and M. Segev, *Nature* **387**, 880 (1997).
- [46] Z. Chen, M. Mitchell, M. Segev, T. Coskun, and D. N. Christodoulides, *Science* **280**, 889 (1998).
- [47] D. N. Christodoulides and R. I. Joseph, *Opt. Lett.* **13**, 794 (1988).
- [48] H. S. Eisenberg, Y. Silberberg, R. Morandotti, A. R. Boyd, and J. S. Aitchison, *Phys. Rev. Lett.* **81**, 3383 (1988).
- [49] Y. Silberberg, *Opt. Lett.* **15**, 1282 (1990).

- [50] M. Brambilla, L. A. Lugiato, F. Prati, L. Spinelli, and W. J. Firth, *Phys. Rev. Lett.* **79**, 2042 (1997).
- [51] V. P. Taranenko, I. Ganne, R. J. Kuszelewicz, and C. O. Weiss, *Phys. Rev. A.*, to be published.
- [52] S. Sears, M. Soljagic, M. Segev, D. Krylov and K. Bergman, Cantor set fractals from solitons, *Physical Review Letters* **84**, 1902 (2000).
- [53] S. M. Sears, M. Soljagic, D. N. Christodoulides and M. Segev, Pattern formation via symmetry breaking in nonlinear weakly correlated systems, *Physical Review E* **65**, 36620 (2002).
- [54] Z. Chen, S. M. Sears, H. Martin, D. N. Christodoulides and M. Segev, Clustering of solitons in weakly correlated systems, *Proceedings of the US National Academy of Science (PNAS)*, **99**, 5223 (2002).
- [55] G. P. Agrawal *Nonlinear Fiber Optics*, Academic Press (2001).

